# EXPERIMENTAL VERIFICATION OF DESIGN PROCEDURES FOR SHEAR AND TORSION IN REINFORCED AND PRESTRESSED CONCRETE

J. A. Ramirez and J. E. Breen

RESEARCH REPORT 248-3

PROJECT 3-5-80-248

# CENTER FOR TRANSPORTATION RESEARCH

| 1. Report No. | 2. Government Accession No. | 3. Recipient's Catalog No. |
|---|---|---|
| FHWA/TX-84/37+248-3 | | |

| 4. Title and Subtitle | 5. Report Date |
|---|---|
| EXPERIMENTAL VERIFICATION OF DESIGN PROCEDURES FOR SHEAR AND TORSION IN REINFORCED AND PRESTRESSED CONCRETE | November 1983 |
| | 6. Performing Organization Code |

| 7. Author's) | 8. Performing Organization Report No. |
|---|---|
| J. A. Ramirez and J. E. Breen | Research Report 248-3 |

| 9. Performing Organization Name and Address | 10. Work Unit No. |
|---|---|
| Center for Transportation Research The University of Texas at Austin Austin, Texas 78712-1075 | |
| | 11. Contract or Grant No. |
| | Research Study 3-5-80-248 |

| 12. Sponsoring Agency Name and Address | 13. Type of Report and Period Covered |
|---|---|
| Texas State Department of Highways and Public Transportation; Transportation Planning Division P. O. Box 5051 Austin, Texas 78763 | Interim |
| | 14. Sponsoring Agency Code |

15. Supplementary Notes

Study conducted in cooperation with the U. S. Department of Transportation, Federal Highway Administration. Research Study Title: "Reevaluation of AASHTO Shear and Torsion Provisions for Reinforced and Prestressed Concrete"

16. Abstract

The object of this study is to propose and evaluate a design procedure for shear and torsion in reinforced and prestressed concrete beams, with the aim of clarifying and simplifying current design requirements and AASHTO requirements.

This report summarizes an extensive experimental verification of a powerful three-dimensional space truss model with variable angle of inclination of the diagonal elements. This conceptual model was developed by European and Canadian engineers over the past fifteen years. The model is shown to be a conservative method of predicting the strength of such members under combined loading. Detailed comparison with current ACI/AASHTO procedures indicate greatly reduced scatter when comparisons are made to test results. Detailed design procedures and specifications, and example applications are given in the final report in this series.

| 17. Key Words | 18. Distribution Statement |
|---|---|
| beams, concrete, reinforced, prestressed, shear, torsion, design, reinforcement, verification, experimental | No restrictions. This document is available to the public through the National Technical Information Service, Springfield, Virginia 22161. |

| 19. Security Classif. (of this report) | 20. Security Classif. (of this page) | 21. No. of Pages | 22. Price |
|---|---|---|---|
| Unclassified | Unclassified | 322 | |

Form DOT F 1700.7 (8-69)

EXPERIMENTAL VERIFICATION OF DESIGN PROCEDURES FOR SHEAR AND TORSION

IN REINFORCED AND PRESTRESSED CONCRETE


by


J. A. Ramirez and J. E. Breen



Research Report No. 248-3

Research Project 3-5-80-248

"Reevaluation of AASHTO Shear and Torsion Provisions for
Reinforced and Prestressed Concrete"




Conducted for

Texas

State Department of Highways and Public Transportation

In Cooperation with the
U. S. Department of Transportation
Federal Highway Administration

by

CENTER FOR TRANSPORTATION RESEARCH
BUREAU OF ENGINEERING RESEARCH
THE UNIVERSITY OF TEXAS AT AUSTIN


November 1983

# PREFACE

This report is the third in a series which summarizes a detailed evaluation of AASHTO design procedures for shear and torsion in reinforced and prestressed concrete beams. The first report summarized an exploratory investigation of the shear transfer between joints using details commonly found in segmental box girder construction. The second report reviews the historical development of design procedures for shear and torsion in concrete members as found in American practice. Both the AASHTO Specifications and the ACI Building Code are examined, since they have been closely related. In addition, this report presents the background and equilibrium relationships for use of a space truss with variable inclination diagonals as a design model. This report summarizes special considerations required for the practical usage of the variable inclination truss model. It also compares the theoretical capacity as computed by the truss model to experimental results for a great variety of previously reported tests as well as the results of tests run in this program to investigate several variables. The fourth and final report in this series draws on the analytical and experimental results presented in the earlier reports. It uses these results to develop procedures and suggested AASHTO Specification procedures for girder shear and torsion. The final report also contains several examples to illustrate the application of the design criteria and procedures.

# S U M M A R Y

The object of this study is to propose and evaluate a design procedure for shear and torsion in reinforced and prestressed concrete beams, with the aim of clarifying and simplifying current design requirements and AASHTO requirements.

This report summarizes an extensive experimental verification of a powerful three-dimensional space truss model with variable angle of inclination of the diagonal elements. This conceptual model was developed by European and Canadian engineers over the past fifteen years. The model is shown to be a conservative method of predicting the strength of such members under combined loading. Detailed comparison with current ACI/AASHTO procedures indicate greatly reduced scatter when comparisons are made to test results. Detailed design procedures and specifications, and example applications are given in the final report in this series.

# CONTENTS

# TABLES

# C H A P T E R  1

## INTRODUCTION

Design provisions for shear and torsion for reinforced and prestressed concrete members and structures in both the AASHTO Specifications (17) and the ACI Building Code (24) have evolved into complex procedures in recent revisions. The complexity of such procedures results from their highly empirical basis and the lack of a unified treatment of shear and torsion. Ironically, such design procedures seem better suited for analysis, since they become cumbersome and obscure when used for design.

Such deficiencies could be overcome if the design procedures in the shear and torsion areas were based on behavioral models rather than on detailed empirical equations. If the design procedures were based on a physical model, the designers would be able to envision the effects of the forces acting on the member, and then provide structural systems capable of resisting those forces. Furthermore, design provisions based on a conceptual model would become more simple and would not require as much test verification.

The present study attempts to answer the challenge posed by the ACI-ASCE Committee 426 (28):

> During the next decade it is hoped that design regulations for shear strength can be integrated, simplified, and given a physical significance so that designers can approach unusual design problems in a rational manner.

1

are generally not in English and are quite complex. The more limited reports, which are in English, have not had wide American readership. The apparent complexity of the proofs of the plasticity theorems as applied to shear and torsion can cause the more design-oriented reader to lose sight of the fact that the authors use these proofs only as a theoretical basis for proving the application of a refined truss model. The model was shown to be a lower bound solution giving the same result as the much more rigorous plasticity upper bound solution. Hence it is a valid solution which correctly represents the failure load.

This report extends the application of the space truss model to consider many special limits and approachs which must be incorporated in the design framework. The highlights of the refined truss model approach are the relatively simple design procedures that can be developed from the space truss model, and the extremely logical way the designer can envision providing and proportioning reinforcement for shear and torsion under special circumstances as in the case of box sections, concentrated loads on lower flanges, etc. Several of these are illustrated in Chapter 2.

However, it was felt that before the generalized refined truss model approach could be used as the basic design procedure in American practice, a complete evaluation of the accuracy of the model using a significant body of the available test data reported in the American literature was necessary. In Chapter 3, thorough comparisons of the space truss model with a wide range of test data and with predicted failure loads from other design procedures are presented.

# C H A P T E R  2

## SPECIAL CONSIDERATION REGARDING THE TRUSS MODEL

### 2.1  Introduction

Before design recommendations based on the space truss model can be proposed, several questions with regard to the behavior of the truss model under special conditions must be addressed.

In Report 248-2, the basic model was presented for the case of a thin-walled box section subjected to a constant shear flow produced by a shear force and/or a torsional moment and for a solid rectangular section subjected to bending and shear but not torsion. However, many questions still remain unanswered, such as the application for other cross sections or for the case when the shear force is not constant through the design region $z \cot\alpha$ such as in beams subjected to distributed loading.

In the space truss model, the ultimate strength of a given section is based on yielding of both the longitudinal and the transverse reinforcement. As a result, it is essential that premature failures caused by crushing of the concrete diagonal strut be avoided. This can be achieved by limiting the compression stresses in the diagonal strut to values equal or less than a certain specified allowable compression stress $f_c$.  However, due to the special conditions existing in the diagonal compression strut, the value of $f_c$ has to be substantially less than the specified compressive strength of the concrete $f'_c$.

5

In this chapter, the relationships derived in Report 248-2 for equilibrium in the space truss model are discussed to the extent necessary to draw conclusions which will permit the presentation of simple but safe and complete design recommendations based on the space truss model.

## 2.2 Effects of Different Types of Loading

The case of members subjected to a constant shear and/or torsion was illustrated in 248-2. In this section the effects of different loading conditions using the truss model are presented. First, the case of beams under uniformly distributed load is considered. Next, the special effects of concentrated loads is considered. The presence of a concentrated load induces a series of diagonal compression forces which "fan out" from the concentrated load. The effects of this disturbance on the assumed regular truss action are considered. Next, the case where heavy concentrated loads are applied near the supports is given. Finally, the case of loadings applied on/or near the bottom face causing the so called "hanger effect" is also included.

2.2.1 Beams Subjected to Uniformly Distributed Load. Consider the case of a simple beam subjected to a uniformly distributed load w as shown in Fig. 2.1. In this case the shear force varies linearly from a maximum at the support to zero at midspan. The analysis of this particular case with the truss model (see Fig. 2.2a) yields, from equilibrium of vertical forces on the free body shown in Fig. 2.2b, the value of the design shear force $V_s$ in the zone zcotα:
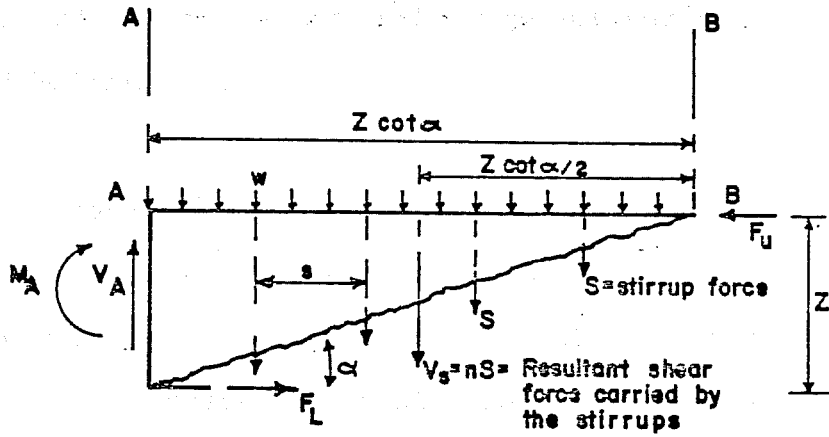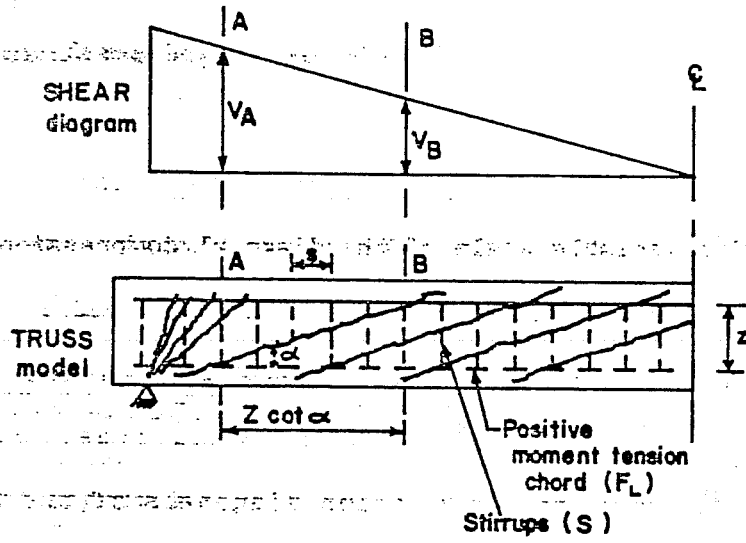
$$+ \quad \Sigma F_v = 0 = V_A - V_S - w \, z \cot \alpha$$

$$+ \quad \Sigma M_B = 0 = -F_L \cdot z + V_A \cdot z \cot \alpha + M_A - V_S \frac{z}{2} \cot \alpha - \frac{w}{2} (z \cot \alpha)^2$$

(b)

Fig. 2.2    Internal truss forces in the case of uniformly distributed loading

shown in Fig. 2.3, compression fans will form both at the support and under the applied concentrated load.

The geometry of the compression fans depends upon the stirrup spacing and the selected angle alpha. Figure 2.4a shows the equilibrium system at the support for the case of $\tan\alpha = 1.0$ and $s = z/2$.

In Fig. 2.4a the horizontal force $\Delta F(v)$ is shown as a tension force in the truss model. However, the minus sign attached to the value of this force in the table shown in Fig. 2.4a indicates that in reality it acts in the opposite direction, thus becoming a compression force. The presence of this horizontal compression force due to the "fanning" effect eliminates the need for longitudinal tension steel near the ends of simply supported beams where the end reaction induces compression (71).

As can be seen from Fig. 2.4a, as soon as the inclination of the diagonal compression force, "D", in the strut reaches the inclination of the chosen angle $\alpha$, the effects of the compression fan vanishes.

Since each of the diagonal compression forces acting at an inclination equal to chosen angle $\alpha$ can be anchored at a joint of the truss, a diagonal compression field with uniform inclination becomes feasible, thus eliminating the need of a compression fan to satisfy equilibrium.

Figure 2.4b illustrates the effect of the compression fan on the required anchorage force for the bottom (tension) chord at the support. For the case shown in Fig. 2.4b, the bottom chord of the truss model
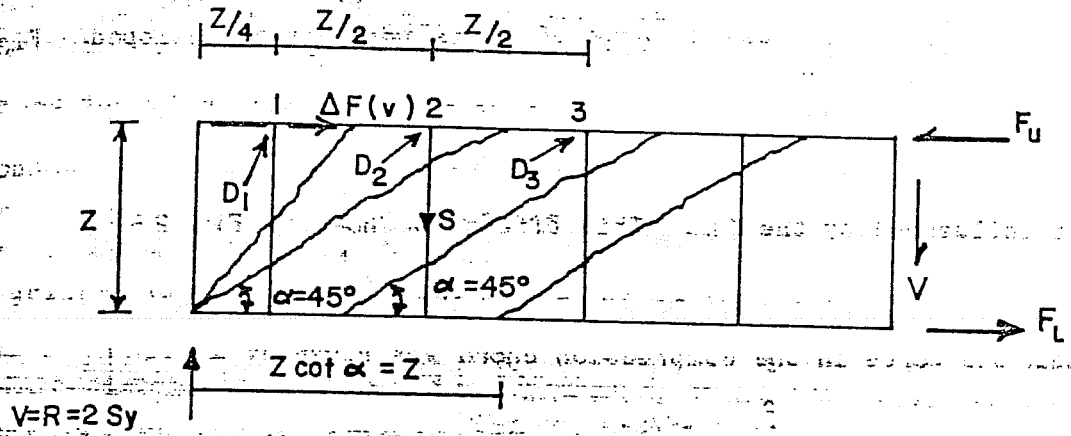
| Point (i) | $\alpha$ (i) | $\cos\alpha$ (i) | $\tan\alpha$ (i) | S (i) | $D_i = S/\sin\alpha$ (i) | $\Delta F(v)$ $D(i)\cos\alpha(i)$ |
|---|---|---|---|---|---|---|
| 1 | 75.96° | 0.24 | 4 | $S_y$ | $1.03S_y$ | $-0.25S_y$ |
| 2 | 53.13° | 0.60 | 4/3 | $S_y$ | $1.25S_y$ | $-0.75S_y$ |
| | | | | | $\Sigma\Delta F(v) = -S_y$ | |
| 3 | 45 | 0.71 | 1 | $S_y$ | $1.41S_y$ | $-S_y$ |

(a) Equilibrium system at support
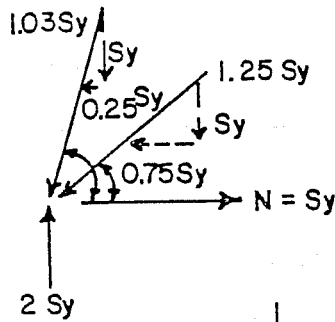
$$\Sigma F_H = 0 = N - 0.25S_y - 0.75S_y$$
$$N = S_y = 1/2\, V \cot\alpha$$

$$F_L = \frac{1}{2} V \cot\alpha$$
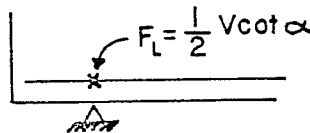
(b) Anchorage force at the support

Fig. 2.4 Compression fan at the support

|  | Point | x | M(s) | $F_u$ |
|---|---|---|---|---|
|  | 1 | $z/4$ | $S_y z/2$ | $S_y/2$ |
|  | 2 | $3z/4$ | $3S_y z/2$ | $3S_y/2$ |
|  | 3 | $5z/4$ | $5S_y z/2$ | $5S_y/2$ |

(a) Force in the upper chord

In figure (a): $-\frac{M}{Z} + \frac{1}{2} V\cot\alpha$, $-\frac{M}{Z}$, $S_y$



In figure (b): $\frac{M}{Z} + \frac{V\cot\alpha}{2}$, $\frac{M}{Z}$, $S_y$
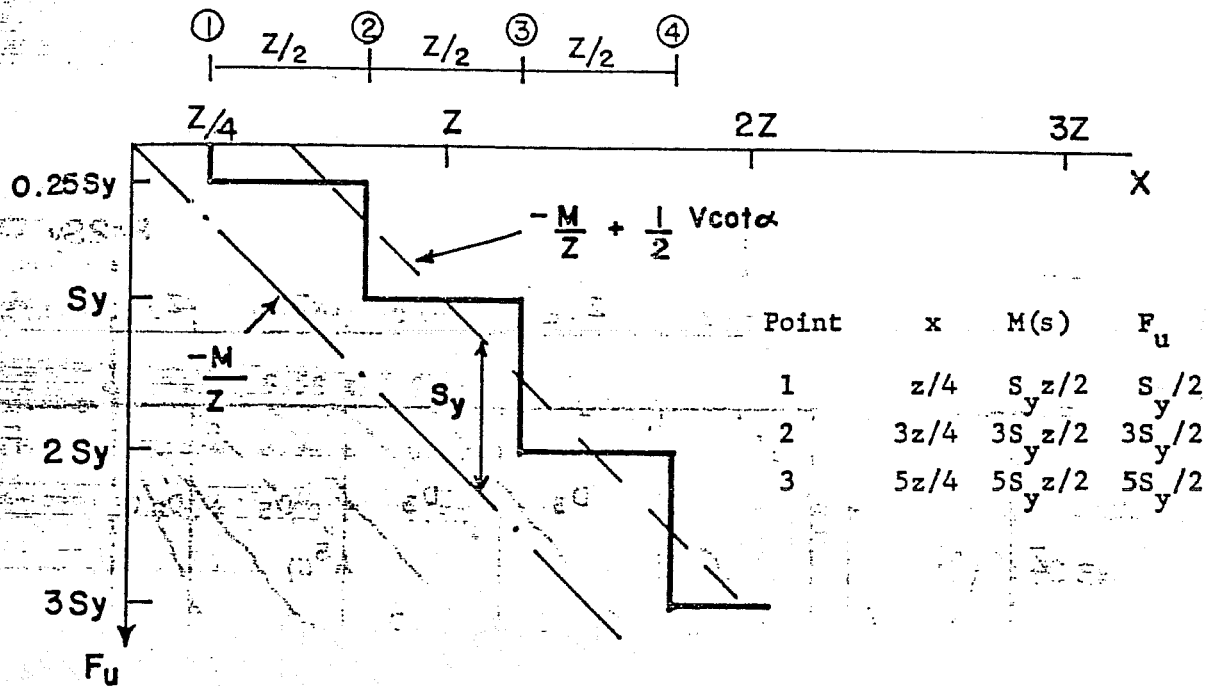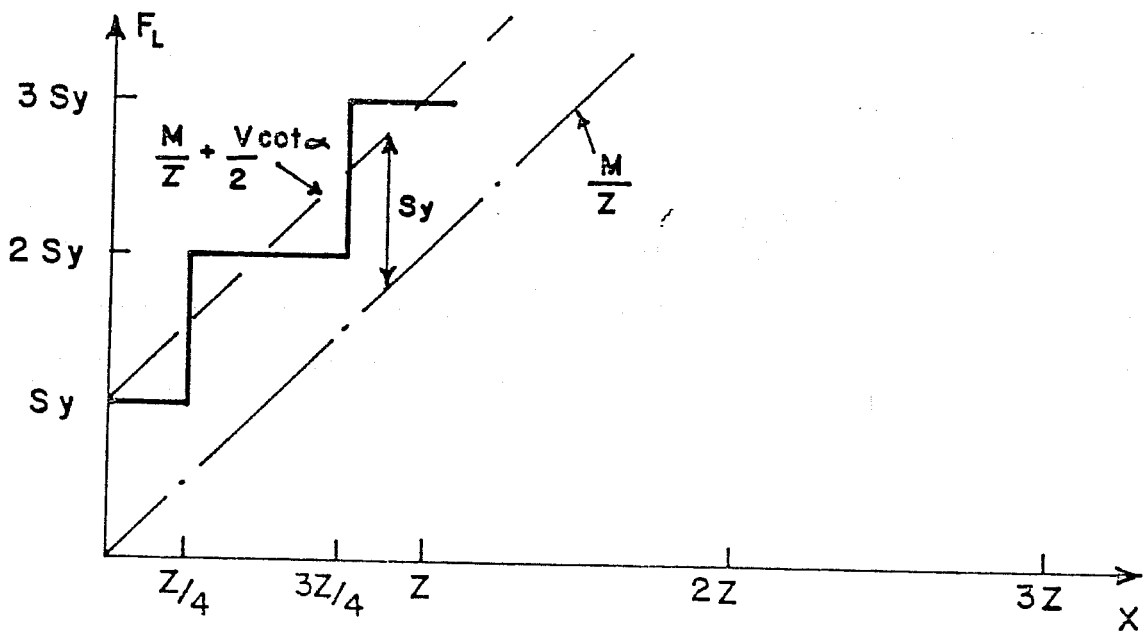
(b) Force in the lower chord

Fig. 2.5  Forces in the top and bottom chords of the truss model
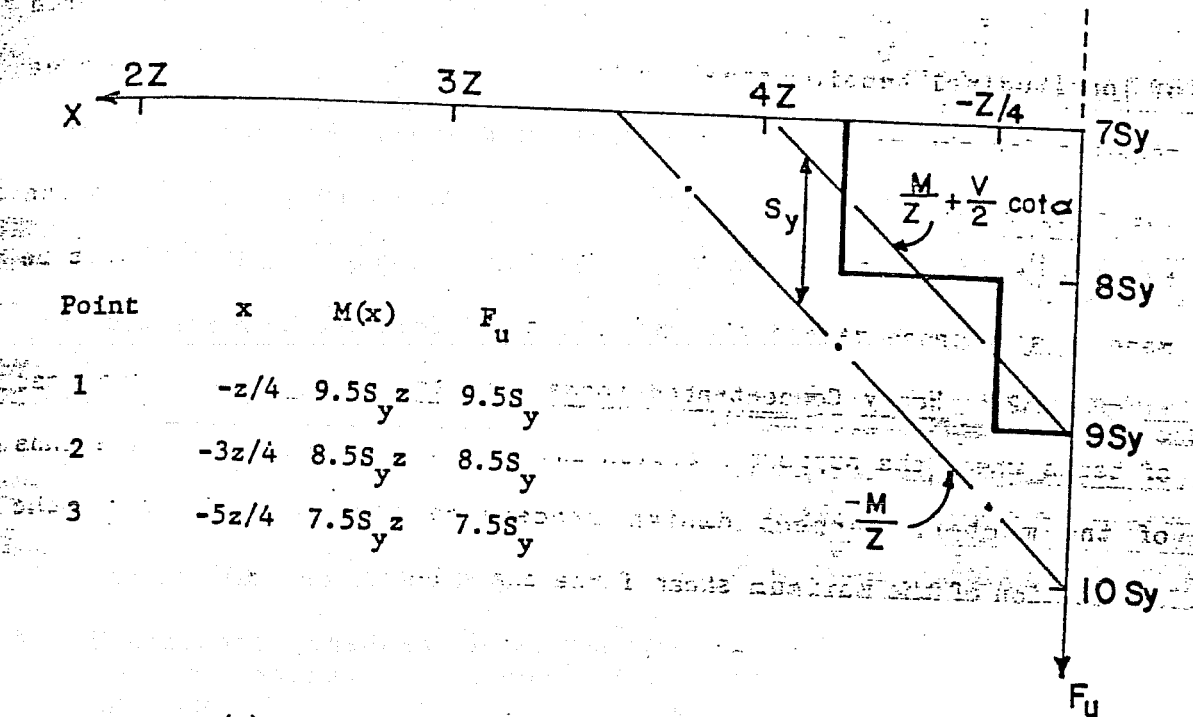
(a) Force in the upper chord (compression)

| Point | x | M(x) | $F_u$ |
|---|---|---|---|
| 1 | $-z/4$ | $9.5S_y z$ | $9.5S_y$ |
| 2 | $-3z/4$ | $8.5S_y z$ | $8.5S_y$ |
| 3 | $-5z/4$ | $7.5S_y z$ | $7.5S_y$ |
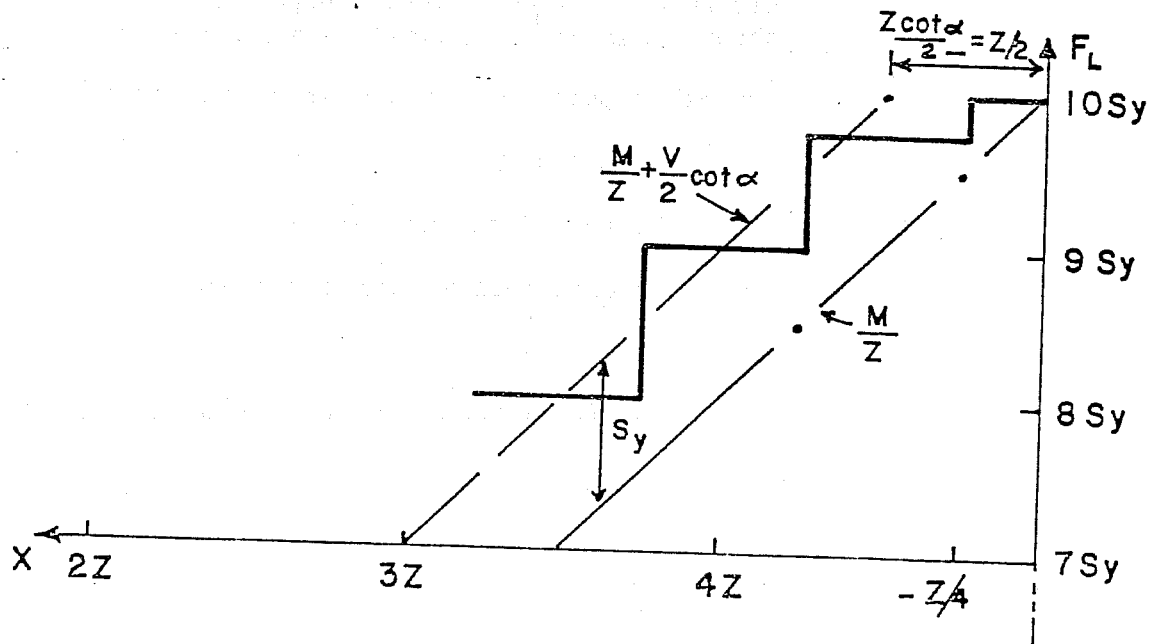
(b) Force in the lower chord (tension)

Fig. 2.7  Forces in the top and bottom chords of the truss model
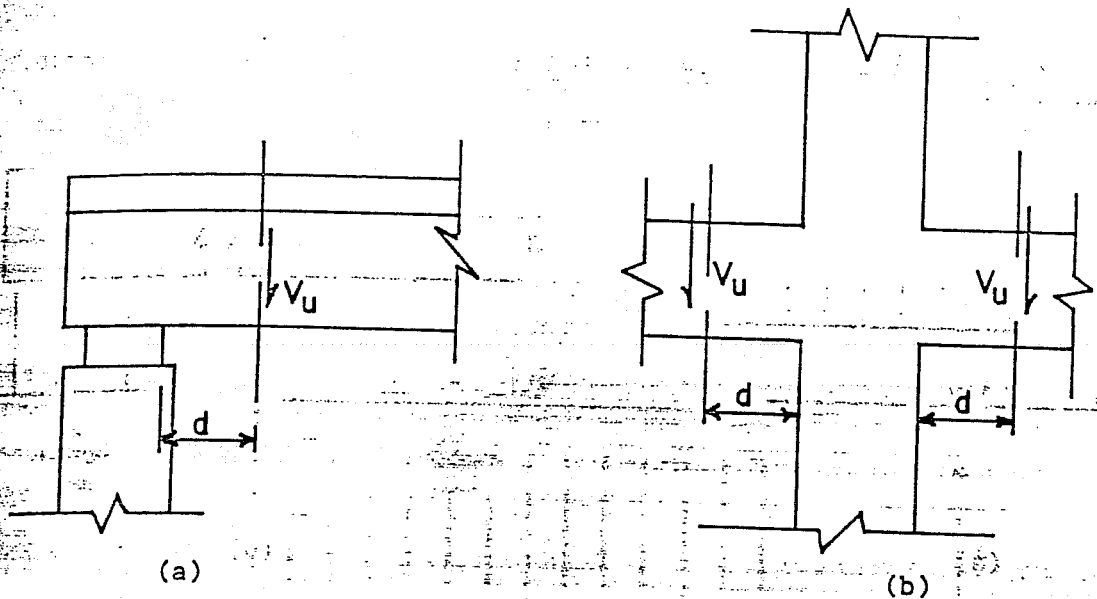
Fig. 2.8  Typical support conditions where the maximum design shear force is that computed at a distance "d" from the face of the support

However, this provision is not always valid. These are two major exceptions. The first one is the case when the support reaction does not induce a state of compression in the end region of the beam. Such is the case of members framing into a supporting member in tension, as seen in Fig. 2.9a. In that case the critical section for shear is taken at the face of the support.

The second major exception is in the case of members where the shear at section between the support and a distance "d" differs radically from the shear at a distance "d". This occurs in brackets, and in beams where a heavy concentrated load is located close to the support such as in bridge bent caps (see Fig. 2.9b). In these cases current shear design provisions recommend (17,24) that the actual shear at the face of the support should be used.

of the support it is recommended that the basic truss model be applied

consistently as recommended by Marti (183,184) as a more general check

than the usual shear friction theory.
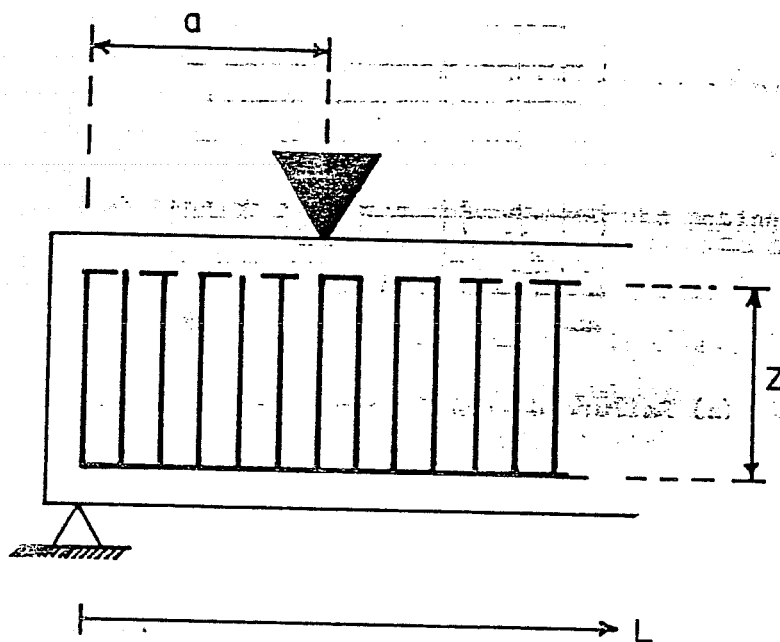


Fig. 2.10 Definition of a/z ratio

In general, tests of beams with a/z ratios less than 0.5 have

shown crack patterns at failure similar, to that shown in Fig. 2.11a.

The pattern of cracks at failure in Fig. 2.11a shows an inclination

which is very close to 90 degrees from the horizontal.  Normally,

therefore, vertical stirrups will not be effective.  However, in the

case of brackets and corbels (see Fig. 2.11b), shear would act along the

vertical plane of the crack.  Vertical slip of one crack face occurs

with respect to the other.  If the crack faces are rough and irregular,

this slip will be accompanied by a horizontal separation of the crack

faces.  Thus it is obvious that horizontal web reinforcement should be

provided (shear friction reinforcement). At ultimate, the horizontal crack separation will be sufficient to stress this reinforcement to its yield point.

Consequently, applying the previous discussion to Fig. 2.11a, it is reasonable to assume that the design of this type of member can be based on a simple truss analogy consisting of the main reinforcement acting as horizontal tension ties and concrete struts acting as inclined compression members. In this strut and tie system shear failure as such is not considered as a primary failure mode. The basic assumptions followed in the construction of this truss model are:

1. Equilibrium must be satisfied.

2. The concrete transmits only compression forces. The strength of the concrete in tension is neglected.

3. The reinforcement acts only as linear members, i.e. dowel effect is neglected.

4. Yielding of the reinforcement will take place at failure.

5. Well-distributed horizontal reinforcement should be placed across the potential length of the vertical cracks to control cracking at service load levels and to ensure the assumed redistribution of internal forces in the cracked state.

In the strut and tie system, provided the anchorage of the tie is adequate, eventual failure is caused either by yielding of the main steel, or by crushing of the concrete in the flexural compression zone or in the diagonal strut. Since brittle failures due to crushing of the concrete must be avoided, the stress in the flexural compression zone and in the diagonal strut should be kept below specified limits. In

In Fig. 2.12a, the case of a truss loaded on the top chord is analyzed and the force in the vertical tension member C is found to be 1.5P (tension). In Fig. 2.12b, the same truss is analyzed but the load is placed on the bottom chord. The tension force in the same member C becomes 2.5P (tension).

The increase in the tension force in the member C when the load is applied at the bottom chord reflects the so called "hanger effect".

The additional area of steel required in the vertical is that necessary to "hang up" the load P by transmitting it from the bottom face to the top of an effective compression strut in the member. For the case of members subjected to an uniformly distributed load w, the additional tension force in the vertical elements when the member is loaded at the bottom chord would be w*s, where "s" represents the spacing between the vertical elements in the truss model.

## 2.3 Compression Strength of the Diagonal Strut

The use of the truss model with variable angle of inclination of the diagonal struts in the design of reinforced and prestressed concrete members requires that the steel reinforcement yield prior to failure of the concrete in compression. Concrete failure can be due to crushing of the bending compression zone or the concrete compression diagonals.

The stresses in the bending compression zone can be determined using the well-known bending theory (135). They are limited by restricting the tensile reinforcement to a fraction of the amount which produces a balanced failure. In the case where torsion exists together with bending the situation is even less critical. Since a torsional

moment introduces longitudinal tension on all faces of the member, it will raise the neutral axis in the case of positive bending moment (tension at the bottom of the member), therefore reducing the compression stresses in the bending compression zone. The same holds true for the case of a negative bending moment (tension at the top) since now the torque will lower the neutral axis, hence reducing the stress in the bending compression zone. Thus, the restrictions on longitudinal reinforcement as a fraction of balanced reinforcement based on simultaneous yielding of the longitudinal steel and crushing of the concrete in the case of pure bending constitutes a safe lower bound for the case of combined torsion and bending.

The concrete compression diagonal struts carry the diagonal forces necessary for truss equilibrium. The stresses $f_d$ in the diagonal compression strut are caused by the diagonal force D. Consider the case of a shear field element subjected to a constant shear flow as shown in Fig. 2.13. From geometric considerations the stress in the diagonal strut caused by the diagonal force D is given by the relation:

$$f_d = \frac{q}{b_w \sin\alpha \cos\alpha} \tag{2.6}$$

where "q" is the shear flow due to shear or shear and torsion. Assuming a constant shear flow over the entire height of the section the term $q/b_w$ becomes the average shear stress "v". Rearranging Eq. 2.6 yields

$$\frac{f_d}{v} = \frac{1}{\sin\alpha \cos\alpha} \tag{2.7}$$

This relation represents the normalized compression stress in the diagonal strut as a function of the angle of inclination $\alpha$ of the strut.

It has been suggested (28,57,58,65) that the limiting value of the average principal compressive stress in the diagonal concrete strut is governed not so much by the compression strength of the uncracked portions of the strut but by the capacity of the interface shear transfer mechanisms, such as aggregate interlock, to transmit the require shear stress across previously existing cracks. When a crack is developed in a concrete mass the surfaces are usually rough and irregular. Movement is then restricted by the bearing and friction of the aggregate particles on the crack surface. Provided that restraint is available to prevent large increases in the crack width, substantial shear forces can be transmitted across the crack interface through the mechanism of aggregate interlock. The principal factors affecting the aggregate interlock are:

1. Quality of the concrete. Usually the top part of a member, because of the particle sedimentation and water gain under the coarse aggregate will contain weaker concrete.

2. The size of the crack width. Smaller crack widths lead to larger shear stresses, but also to more sudden failures.

Tests by T. Paulay and P. J. Loeber (32), in which the crack width increased proportionally with the applied load, verified that the stiffness of the aggregate interlock mechanism gradually decreased as the shear stress across the interface increased. In order for the aggregate interlock mechanism to remain effective, the crack width should be limited. For larger crack widths only limited transfer of shear forces across the crack interfaces is possible and, thus, no

Equations 2.10, for the case of yielding of the transverse reinforcement [$\varepsilon_s = \varepsilon_y$], and 2.11, when the longitudinal reinforcement yields [$\varepsilon_1 = \varepsilon_y$], are shown in Fig. 2.15.

From Fig. 2.15 it can be seen that, for an inclination of the compression diagonals of $\alpha = 45$ degrees, the crack parameter $\varepsilon_r$ and hence, the crack width becomes a minimum for yielding of both the longitudinal and stirrup reinforcement. A smaller angle $\alpha$ requires asymptotically increasing crack opening and stirrup strains to obtain yielding of the longitudinal reinforcement. An angle larger than 45 degrees will demand larger crack openings and longitudinal strains to obtain yielding of the transverse reinforcement. Therefore, the mean crack strain is largely dependent upon the angle of inclination of the diagonal compression strut. Since the aggregate interlock disintegrates with large crack widths, and the mechanism of shear transfer in the diagonally cracked concrete is largely dependent on the aggregate interlock, it is apparent that the maximum compressive stress that the diagonal strut can take will be a function of the angle $\alpha$.

Equation 2.7, which relates the stress in the diagonal compression strut and the angle of inclination $\alpha$ of this element, is plotted in Fig. 2.16.

From Fig. 2.16 it can be seen that the compression stress $f_d$ in the diagonal strut does not vary significantly within the limits of the angle $\alpha$ proposed in Report 248-2. The maximum difference from the minimum value at 45 degrees is only 25%. Thus, within the limits for the angle of inclination of the diagonal compression strut,
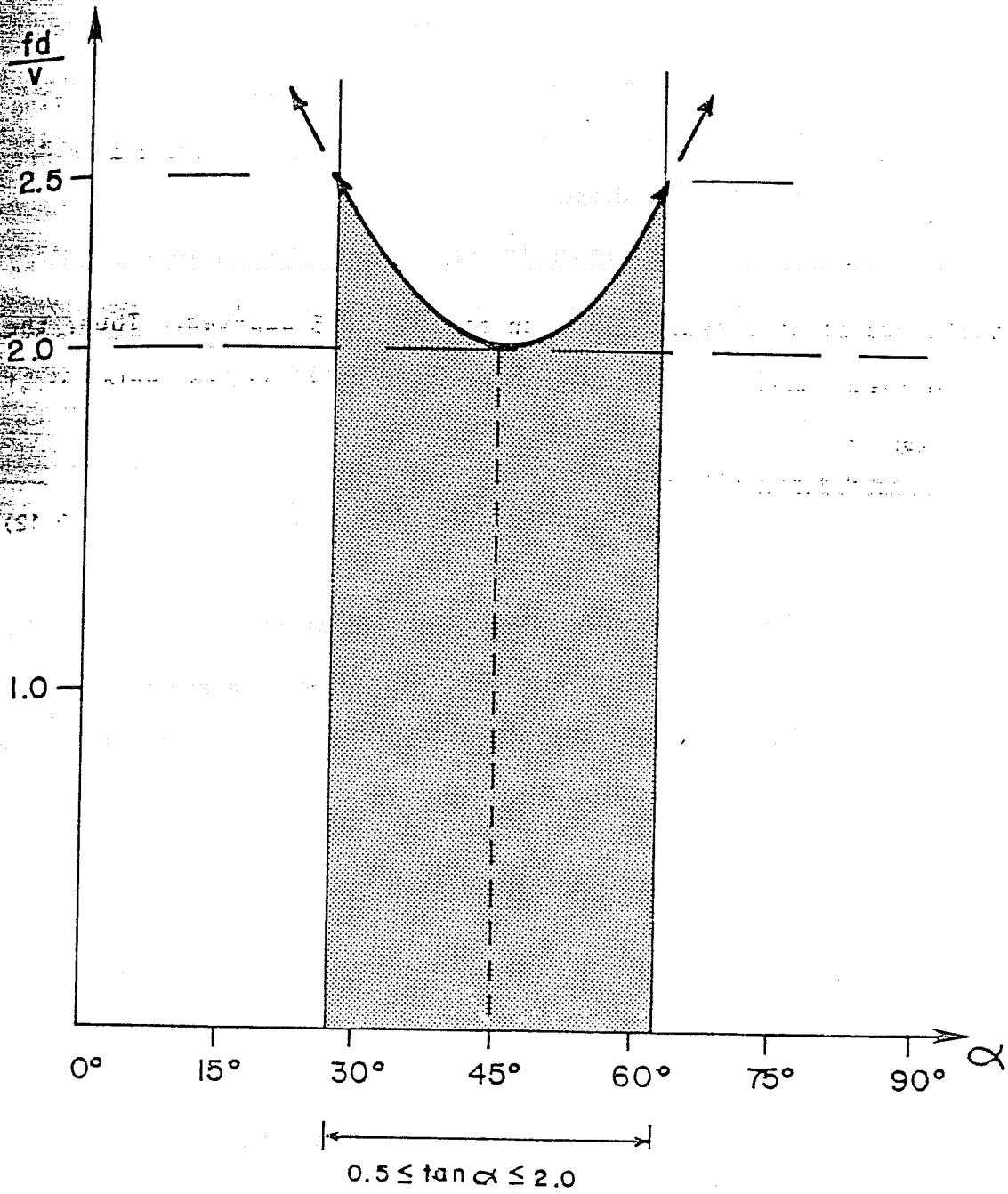
Fig. 2.16 Stress $f_d$ as a function of the angle

compression stress in the diagonal strut should be a function of the average principal compressive strain in the strut $\epsilon_d$, the ratio of the maximum shear strain $\gamma_m$ (i.e. the diameter of the strain circle), and the 28 day concrete compression strength $f_c'$ (see Fig. 2.17).

$$\gamma_m = \epsilon_L + \epsilon_s + 2\epsilon_d$$

$\epsilon_s$ = stirrup strain

$\epsilon_L$ = Longitudinal steel strain
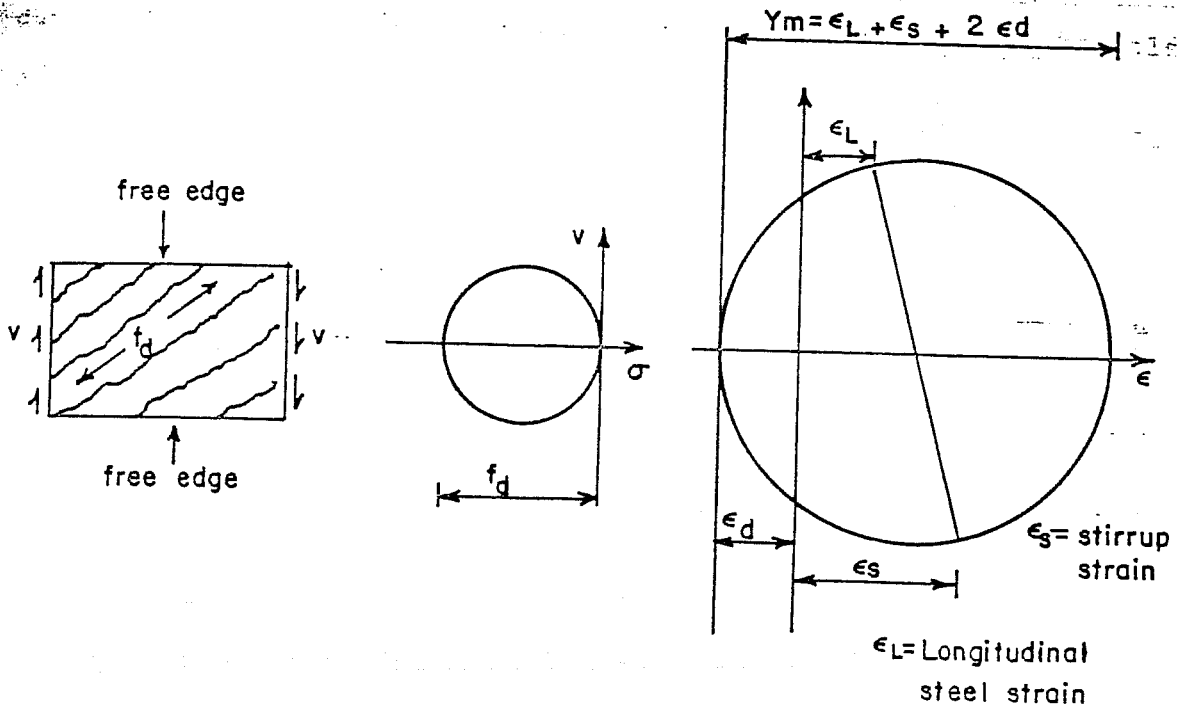
(a) Diagonally cracked concrete

(b) Stress circle

(c) Strain circle

Fig. 2.17  Stress and strain conditions for diagonally cracked concrete neglecting principal tensile stress

Thürlimann cites several factors which influence the value of $f_c$. Due to the fact that the stirrups across the diagonal tension cracked concrete are in tension, the diagonal concrete strut is then in a biaxial state of stress which reduces its compressive strength. Another factor is the redistribution of forces in the member due to the different ratios of longitudinal to transverse reinforcement which may cause the failure crack to be at an inclination other than the 45 degree angle corresponding to initial diagonal tension cracking of the concrete. Another important factor is the undesirability of a failure due to crushing of the concrete in the web because of its brittle nature.

Another factor considered was the fact that in the case of torsion the twisting of the beam induces an additional compression stress into the diagonal. Thürlimann and Lampert (95) stated that the increase in the diagonal compression stress was due to a distortional effect in the walls of the cross section. Through twisting, the originally plane walls of the section are distorted to hyperbolic paraboloids (Fig. 2.19) limited by four straight edges.

The distorted wall constitutes then a hyperbolic paraboloid shell subjected to a uniform shear flow "q". The entire shell when loaded in this fashion is subjected solely to pure shear stresses of constant intensity (see Fig. 2.20).

This state of pure shear, which actually resolves into principal stresses of equal and opposite magnitude (tension and compression) acting on sections at 45 degrees to the shear plane, can be deduced from

purely physical considerations without recourse to differential equations.
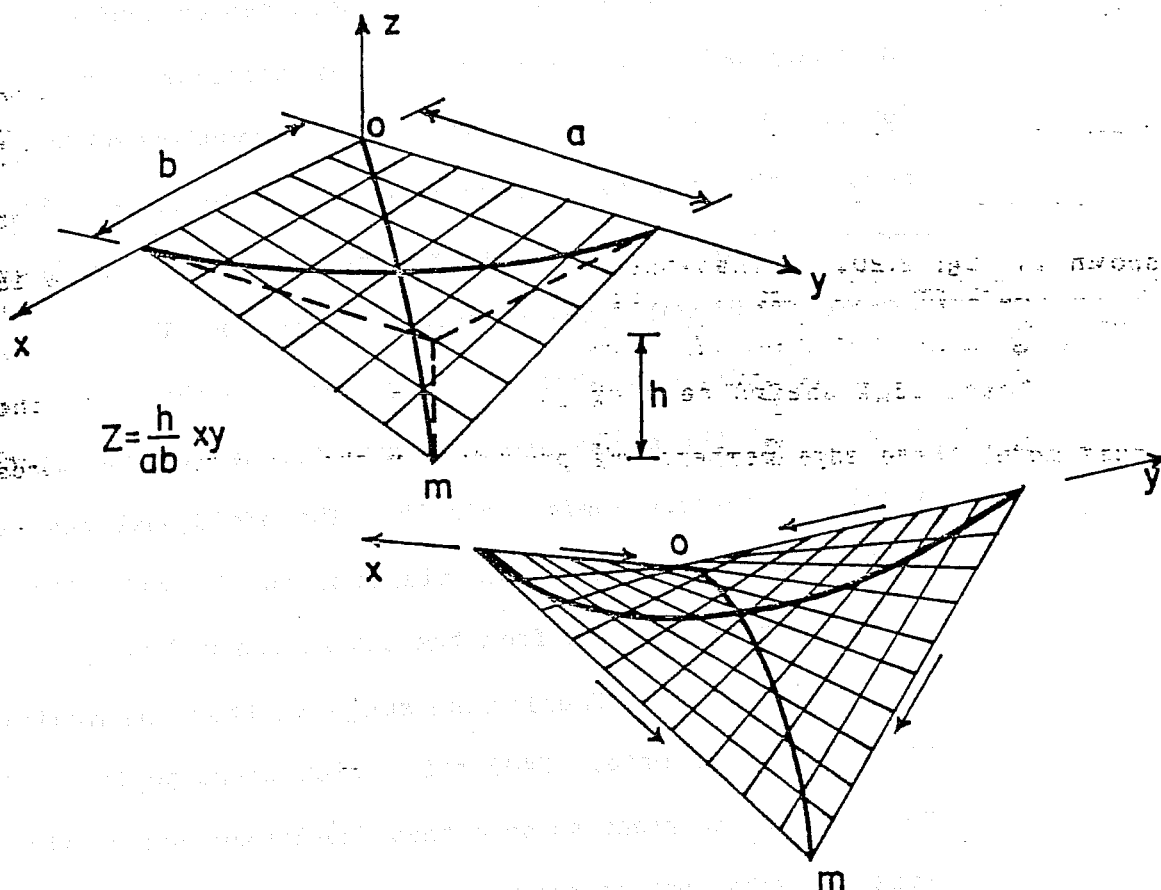
$$Z = \frac{h}{ab} xy$$

Fig. 2.21   Sections of a hyperbolic paraboloid surface taken
at 45 degrees to the coordinate axis

As shown in Fig. 2.21, sections of a hyperbolic paraboloid surface taken at 45 degrees to the coordinate axis form identical parabolic arches.   In other words, the surface shown in Fig. 2.21 can be obtained by moving a parabolic curve along curve o-m.   The parabolas parallel to the curve o-m curve downward, whereas those at right angles to these parabolas curve in the opposite direction.   Assuming that the
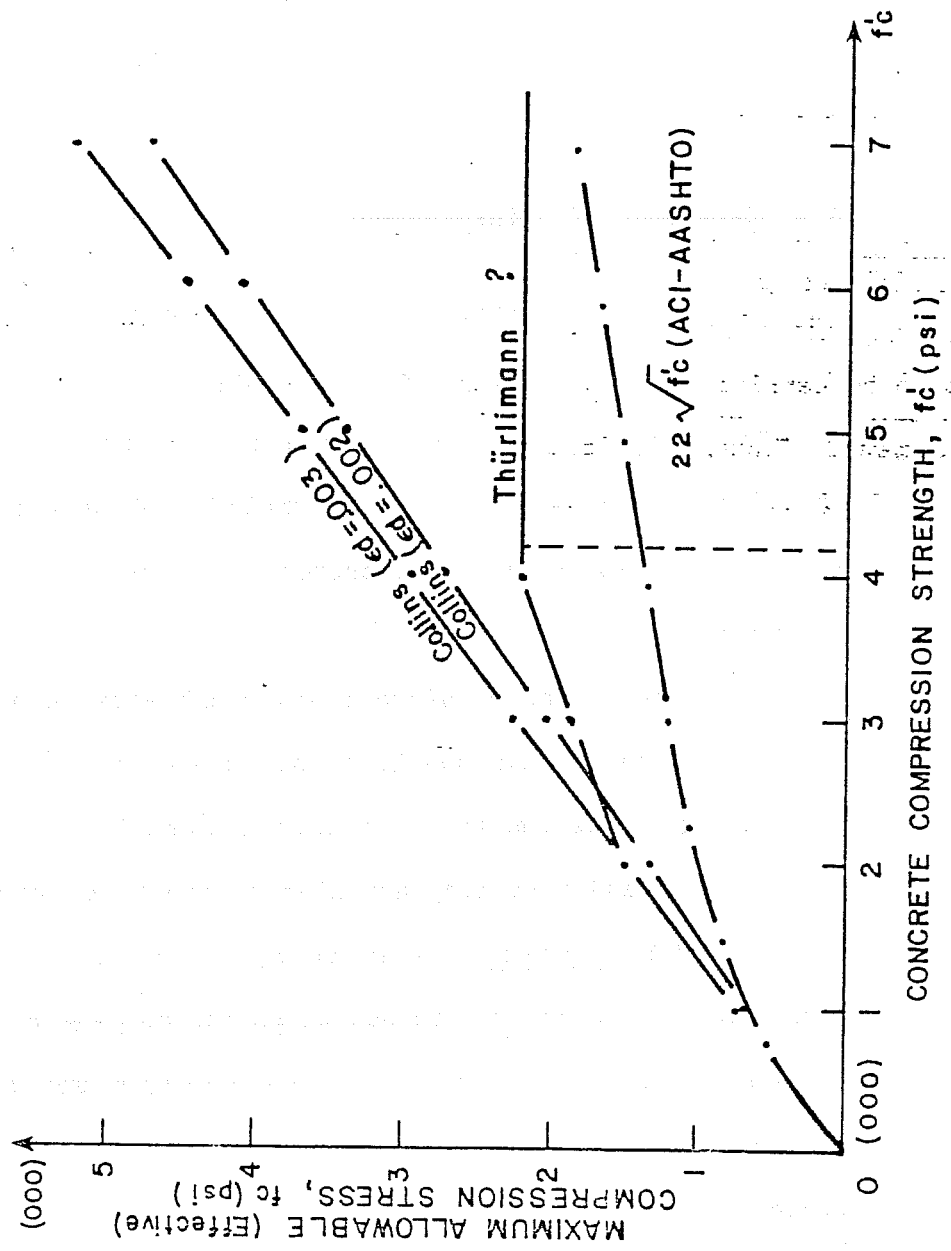
Fig. 2.22 Web crushing limits

equilibrium. It is primarily a strength problem because the structure, or its component, will collapse if the torsional resistance cannot be supplied.
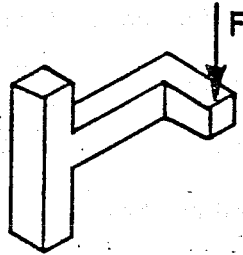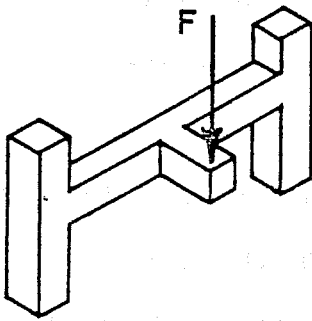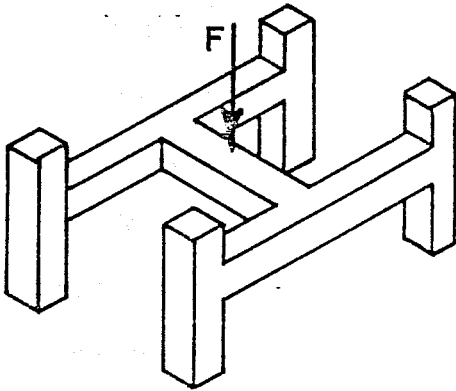
| | Equilibrium torsion | Compatibility torsion |
|---|---|---|
| Statically determinate structures |  | Impossible |
| Statically indeterminate structures |  |  |

Fig. 2.23 Torsion in statical systems

As shown in Fig. 2.23, in statically determinate structures only equilibrium torsion exists, while in indeterminate structures both types are possible. If equilibrium is possible in a system even if the torsional stiffness is neglected in the service load state or even if the torsional resistance is neglected in the ultimate state, then one is dealing with compatibility torsion. In this case torsional moments are developed by resistance to rotation and may be relieved when local

Specific guidelines to compute the minimum amount of torsional reinforcement that should be provided in the case of compatibility torsion are given in Report 248-4F.

This differentiation between equilibrium torsion and compatibility torsion is also required when properly detailing the reinforcement. In the case of compatibility torsion, the function of the reinforcement consists for the most part in providing crack control. Hence, the distribution is more important than the amount. The case of equilibrium torsion is different. Here the amount of reinforcement becomes equally as important as its distribution. When dealing with equilibrium torsion it is necessary to both provide enough reinforcement to resist the torsion required by statics and to properly detail of reinforcement to ensure that such strength can be fully developed.

In designing a member subjected to torsion, it is necessary in order to provide adequate crack control that the longitudinal steel be uniformly distributed around the perimeter of the cross section. The trusslike behavior of the member shows that the longitudinal steel in each corner of the section is anchoring the diagonal compression struts. If the reinforcement at the corners is too weak, a brittle premature failure will result from the bulging out of the corner bars (see Fig. 2.24). For this reason, ductility and strength requirements would be better served by concentrating a considerable amount of the required longitudinal steel for torsion at the corners of the cross section. However, a torsional moment causes a general lengthening of the member. Hence, longitudinal steel anywhere in the cross section can be effective
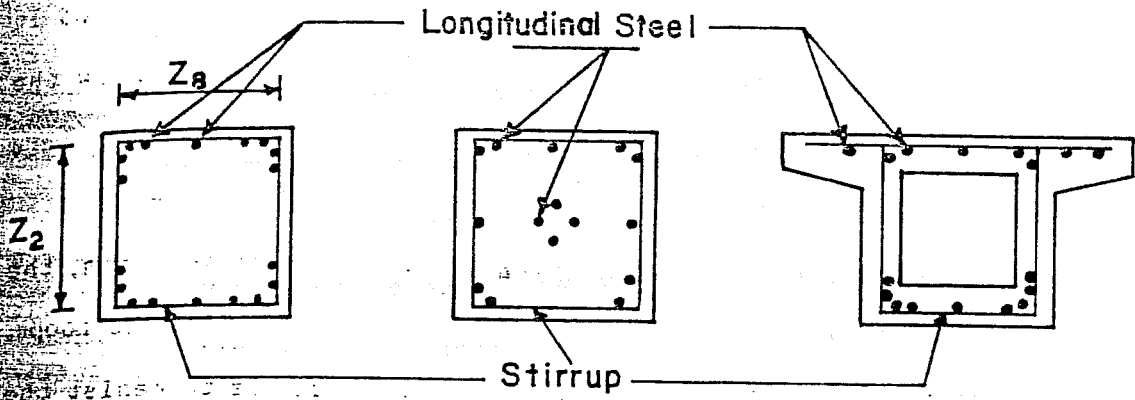
(a) Sections with same ultimate torque
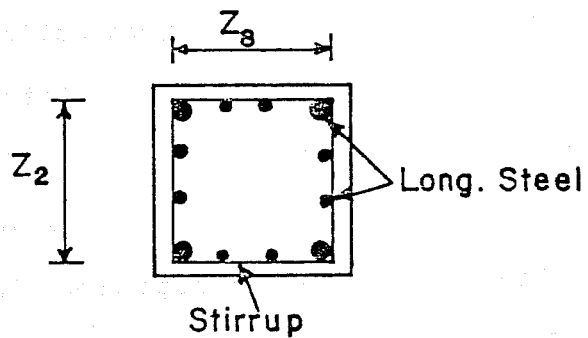


(b) Optimal distribution of longitudinal steel

Fig. 2.25   Distribution of the longitudinal steel

his
e of
d it
the
here

the
ops.
the
hey
see
ng
al
to
he
os
g.
t
e
t
m
e
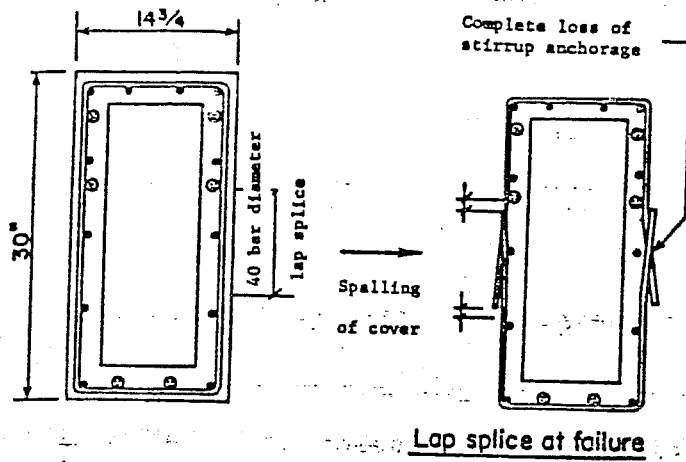


(a) Lap splice inadequate detail for torsion
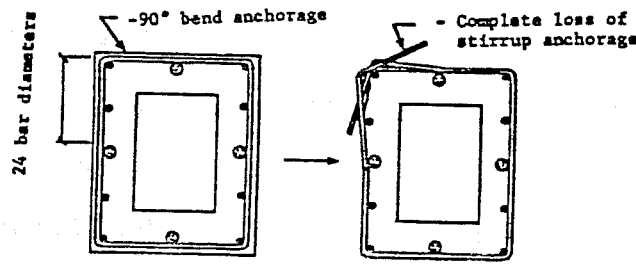
(b) 90 degree hook inadequate detail for torsion
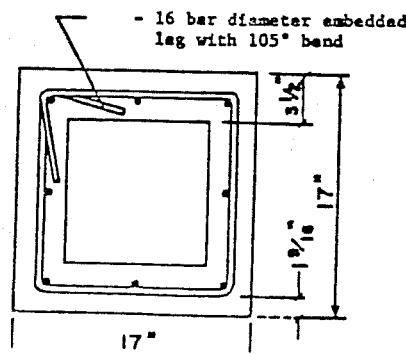
(c) Properly detailed transverse reinforcement

Fig. 2.26   Stirrup anchorage details [from Ref. 118]

Thus, it is suggested that when setting the maximum stirrup spacing the value of $\tan\alpha = 1.0$ be used regardless of the assumed angle of inclination at failure.

As a result, the maximum stirrup spacing for torsion is then $s_{max} \leq h_2/2$, which is similar to the limit proposed by Thürlimann of $h_2/2$ but less than 8". Therefore, it is felt that the use of Thürlimann's proposal is more practical and reasonable.

2.4.2 <u>Shear.</u> Detailing for shear strength requires that just as in the case of torsion, both the longitudinal and the transverse reinforcement must be properly anchored so as to allow the development of their full tensile strength. Required anchorage can be provided by means of adequate straight embedment length, standard hooks or even mechanical anchorage.

The function of all of the reinforcement has been nicely explained by Collins and Mitchell (56), and is fully illustrated in Fig. 2.27. From Fig. 2.27, it is apparent that the function of the longitudinal steel is to act as a tension chord as required for flexure and to balance the horizontal components of the diagonal compression struts. In addition, it must provide adequate end support for the stirrup reinforcement. In the truss model the longitudinal tension chords must tie the beam together along its longitudinal axis and be properly anchored at the ends.
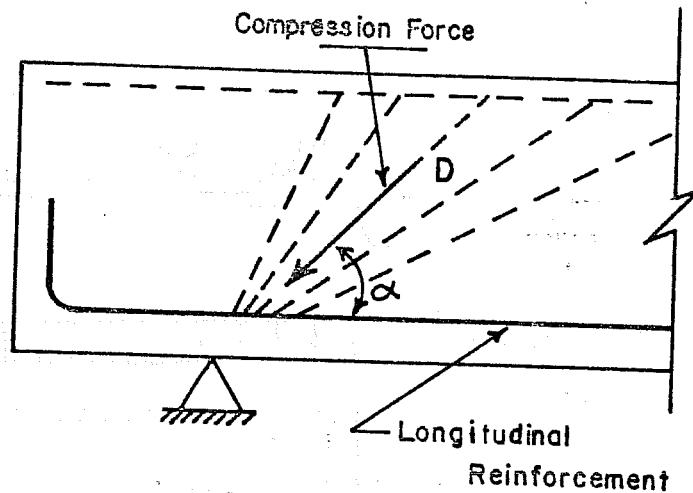
Fig. 2.28   Anchorage of reinforcement at support

the bottom (tension of flexure) chord requires an anchorage length such that a force equal to $V \cot\alpha/2$ is adequately developed (see Fig. 2.4b).

In a more physical sense, the concrete compression strut is "pushing" on the end of the beam, and the smaller the angle of inclination, the more anchorage force that would be required at the support.

(b) Curtailment of the longitudinal steel

Consider the case of curtailment of the longitudinal reinforcement (see Fig. 2.29a).  The question is how far should the longitudinal steel extend, distance $l_s$ beyond the point at which it is no longer required for flexure.  In Report 248-2 it was shown that the force in the lower tension chord is found as:

$$F_1 = (M/z) + [(V \cot\alpha)/2] \tag{2.16}$$

From Fig. 2.29b the step in the diagram due to the change in steel is given by:

$$L_{AB} \left(\frac{dF_L}{dx}\right) = \Delta A_L \, f_{yL} \tag{2.17}$$

and

$$\frac{dF_L}{dx} = \frac{d}{dx} \left(\frac{M}{2} + \frac{1}{2} V \cot\alpha\right) \tag{2.18}$$

Since the shear force V is constant and the angle of inclination of the diagonal compression strut is assumed constant in the design process Eq. 2.18 yields:

$$\frac{dF_L}{dx} = \frac{1}{z}\frac{dM}{dx} = \frac{V}{z} \tag{2.19}$$

Substituting in Eq. 2.17 yields:

$$L_{AB} = \Delta A_L \, f_{yL} \, z/V \tag{2.20}$$

thus, from Fig. 2.29b

$$L_s = L_a - L_{AB} = L_a - \frac{\Delta A_L * f_{yL} * z}{V} \tag{2.21}$$

This equation is also applicable when detailing positive moment tension reinforcement at points of inflection and simple supports. In the current ACI Code (24) a similar requirement is established for the adequate development of the positive moment tension reinforcement at simple supports and points of inflection. This reinforcement is limited to a diameter such that the development length, $l_d$, required to develop

Substituting in Eq. 2.17 yields

$$L_{AB} = \frac{\Delta A_L f_{yL}}{\frac{V}{z} + \frac{w}{2} \cot\alpha} \tag{2.26}$$

Thus from Fig. 2.29b

$$L_s = L_a - L_{AB} = L_a - \frac{\Delta A_L f_{yL}}{\frac{V}{z} + \frac{w}{2} \cot\alpha} \tag{2.27}$$

where $l_s$ represents the supplemental length required beyond the theoretical cut-off point.

## II) Transverse Reinforcement

The transverse reinforcement in the truss model provides, as shown in Fig. 2.27, the vertical tension ties to resist the vertical component of the diagonal compression struts. All stirrups must be properly anchored in the compression and tension zones of the member. The cracking of the concrete in the tension zone demands that the stirrup be continuous throughout this zone. No splicing of stirrups should be permitted.

Typical prestressed beam stirrup detailing as shown in Fig. 2.30a is not unadmissible. Such details are often used to simplify plant fabrication. The reason it should not be used is that the cracking of the concrete in the tension zone would destroy the bond between the concrete and the stirrups. This means that stirrup tension force could not be developed. Also, as shown in Fig. 2.27, the stirrups must provide effective reactions for the diagonal compression struts to bear against, both in the tension and compression zones. This detail

fails in both respects. A clear example of the type of failure this improper detailing can lead to is illustrated in Chapter 3 of this study in the section dealing with failures due to inadequate detailing.

For the same general reasons, detailing of stirrups such as the ones shown in Fig. 2.30b, is also undesirable. Figure 2.30c shows some examples of adequate detailing. From the study of members subjected to bending and shear using the truss analogy it is clear that the diagonal compression struts can only be anchored at the joints of the truss, i.e. intersection points between the transverse and the longitudinal reinforcement. The loads can only be transmitted at the joints of the truss because the members of a truss can only resist axial forces and their resistance to direct bending (i.e. loads applied to the member between the joints), or direct shear (dowel action) is almost negligible. For this reason, the stirrup which is the vertical tension member, must be able to develop its full strength over the entire height between the top and bottom joints of the truss. Hooks of the stirrups should be anchored around large longitudinal bars in order to distribute the concentrated force from the stirrups. A highly recommended practice would be to always bend stirrups around longitudinal bars, and terminate them only in the compression zone with at least a 135 degree hook at the ends.

In the detailing of transverse reinforcement it is also important to point out the width effect. This is important in the case of members having large web widths, and where more than two bars are used to resist flexure (see Fig. 2.31). In this case it is important to

like a deep beam, and its load-carrying capacity will be exhausted when the concrete fails near the bearing due to the concentration of the diagonal compression stresses. Based on this assumption and test results Leonhardt and Walther suggested that when large shear stresses exist in the member, the transverse spacing of stirrup legs should not exceed 7.5 in.. In the case of members with small nominal shear stresses it was suggested that the transverse spacing of stirrup legs can be made 15 in. or more but not exceed the effective depth, "d" of the member.

An upper limit on the maximum longitudinal stirrup spacing must be imposed to avoid the concentration of large compression forces at the joints between the stirrups and longitudinal chords and to ensure that all compression struts have effective reactions to bear against. The space truss model assumes a uniform distribution of the diagonal compression struts over the length of the beam. With large stirrup spacings these inclined struts react most effectively at the stirrup locations. These local concentrations may induce premature failures due to crushing of the diagonal strut or bulging out of the corner longitudinal bars.

The current ACI Building Code (24) and AASHTO Standard Specifications (12) require a maximum stirrup spacing for reinforced concrete beams of no more than d/2 or d/4 depending on the level of shear stress but in any case no more than 24 in. (d being the distance between the extreme compression fiber and the centroid of the tension reinforcement). In the case of prestressed concrete beams the stirrup

1.0 should be used when setting the maximum stirrup spacing. This yields a maximum stirrup spacing of z/2 which is similar to the one proposed in the Swiss Code (156). Since the maximum shear stress is limited to $15\sqrt{f_c'}$ in order to prevent diagonal crushing it seems reasonable to suggest a maximum stirrup spacing of $S_{max} \leq z/2$ but no more than 12 in.

## 2.5 Uncracked, Transition, and Full Truss States

In the behavior of reinforced and prestressed concrete beams subjected to shear or shear and torsion, as in the case of flexure, three well-defined failure states can be distinguished. The first is the uncracked state. This state is terminated in the case of shear by a shear failure when first inclined cracking of the web occurs. Then, there is a transition state for the section at which failure might be in between the uncracked state and its ultimate full truss state. While the member is in the transition state more cracking takes place and there is a redistribution of internal forces in the member. This redistribution of forces is possible due to the aggregate interlock forces and the concrete tensile strength. Failure occurs with the aggregate interlock and similar mechanisms supplementating the truss behavior. Lastly, a member may fail in the full truss state.

In the truss model, the inclination of the inclined compression strut is the inclination at ultimate and not first inclined cracking. The inclination at ultimate may coincide with the inclination at first inclined cracking but this does not necessarily have to be the case.

In terms of nominal shear stress v, which may be expressed as

$$v = q/b_w \qquad (2.29)$$

Hence, Eq. 2.28 becomes

$$v_{max} = f_{d\ max}/2 \qquad (2.30)$$

The nominal shear stress in the case of shear since $q(V) = V/z$ results in:

$$v = V/[z\ b_w] \qquad (2.31)$$

for the case of torsion since $q(T) = T/(2A_o)$ yields:

$$v = T/[2A_o\ b_w] \qquad (2.32)$$

From tests (48,95,96,101) and experience Thürlimann (162) suggests that for values of $v/v_{max}$ of less than approximately 1/6, a reinforced concrete section will remain uncracked. For a ratio greater than 1/6 and less than approximately 1/2, the section is in the transition state between uncracked and the full truss state. In this transition state the concrete tensile strength will provide a continuously diminishing additional shear strength (see Fig. 2.32).

For the values of $v/v_{max}$ between 1/2 and 1, the section is in the full truss state, where the total ultimate strength of the section is provided by the truss system.
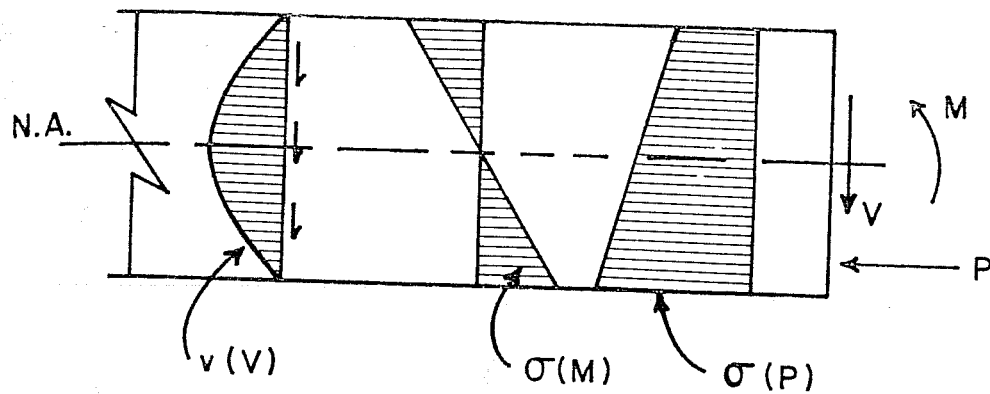
Fig. 2.33  State of stresses in an uncracked prestressed section

maximum tensile stress $\sigma_1$ equals the maximum applied shear stress $v$ being the radius of the Mohr circle.  In Fig. 2.34b, the Mohr circle corresponding to the state of stress shown in Fig.  2.33 for an element at the neutral axis is shown.  The principal tensile stress resulting in the section is smaller than the actual applied shear stress.  Thus, the load required to produce diagonal tension cracking in the member increases.  The resulting effect is that the uncracked state of the member is increased.  For this reason Thürlimann (162) suggests that an increase in the upper limit of the uncracked state from a value of $v/v_{max}$ of 1/6 to 1/3 should be considered for prestressed concrete.

The higher limit is also based on the observation of actual test beams and practical experience.

Therefore, the concrete contribution factor in the transition zone in the case of prestressed concrete members can be derived by

moving the limit of the uncracked state up to $v = 1/3\, v_{max}$ This results in a concrete contribution factor C.F equal to (see Fig. 2.32):

$$C.F. = 2 - 3\, v/v_{max} \geq 0 \tag{2.33}$$

Many times because of the design process followed, loading conditions, clear span length, or even architectural constraints, flexure will control the design of a given member. In such case the shear stress on the cross section, defined as $v_u = V_u/[b_w z]$ for shear, and $v_u = T_u/[2A_o b_e]$ for torsion, might be of such low magnitude that the member at failure as far as shear stresses are concerned would be in a transition state between its uncracked condition and the behavioral state where the truss action would provide the entire resistance of the member. Moreover, the limits previously proposed for the inclination of the diagonal strut, and in particular the lower limit of 26 degrees, which is established in order to prevent extensive web cracking under service load conditions, might sometimes force a member into this transition state.

For members in the transition state, components of the shear failure mechanism, such as aggregate interlock, and the concrete tensile strength, become of importance. The contribution of these mechanisms to the ultimate strength of the member is reflected in the additional concrete contribution to the shear and/or torsional capacity of the member in this transition state, and as such should be considered in the actual design process.

Since the core offers no contribution to the torsional strength, and, in the cracked state the outer concrete shell may eventually spall off, it is reasonable to consider an effective web thickness "$b_e$" to determine the concrete stresses in the diagonal strut. Based on experimental evidence Thurlimann and Lampert (93) proposed that the thickness of this effective web should be taken as the smaller of the two values:

$$b_e = d/6 \quad \text{or} \quad b_e = d_o/5 \tag{2.34}$$

where "d" is the diameter of the largest inscribed circle in the cross section and $d_o$ is the diameter of the circle inscribed in the largest area enclosed by the centroids of the longitudinal chords in the cross section (see Fig. 2.35). More recent studies provide detailed information of $b_e$ (56,180).
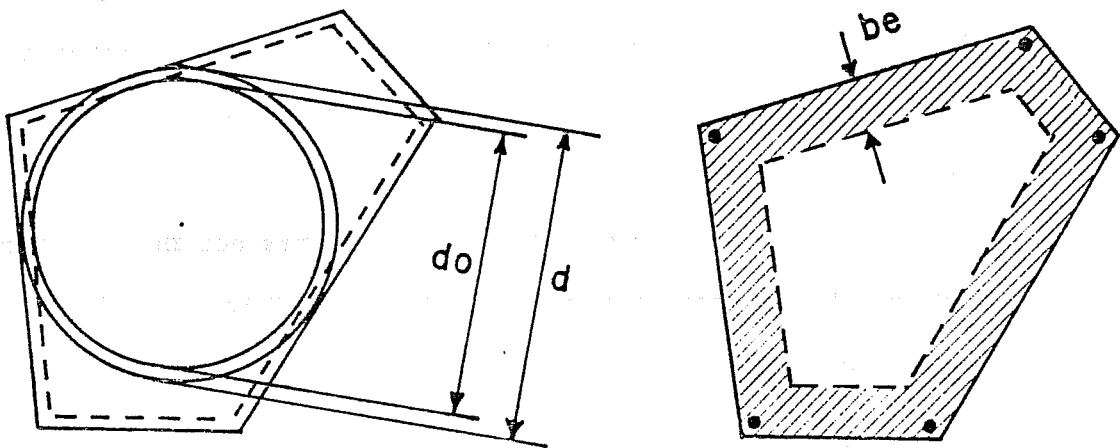


Fig. 2.35  Effective web thickness for solid cross sections

review, Campbell and Batchelor, based on tests of I-beams with thin webs conducted by Chitnuyanondh (47), proposed that when the truss model with variable angle of inclination is used in the design, the effective web width of the members may be computed using the following relations:

$$b_e = b_w - 0.75d_d \tag{2.35}$$

for an ungrouted duct, and

$$b_e = b_w - 0.33d_d \tag{2.36}$$

for a grouted tendon. In Eqs. 2.35 and 2.36, $d_d$ represents the diameter of the duct. These equations were derived from tests on beams containing a single duct in the web and with a $d_d/b_w$ ratio of 0.46.

Leonhardt (100) suggested that if multiple ducts having a diameter $d_d$ greater than 1/10 of the web width are located in the web, then the effective web width "$b_e$" should be taken as:

$$b_e = b_w - \Sigma d_d \tag{2.37}$$

for ungrouted ducts, and

$$b_e = b_w - 0.67 \Sigma d_d \tag{2.38}$$

for the case of grouted ducts. These equations may be applied when more than one duct is located at the same level in a web as indicated by the summation sign. Smaller values for the web width are obtained when these relations are used instead of Eqs. 2.35 and 2.36 as should be

If all the cross sections in a member subjected to twisting are free to warp (unrestrained torsion), the longitudinal elements (lines) of the surface of the twisted member remain practically straight lines with negligible change in their lengths, unless the angle of twist per unit lange is very large and the cross sections are unusually extended. Hence, longitudinal stresses may usually be neglected. As a consequence, it is reasonable to assume that a torsional moment in this case produces pure shearing stresses distributed over the ends as well as all other cross sections of the member. In the use of the truss model as a design procedure, this type of torsion is referred to as circulatory torsion. When this type of torsion exists, the cross section of the member can be replaced by corresponding hollow sections using the truss model. The resultant shear stresses will then generate a uniform shear flow around the perimeter of the cross section.

If, however, any cross section of the member subjected to a torsional moment is held rigidly (see Fig. 2.36) and, as a consequence, the warpage is restrained (restrained torsion), then the longitudinal elements of the surface become curved with marked changes in their lengths. The resulting longitudinal stresses in the outer elements of the flanges are not negligible. The torsional moment T is transmitted along the member near the free end mainly by torsional shearing stresses (see Fig. 2.36c). However, near the fixed end the torsional moment is transmitted mainly by the lateral shearing forces V (see Fig. 2.36a) which accompany the lateral bending of the flanges. At intermediate sections (see Fig. 2.36b), the torsional moment will be transmitted by a

(a) Closed box section



(b) Nonwarping sections
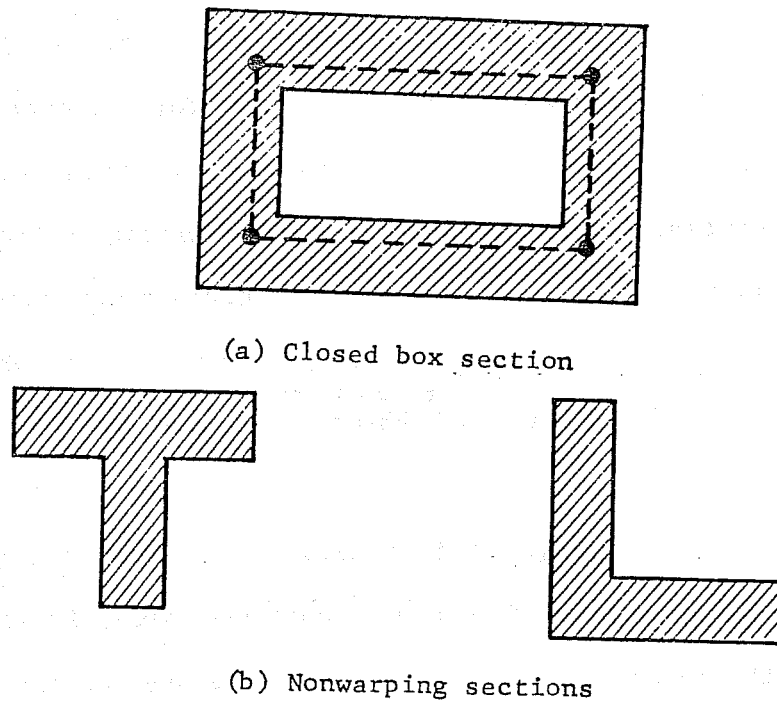
Fig. 2.37  Sections not influenced by the restraining effect
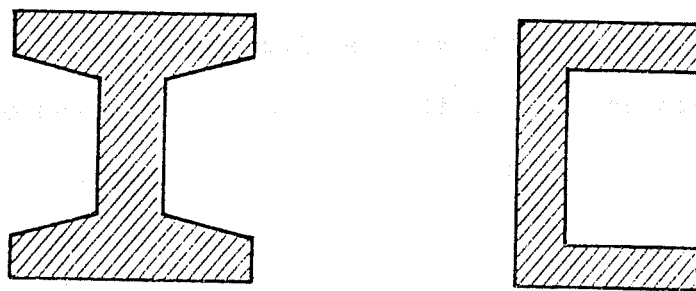


Fig. 2.38  Sections influenced by the restraining effect

and $\epsilon_d$ = diagonal compressive strain. This geometric relation is presented as the compatibility equation assuming coinciding principal stress and strain axes in the cracked concrete. It relates the strains in the concrete diagonals, the longitudinal steel, the transverse steel, and the angle of inclination of the diagonal compression strut. However, this equation is not valid in the case of combined actions.

In Chapter 3 the ultimate load predictions based on the truss model are also evaluated using test results of beams where the warping torsion effects are of significance.

2.6.3 Strand Draping. In general, it is considered that draping of the prestressing tendons will produce an upward vertical component which will counteract the downward shear force acting on a section (see Fig. 2.39).



Geometrc:

$$V_{ps} = f_{pse} A_{psd} \sin\theta$$

$f_{pse}$: Effective prestressing stress after losses

$A_{psd}$: Area of prestress draped strands

$V_{ps}$ : Upward vertical component of the prestressing force
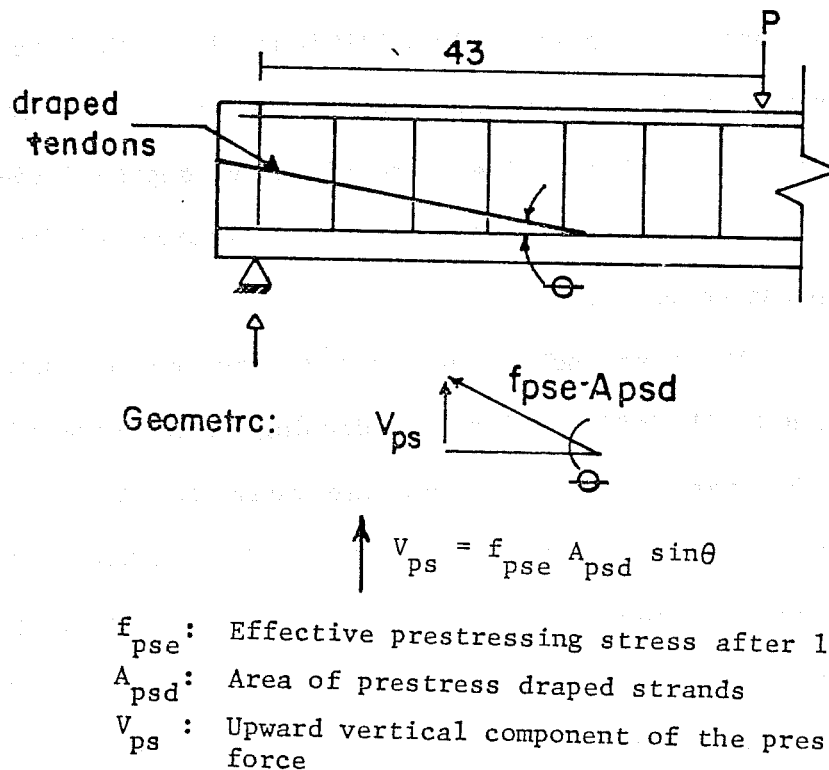
Fig. 2.39 Strand draping effect

Fig. 2.40. Due to the inclination of the tendons, the section shown in Fig. 2.40 undergoes a twist. The tangential components of the forces in the tendons then help to resist the applied torque.
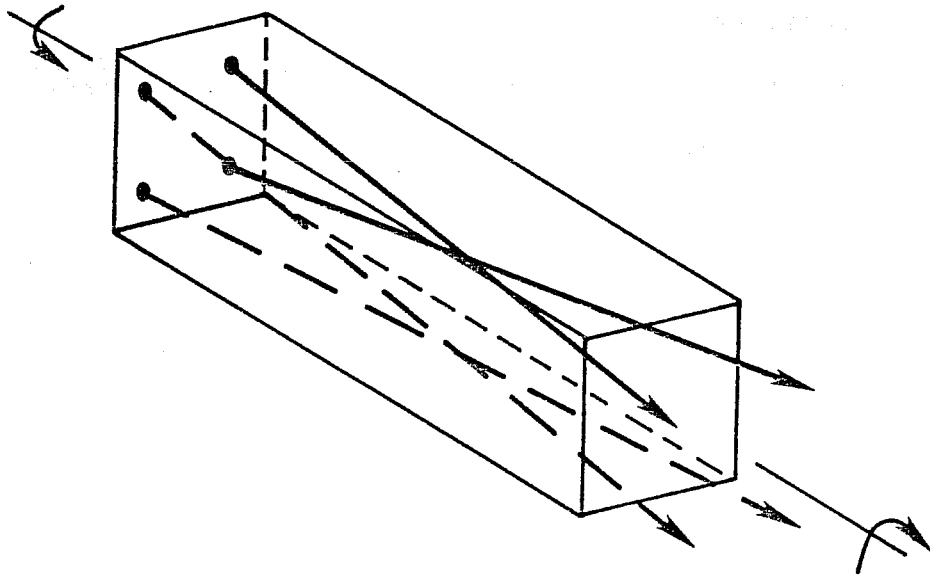
Fig. 2.40 Prestressed beam with inclined tendons in the case of torsion

However, in view of the lack of test data in this area, it is recommended that at least the area of longitudinal steel required from equilibrium consideration in the truss model to take care of the torsional and shear stresses, as derived in Report 248-2, should remain straight throughout the entire length of the member to provide effective truss action and prevent premature failures.

# CHAPTER 3

## EXPERIMENTAL VERIFICATION OF THE SPACE TRUSS MODEL

### 3.1 Introduction

Before the generalized variable inclination truss model approach is adopted as the basis of a design procedure in American practice, a complete evaluation of the accuracy of the model is necessary. Such an evaluation should check the accuracy of this model using a significant body of the available test data reported in the American literature which has formed the basis for current procedures. This model should be shown accurate and safe in comparison with such data. This chapter details the results of such an evaluation.

Using both tests reported in the literature and test results from beams tested in this program, truss model predicted ultimate values are compared with test results.

Since the truss model is to be proposed only for the design of underreinforced sections, a differentiation is made in the analysis of the test results. The specimens in which the reinforcement yielded at failure are differentiated from those in which yielding of the reinforcement was not reached or where failure was due to poor detailing. In the section dealing with the strength of the diagonal compression strut the results of beams where web crushing was observed at failure are used to propose web crushing limits.

Tests reported by Hsu (82) on reinforced concrete rectangular beams.

| (1) Member ID | (2) r | (3) Tu(Eq.3.1) (K-in) | (4) Ttest (K-in) | (5) $\alpha$(Eq.3.2) (degrees) | (6) Level of Prestress $\frac{\sigma}{f'c}$ | (7) $\frac{Ttest}{Tu(theory)}\frac{(4)}{(3)}$ |
|---|---|---|---|---|---|---|
| B1 | 1.0 | 174.0 | 197 | 45 | 0 | 1.13 |
| B2 | 1.0 | 250.0 | 259.0 | 44 | 0 | 1.04 |
| B3 | 1.0 | 354.0 | 332.0 | 43 | 0 | 0.94 |
| B4 | 1.0 | 473.0 | 419.0 | 43 | 0 | 0.89 |
| B9 | 1.0 | 250.0 | 264.0 | 34 | 0 | 1.06 |
| M1 | 1.0 | 222.0 | 269.0 | 39 | 0 | 1.21 |
| M2 | 1.0 | 313.0 | 359.0 | 39 | 0 | 1.15 |
| I2 | 1.0 | 272.0 | 319.0 | 45 | 0 | 1.17 |
| I3 | 1.0 | 370.0 | 404.0 | 43 | 0 | 1.09 |
| I4 | 1.0 | 471.0 | 514.0 | 44 | 0 | 1.09 |
| I5 | 1.0 | 602.0 | 626.0 | 44 | 0 | 1.04 |
| J2 | 1.0 | 266.0 | 258.0 | 45 | 0 | 0.97 |
| G2 | 1.0 | 299.0 | 357.0 | 44 | 0 | 1.19 |
| G4 | 1.0 | 537.0 | 574.0 | 43 | 0 | 1.07 |
| G6 | 1.0 | 317.0 | 346.0 | 45 | 0 | 1.09 |
| G7 | 1.0 | 441.0 | 406.0 | 44 | 0 | 1.06 |
| G8 | 1.0 | 602.0 | 650.0 | 44 | 0 | 1.08 |
| N1 | 1.0 | 86.0 | 81.0 | 49 | 0 | 0.94 |
| N2 | 1.0 | 137.0 | 128.0 | 49 | 0 | 0.93 |
| N3 | 1.0 | 129.0 | 108.0 | 49 | 0 | 0.84 |
| K1 | 1.0 | 101.0 | 136.0 | 44 | 0 | 1.35 |
| K2 | 1.0 | 168.0 | 210.0 | 44 | 0 | 1.25 |
| K3 | 1.0 | 219.0 | 252.0 | 43 | 0 | 1.15 |

*Note: Specimens B5,B6,B7,B8,B10,D1,D2,D3 D4,M3,M4,M5,M6,I6,J1,J3,J4,G1,G3, G5,N1a,N2a,N4,K4,C1,C2,C3,C4,C5, and C6 are reported in Secs.3.6 and 3.7

$\overline{x}$ = 1.07

S = 0.12

Table 3.1  Data for reinforced concrete rectangular beams

The value of "r" represents the ratio of the yield force of the top chord to the yield force of the bottom chord. The level of prestress is defined as the ratio between the average effective prestress in the cross section $[f_{se}*A_{pse}]/[A_{gross}*f'_c]$, where $f_{se}$ is the effective prestress force in the strand or wire, $A_{pse}$ is the total area of prestressing steel, $A_{gross}$ represents the total cross-sectional area of the member, and $f'_c$ is the concrete compressive strength.

In Fig. 3.1, a comparison between the test observed values and the predicted truss values for the data in Tables 3.1 and 3.2 is shown. As can be seen from this figure the truss model adequately predicts the ultimate strength in the case of pure torsion, provided that failures due to poor detailing or crushing of the concrete are prevented. The mean for all test prediction values is 1.07 with a standard deviation of 0.15.

In Sec. 2.6.2, the effect of the cross-sectional shape on the torsional ultimate strength was discussed. As long as the cross section is free to warp or the cross-sectional shape is nonwarpable such as in the case of rectagular, T, or L sections, the restraining effect will be of no significance.

Table 3.3 and Fig. 3.2 give a comparison between the ultimate test values for reinforced concrete L-sections. Again, there is a substantial agreement between test and theory, although the mean for all test/prediction values is 1.14 with a standard deviation of 0.17. These values are higher than those for rectangular sections as might be expected.

Tests reported by Liao and Ferguson (104) on reinforced concrete L-beams

| (1) Member ID | (2) r | (3) Tu(Eq.3.1) (in.-kip) | (4) Ttest (in-KIP) | (5) α(Eq.3.2) (degrees) | (6) Level of Prestress | (7) $\frac{\sigma}{f'c}$ $\frac{Ttest\ (4)}{T(theory)(3)}$ |
|---|---|---|---|---|---|---|
| PT-1 | 1.0 | 10.7 | 9.8 | 9 | 0 | 0.92 |
| PT-2 | 1.0 | 17.8 | 17.1 | 16 | 0 | 0.96 |
| PT-7 | 1.0 | 10.7 | 11.9 | 31 | 0 | 1.11 |
| PT-8 | 1.0 | 17.9 | 18.4 | 16 | 0 | 1.03 |

Tests reported by Rajagopalan and Ferguson (140) on reinforced concrete L-beams

| (1) Member ID | (2) r | (3) Tu(Eq.3.1) (in-KIP) | (4) Ttest (in-KIP) | (5) α(Eq.3.2) (degrees) | (6) Level of Prestress | (7) $\frac{\sigma}{f'c}$ $\frac{Ttest\ (4)}{T(theory)(3)}$ |
|---|---|---|---|---|---|---|
| R-7 | 1.0 | 11.2 | 13.5 | 18 | 0 | 1.21 |
| R-8 | 1.0 | 8.1 | 11.2 | 12 | 0 | 1.38 |
| R-17 | 1.0 | 23.5 | 27.7 | 24 | 0 | 1.18 |
| R-19 | 1.0 | 16.7 | 22.5 | 17 | 0 | 1.35 |
| | | | | | X = | 1.14 |
| | | | | | S = | 0.17 |

Table 3.3   Test data of reinforced concrete L-beams
subjected to restrained torsion

Table 3.4 and Fig. 3.3 give a comparison between the ultimate test values and the truss model predictions for prestressed concrete beams subjected to pure torsion. The data presented include tests performed on both hollow and solid rectangular sections in addition to inverted T-beam bent caps.

From Table 3.4 and Fig. 3.3, it is apparent that the truss model adequately predicts the ultimate strength of both solid and hollow prestressed concrete members as long as yielding of the transverse and the longitudinal reinforcement at ultimate is ensured by designing underreinforced sections and avoiding premature failures due to poor detailing. The mean for all test predicted values is 1.01 with a standard deviation of 0.16.

The consequences of restraining the torsional warping of the cross section in the case of sections influenced by the restraining effect such as I-beams, is illustrated in Table 3.5 and Fig. 3.4. The results of tests on reinforced and prestressed concrete I-beams subjected to pure torsion presented in Table 3.5, are compared with the ultimate value predicted by the truss model. In this case, the mean for all test predicted values is 1.5 with a standard deviation of 0.68. From Fig. 3.4, it is apparent that the truss model tends to give more conservative estimates of the actual ultimate capacity of these members than for unrestrained warping cases. However, for the case of low values of the angle $\alpha$ (15 degrees to 30 degrees), and provided yielding of the stirrups and the longitudinal steel takes place at failure, it shows good agreement with the actual test values.
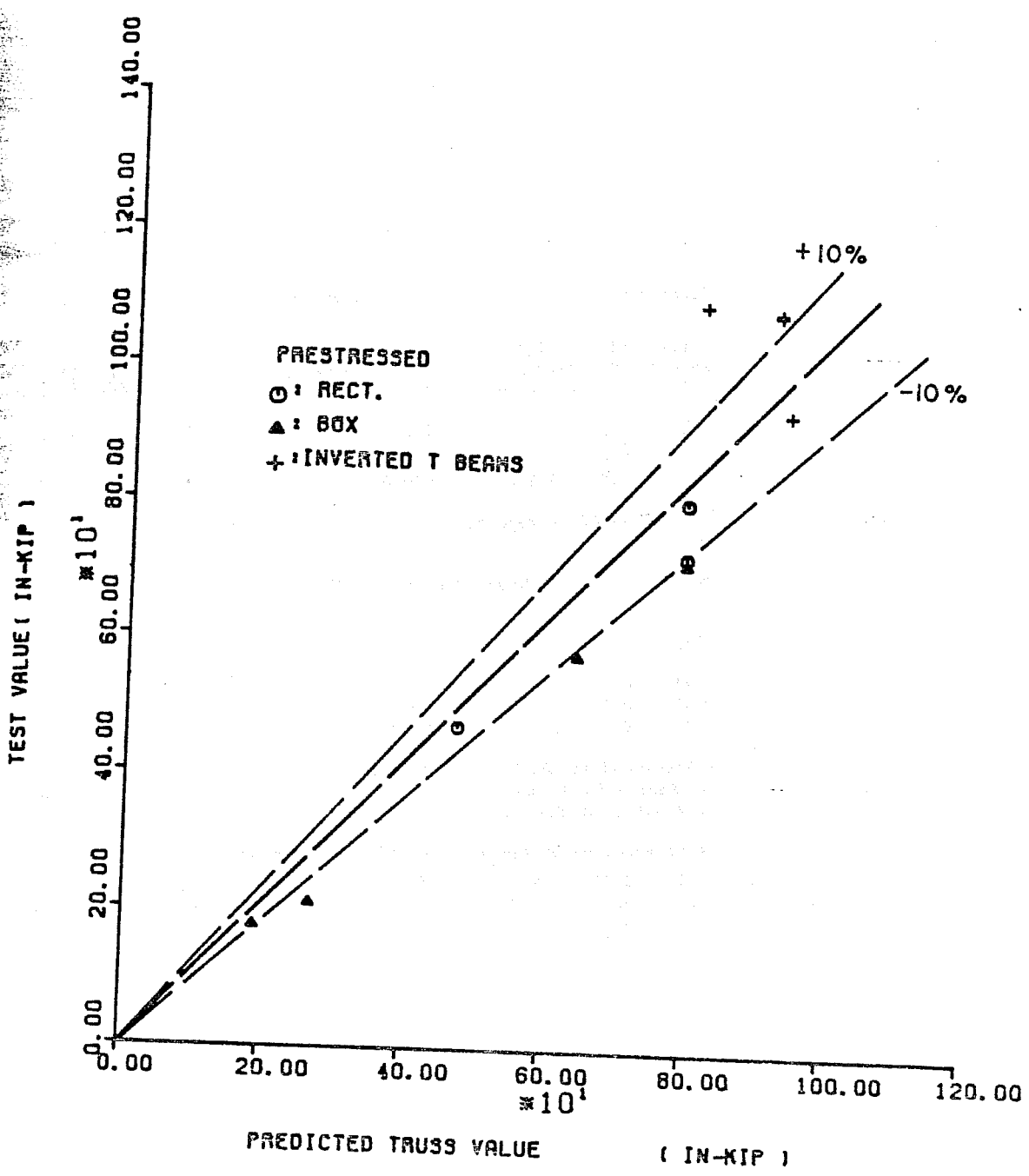
Fig. 3.3   The truss model in the case of prestressed concrete members
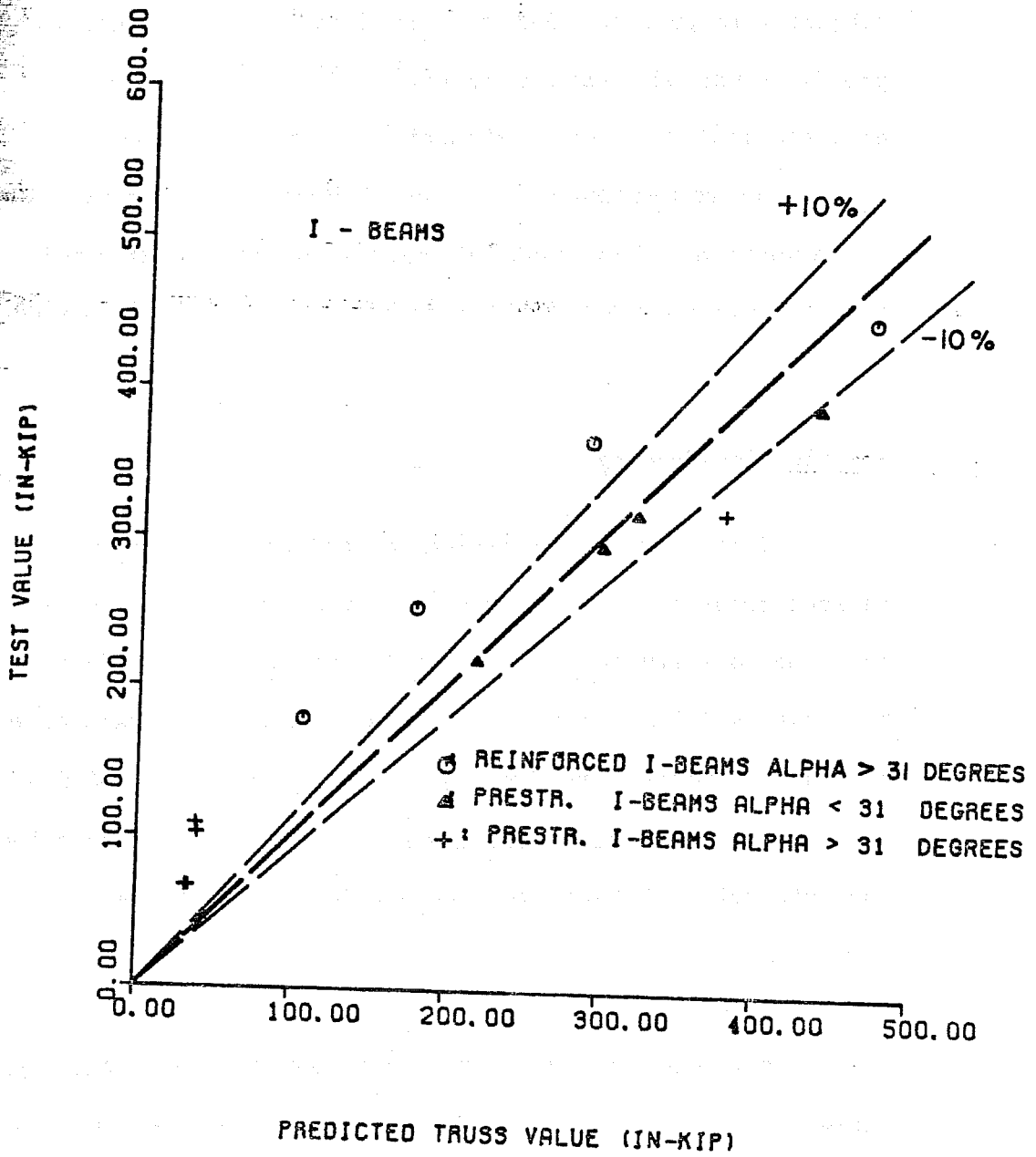
Fig. 3.4  Comparison between test values and truss model
prediction in the case of pure torsion in
I-beams where warping of the cross section is
restrained

$T_u$ and $M_u$ are the ultimate load combinations of torsional and bending moments, "r" is the ratio of the longitudinal reinforcement $F_{yu}/F_{yl}$, where $F_{yu}$ represents the total tension force $A_{yu}*f_y$ provided by the longitudinal reinforcement at the side of the member where the applied bending moment induces compression, and $F_{yl}$ is the total tension force $A_{yl}*f_y$ provided by the longitudinal reinforcement at the side of the member where the applied bending moment induces tension. $T_{uo}$ represents the ultimate torsional capacity of the section, when the applied bending moment $M_u$ is zero. (See Eq. 3.33 of Report 248-2.)

$$T_{uo} = 2 A_0 \left[\frac{R_{ymin}}{u} \frac{S_y}{s}\right]^{0.5} \tag{3.4}$$

$M_{uo}$ is the ultimate bending strength of the section, when the applied torsional moment $T_u$ is zero.

$$M_{uo} = F_{yL}*z \tag{3.5}$$

The derivation and the terms in Eqs. 3.4 and 3.5 have been fully explained in Report 248-2. (See Eqs. 3.33 and 3.48 of Report 248-2.)

Equation 3.6 (see Eq. 3.56 of Report 248-2) represents the interaction between bending and torsion at ultimate, when yielding of the longitudinal reinforcement takes place at the side of the member where the applied bending moment induces compression.

$$1 = \left(\frac{T_u}{T_{uo}}\right)^2 - \left(\frac{M_u}{M_{uo}}\right) \frac{1}{r} \tag{3.6}$$

Tests reported by Gesund, Schuette, Buchanan and Gray (70)

| (1) Member ID | (2) r | (3) $\dfrac{M_{test}}{M_{uo}}$ | (4) $\dfrac{T_{test}}{T_{uo}}$ | (5) Level of Prestress $\sigma/f'$ | (6) I | (7) Failure mode |
|---|---|---|---|---|---|---|
| 2 | 0.7 | 0.50 | 0.77 | 0 | 0.94 | Yielding of |
| 3 | 0.7 | 0.60 | 0.50 | 0 | 0.81 | |
| 4 | 0.7 | 0.70 | 0.50 | 0 | 0.90 | |
| 5 | 0.7 | 0.80 | 0.60 | 0 | 1.04 | longitudinal |
| 6 | 0.7 | 0.90 | 0.40 | 0 | 1.01 | |
| 7 | 0.7 | 0.90 | 0.20 | 0 | 0.93 | |
| 8 | 0.7 | 0.92 | 0.30 | 0 | 0.98 | and transverse |
| 9 | 0.7 | 0.40 | 1.15 | 0 | 1.18 | |
| 10 | 0.7 | 0.60 | 0.80 | 0 | 1.03 | |
| 11 | 0.7 | 0.40 | 0.90 | 0 | 0.98 | reinforcement |
| 12 | 0.7 | 0.70 | 0.70 | 0 | 1.03 | |

* Specimen 1 is reported
  in Sec. 3.7

$X = 0.98$
$S = 0.09$

Table 3.6  Data on reinforced concrete rectangular
beams with r = 0.7
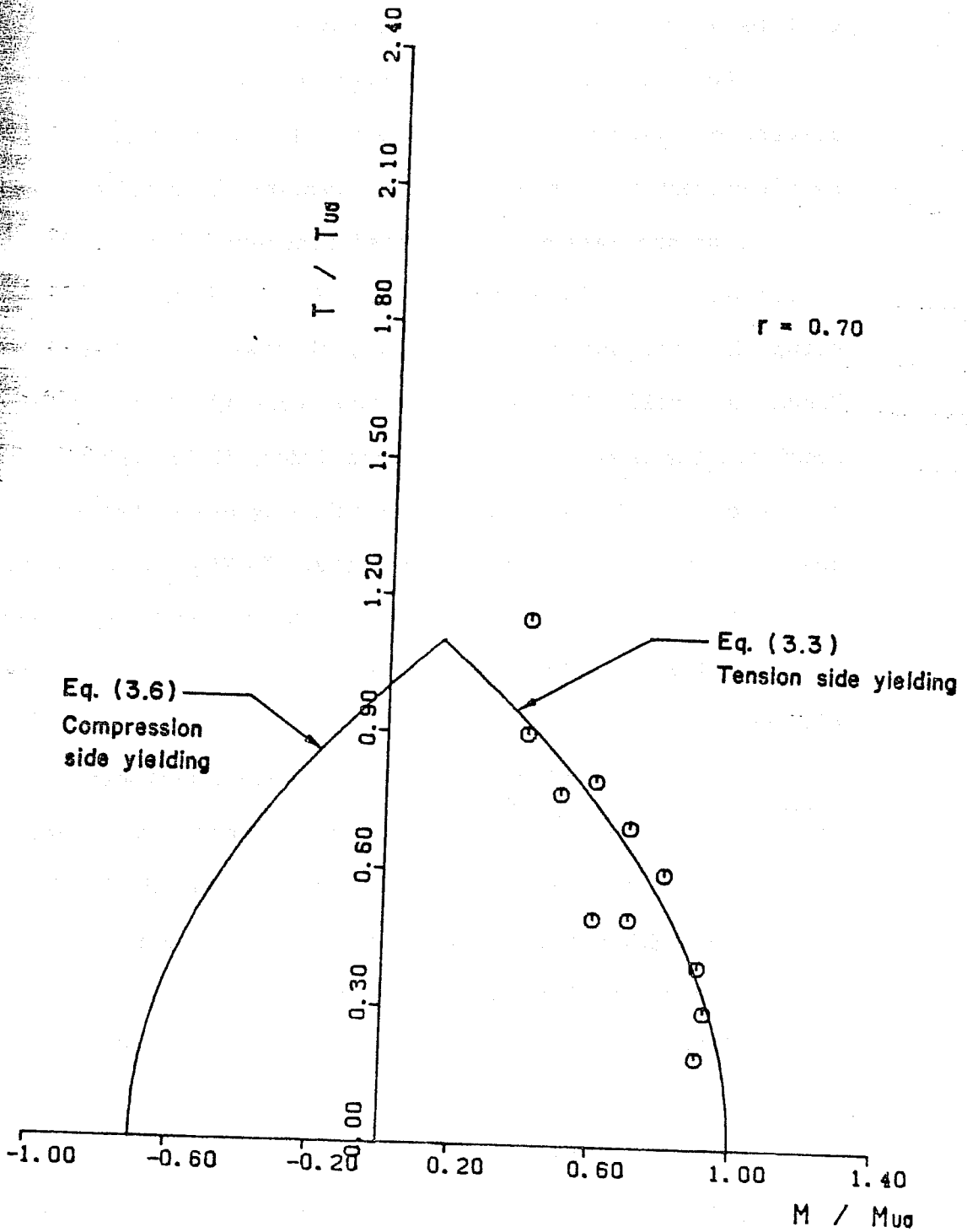
Fig. 3.6   Torque-bending interaction diagram for rectangular reinforced concrete beams with r = 0.7

Tests reported by Rangan and Hall (144) on Prestressed concrete box beams

| (1) Member ID | (2) r | (3) $\dfrac{Mtest}{Muo}$ | (4) $\dfrac{Ttest}{Tuo}$ | (5) Level of Prestress $\sigma/f'c$ | (6) I | (7) Failure Mode |
|---|---|---|---|---|---|---|
| A1 | 0.33 | 1.16 | 0.92 | 0.03 | 1.36 | |
| A2 | 0.33 | 0.88 | 0.94 | 0.04 | 1.14 | |
| A3 | 0.33 | 0.82 | 1.08 | 0.04 | 1.15 | Yielding of |
| A4 | 0.33 | 0.74 | 1.18 | 0.04 | 1.14 | |
| A5 | 0.33 | 0.60 | 1.29 | 0.03 | 1.10 | |
| B1 | 0.33 | 1.14 | 0.90 | 0.04 | 1.34 | the bottom |
| B2 | 0.33 | 0.86 | 0.90 | 0.04 | 1.10 | |
| B3 | 0.33 | 0.74 | 1.00 | 0.04 | 1.05 | longitudinal |
| B4 | 0.33 | 0.70 | 1.10 | 0.04 | 1.07 | |
| B5 | 0.33 | 0.55 | 1.18 | 0.05 | 1.01 | |
| C1 | 0.33 | 1.11 | 0.88 | 0.05 | 1.31 | and stirrup |
| C2 | 0.33 | 0.84 | 0.89 | 0.05 | 1.08 | |
| C3 | 0.33 | 0.72 | 1.15 | 0.05 | 1.11 | reinforcement |
| C4 | 0.33 | 0.67 | 1.06 | 0.05 | 1.03 | |
| C5 | 0.33 | 0.52 | 1.10 | 0.05 | 0.94 | |

$X = 1.13$
$S = 0.12$

Table 3.7  Data for prestressed concrete box beams
with $r = 0.33$

Tests reported by Pandit and Warwaruk (33) on reinforced concrete
beams of rectangular cross section

| (1) Member ID | (2) r | (3) $\dfrac{Mtest}{Muo}$ | (4) $\dfrac{Ttest}{Tuo}$ | (5) Level of Prestress $\sigma / f'_c$ | (6) I | (7) Type of failure |
|---|---|---|---|---|---|---|
| E1 | 1.0 | 0.86 | 0.67 | 0 | 1.23 | Yielding of the bottom |
| E2 | 1.0 | 0.48 | 0.89 | 0 | 1.16 | longitudinal and stirrup reinforcement |

* Specimens B2,B3,C1 and C2
  are reported in Table 3.9;D1,D2,
  D3 are reported in Sec. 3.7.

X = 1.20
S = 0.05

Tests reported by Mitchell and Collins (56) on prestressed concrete
box beams

| TB1 | 1.0 | 0.40 | 1.16 | 0.19 | 1.38 | Yielding of the |
|---|---|---|---|---|---|---|
| TB2 | 1.0 | 0.70 | 1.01 | 0.17 | 1.42 | bottom longitudinal |
| TB3 | 1.0 | 0.98 | 0.55 | 0.23 | 1.23 | and stirrups |

X = 1.34
S = 0.10

Overall X = 1.28
S = 0.11

Table 3.8   Test data on reinforced and prestressed concrete
beams with r = 1.0

tests on reinforced concrete beams of solid rectangular cross section, and prestressed concrete box beams, all with ratio of longitudinal steel "r" of 0.50.

In Fig. 3.9 the test data shown in Table 3.9 are compared with the truss model ultimate load interaction between torsion and bending. In this case the mean of the dispersion index is 1.06 and the standard deviation 0.09. Again, the truss model predictions seem to be in reasonable and generally conservative agreement with observed test values.

The versatility of the truss model allows the analysis of the interaction between torsion and bending in members with complex cross sections. Figure 3.10 shows the results presented in Table 3.10 for a series of tests conducted by Taylor and Warwaruk (161) on prestressed concrete double celled box beams with a longitudinal ratio "r" of 0.25. For these specimens, the mean of the dispersion index is 1.32 and the standard deviation 0.16.

As shown in Fig. 3.10, the truss model ultimate load interaction equations conservatively and adequately predict the ultimate load capacity in combined torsion and bending of such members.

The evaluation of the truss model in the case of reinforced and prestressed concrete members subjected to combined torsion and bending shows that the model can safely predict the ultimate load capacity of such members, as long as yielding of the longitudinal and transverse reinforcement is insured by designing underreinforced sections, and premature failures due to poor detailing are avoided.
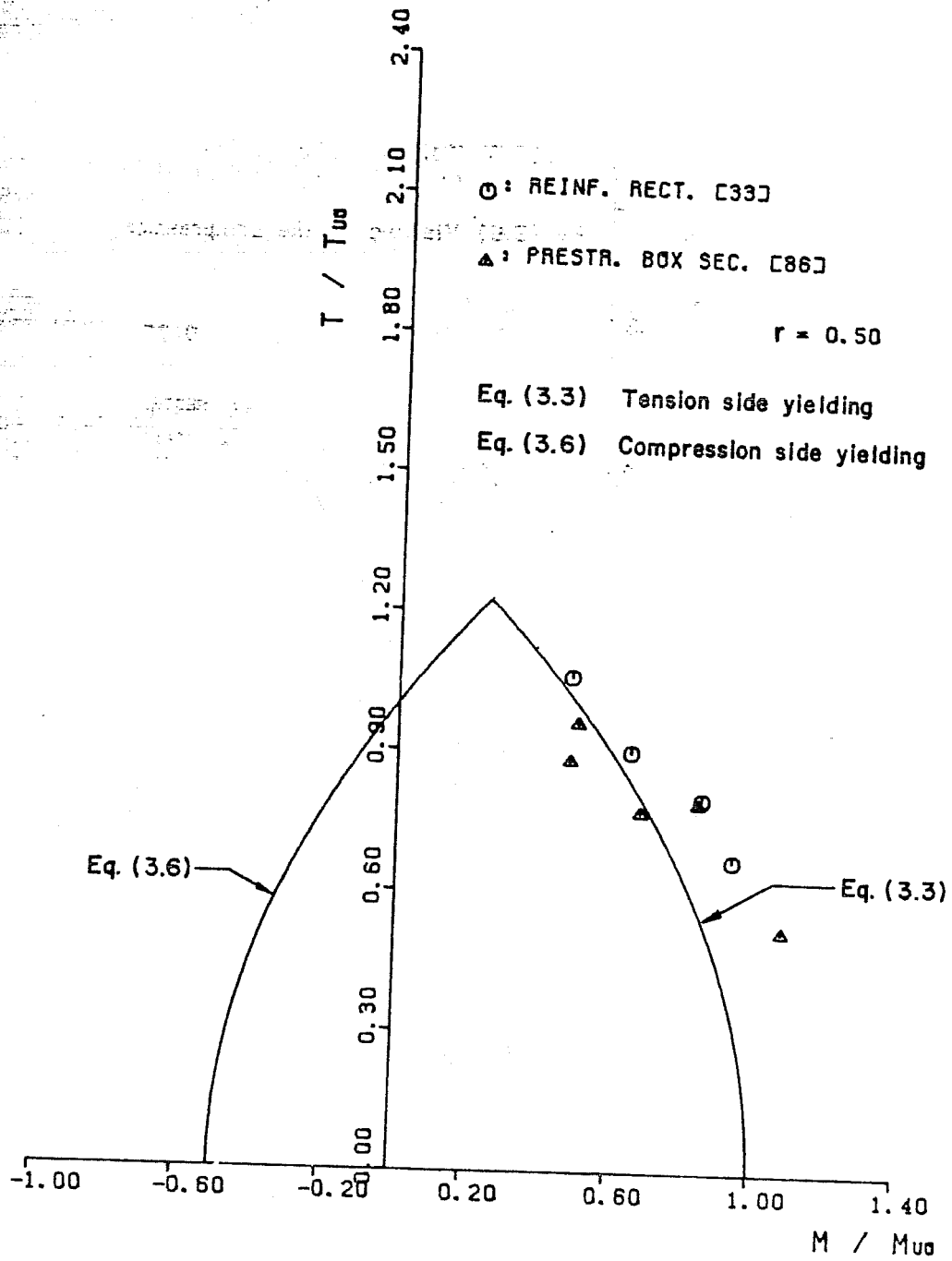
Fig. 3.9   Evaluation of the truss model predictions in
           the case of members of various cross sections

Tests reported by Warwaruk and Taylor (161) on Prestressed concrete
2 cell box beams

| Member ID | r | $\frac{Mtest}{Muo}$ (in-Kip) | $\frac{Ttest}{Tuo}$ (in-kip) | Level of prestress $\sigma/f'c$ | I | Type of failure |
|---|---|---|---|---|---|---|
| R1 | 0.24 | 1.11 | 1.28 | 0.07 | 1.39 | Yielding of the |
| R2 | 0.24 | 1.13 | 0.92 | 0.07 | 1.44 | stirrups and bottom |
| R5 | 0.24 | 0.66 | 1.50 | 0.07 | 1.14 | longitudinal steel |

* Specimens T1,T2 are reported    X = 1.32
  in Sec. 3.7                      S = 0.16

Table 3.10   Data from tests reported by Warwaruk and
             Taylor (161) on prestressed

section when both $T_u$ and $M_u$ are zero, as given by Eq. 3.4. $M_u$ represents the pure moment capacity of the member when $V_u$ and $T_u$ are zero. The value of $T_{uo}$ is given by Eq. 3.5. $V_{uo}$ is the reference value in the case of pure shear as defined by Eq. 3.72 of Report 248-2. For sections with positive bending type reinforcement $[F_{yl} > F_{yu}]V_{uo}$ is given by

$$V_{uo} = n*[2F_{yu}S_y \ z/s]^{0.5}$$

(3.9)

where $F_{yu}$ is the tensile force capacity per web element in the truss model chord where the applied moment induces compression and "n" is the number of webs resisting the applied shear force. This derivation assumes the use of doubly reinforced sections in the design of members subjected to a combination of torsion, bending and shear. Since the resultant horizontal force due to shear always produces tension components in the lower and upper chords, the feasible maximum capacity is dictated by the weaker of the two longitudinal chords $[F_{yl} > F_{yu}]$ in terms of tensile capacity.

The alternate case studied considers yielding of the stirrups at failure along with yielding in tension of the longitudinal reinforcement in the truss model chord in which the applied moment would induce compression $[F_{yu}]$. For this case, the ultimate load interaction of the member is evaluated using Eq. 3.10 (see Eq. 3.83 of Report 248-2).

$$(\frac{T_u}{T_{uo}})^2 + (\frac{V_u}{V_{uo}})^2 - \frac{1}{r} \frac{M_u}{M_{uo}} = 1$$

(3.10)

Tests reported by Collins, Walsh, Archer and Hall (33) on
Rectangular Solid sections (R)

| (1)<br>Member ID<br>and Section<br>Type | (2)<br>r | (3)<br>$\dfrac{Mtest}{Muo}$ | (4)<br>$\dfrac{Ttest}{Tuo}$ | (5)<br>$\dfrac{Vtest}{Vuo}$ | (6)<br>Level of<br>Prestress<br>$\sigma/f'_c$ | (7)<br>I | (8)<br>Type of failure |
|---|---|---|---|---|---|---|---|
| RE2  (R) | 1.0 | 0.26 | 0.91 | 0.03 | 0.0 | 1.05 | |
| RE3  (R) | 1.0 | 0.37 | 0.89 | 0.05 | 0.0 | 1.09 | Stirrups and |
| RE4  (R) | 1.0 | 0.70 | 0.81 | 0.08 | 0.0 | 1.24 | bottom steel |
| RE5  (R) | 1.0 | 0.89 | 0.72 | 0.10 | 0.0 | 1.30 | yielded |
| RE4*(R) | 1.0 | 1.10 | 0.41 | 0.12 | 0.0 | 1.25 | |
| RB1  (R) | 0.26 | 0.02 | 0.75 | 0.01 | 0.0 | 0.80 | |
| RB3*(R) | 0.26 | 0.02 | 0.77 | 0.01 | 0.0 | 0.81 | Stirrups and top<br>steel yielded |
| RB5  (R) | 0.26 | 0.94 | 0.77 | 0.34 | 0.0 | 1.11 | Stirrups and |
| RB5A(R) | 0.26 | 1.00 | 0.70 | 0.39 | 0.0 | 1.16 | bottom longitudinal |
| RB6  (R) | 0.26 | 1.06 | 0.60 | 0.41 | 0.0 | 1.19 | steel yielded |

$$X = 1.09$$
$$S = 0.20$$

Tests reported by Liao and Ferguson (104) on L-sections (L)

| | | | | | | | |
|---|---|---|---|---|---|---|---|
| 3LS-6(L) | 1.0 | 0.29 | 0.99 | 0.29 | 0.0 | 1.20 | Torsion + shear |
| 3LS-8(L) | 1.0 | 0.27 | 0.88 | 0.27 | 0.0 | 1.07 | |
| 3LS-3(L) | 1.0 | 0.68 | 0.62 | 0.38 | 0.0 | 1.18 | shear |
| 1.5LS-1(L) | 1.0 | 0.40 | 0.73 | 0.44 | 0.0 | 1.10 | torsion + shear |
| 3LS-2(L) | 1.0 | 0.51 | 0.77 | 0.57 | 0.0 | 1.30 | shear |
| 1.5LS-2(L) | 1.0 | 0.29 | 0.89 | 0.59 | 0.0 | 1.20 | torsion + shear |

* Specimens 3LS-4 and 3LS-7 are    X =    1.18
  reported in Sec. 3.7             S =    0.08

Table 3.11   Test data from reinforced concrete members
             subjected to torsion-bending-shear

Tests reported by Mukherjee and Warwaruk (123) on Prestressed concrete rectangular sections

| (1) Member ID Section Ty. ( ) | (2) r | (3) $\frac{M_{test}}{M_{uo}}$ | (4) $\frac{T_{test}}{T_{uo}}$ | (5) $\frac{V_{test}}{V_{uo}}$ | (6) Level of Prestress $\sigma/f'_c$ | (7) I | (8) Type of failure |
|---|---|---|---|---|---|---|---|
| V102 (R) | 1.0 | 0.99 | 0.61 | 0.21 | 0.11 | 1.33 | |
| V104 (R) | 1.0 | 0.34 | 1.03 | 0.09 | 0.11 | 1.22 | |
| V105 (R) | 1.0 | 0.08 | 1.03 | 0.04 | 0.11 | 1.07 | Yielding of the stirrups |
| V123 (R) | 1.0 | 0.54 | 1.09 | 0.16 | 0.11 | 1.42 | and bottom |
| V124 (R) | 1.0 | 0.32 | 1.18 | 0.10 | 0.11 | 1.36 | longitudinal |
| V125 (R) | 1.0 | 0.09 | 1.18 | 0.04 | 0.11 | 1.23 | steel |
| S1 (R) | 1.0 | 0.89 | 0.87 | 0.19 | 0.11 | 1.46 | |
| S2 (R) | 1.0 | 0.84 | 0.66 | 0.16 | 0.11 | 1.23 | |

\* Specimens V107, V122, V127, V202, V203, V204, V205, V207, V223, V224, V225, and V227 are reported in Sec. 3.7

X = 1.29
S = 0.13

Tests reported by Johnston and Zia (86) on Prestressed concrete box sections

| | | | | | | | |
|---|---|---|---|---|---|---|---|
| H-4-3-5 (R) | 0.5 | 0.45 | 0.75 | 0.41 | 0.09 | 0.85 | |
| H-6-3-3 (R) | 0.5 | 0.69 | 0.70 | 0.38 | 0.09 | 1.02 | |
| H-6-3-4 (R) | 0.5 | 1.12 | 0.58 | 0.42 | 0.09 | 1.36 | Yielding of |
| H-6-3-5 (R) | 0.5 | 1.07 | 0.40 | 0.42 | 0.09 | 1.24 | |
| H-6-6-3 (R) | 0.5 | 0.50 | 0.79 | 0.44 | 0.10 | 0.92 | stirrups and |
| H-4-3-3 (R) | 0.5 | 0.49 | 0.50 | 0.55 | 0.10 | 0.79 | |
| H-4-6-3 (R) | 0.5 | 0.53 | 0.55 | 0.60 | 0.09 | 0.86 | bottom steel |
| H-6-6-4 (R) | 0.5 | 1.10 | 0.28 | 0.62 | 0.10 | 1.38 | |
| H-6-6-5 (R) | 0.5 | 1.05 | 0.54 | 0.59 | 0.10 | 1.41 | |
| H-4-6-2 (R) | 0.5 | 0.45 | 0.37 | 0.81 | 0.09 | 0.80 | |
| H-4-6-4 (R) | 0.5 | 0.86 | 0.41 | 0.88 | 0.10 | 1.37 | |

\* Specimens H-4-3-1,H-4-3-2, H-4-6-1,H-4-6-3,H-4-6-5,H-6-3-1 H-6-3-2,H-6-6-1,H-6-6-2 are reported in Sec. 3.7

X = 1.09
S = 0.26

Table 3.13  Test data from prestressed concrete members subjected to torsion-bending-shear

than the test values. Hence, the truss model is conservative in such cases. I = 1 indicates that the obtained test results and the predicted values are exactly the same. Finally, I < 1 indicates that the predicted values were larger than the actual test results and thus the theory would be unconservative for such specimens. The values of the mean (X) and standard deviation (S) are provided at the bottom of each group of tests. In addition, the values of the mean and the standard deviation of all the reinforced and prestressed concrete members studied are provided at the bottom of Tables 3.12 and 3.14, respectively.

For the case of reinforced concrete members the mean of the dispersion coefficient is 1.10 and the standard deviation 0.15. This indicates that the truss model predictions were very good and in general conservative.

For the case of all the prestressed concrete members shown in Table 3.13 and 3.14 the mean of the dispersion coefficient is 1.14 and the standard deviation 0.24. This indicates a reasonable agreement between test results and truss model predictions. The truss model is more conservative for prestressed concrete members than for reinforced concrete members, and a larger scatter is observed as shown by the standard deviation value of 0.24. However, in spite of the large standard deviation, no test result was less than 80% of the predicted value.

To illustrate the predicted truss model ultimate load interaction evaluated by means of Eqs. 3.8 and 3.11 some of the test
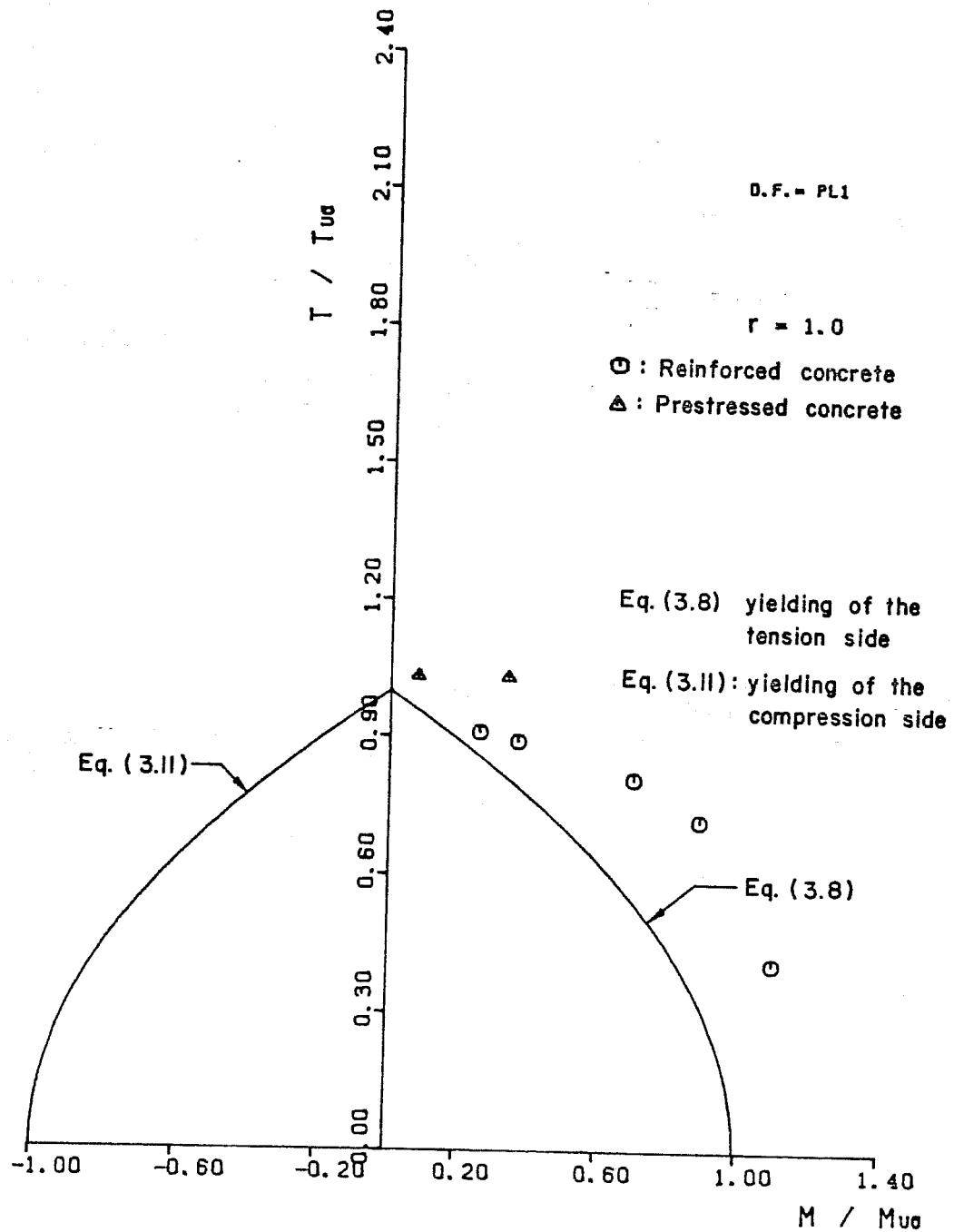
Fig. 3.11  Torsion-bending-shear interaction with $V_u/V_{uo} = 0.75$ for reinforced and prestressed concrete specimens
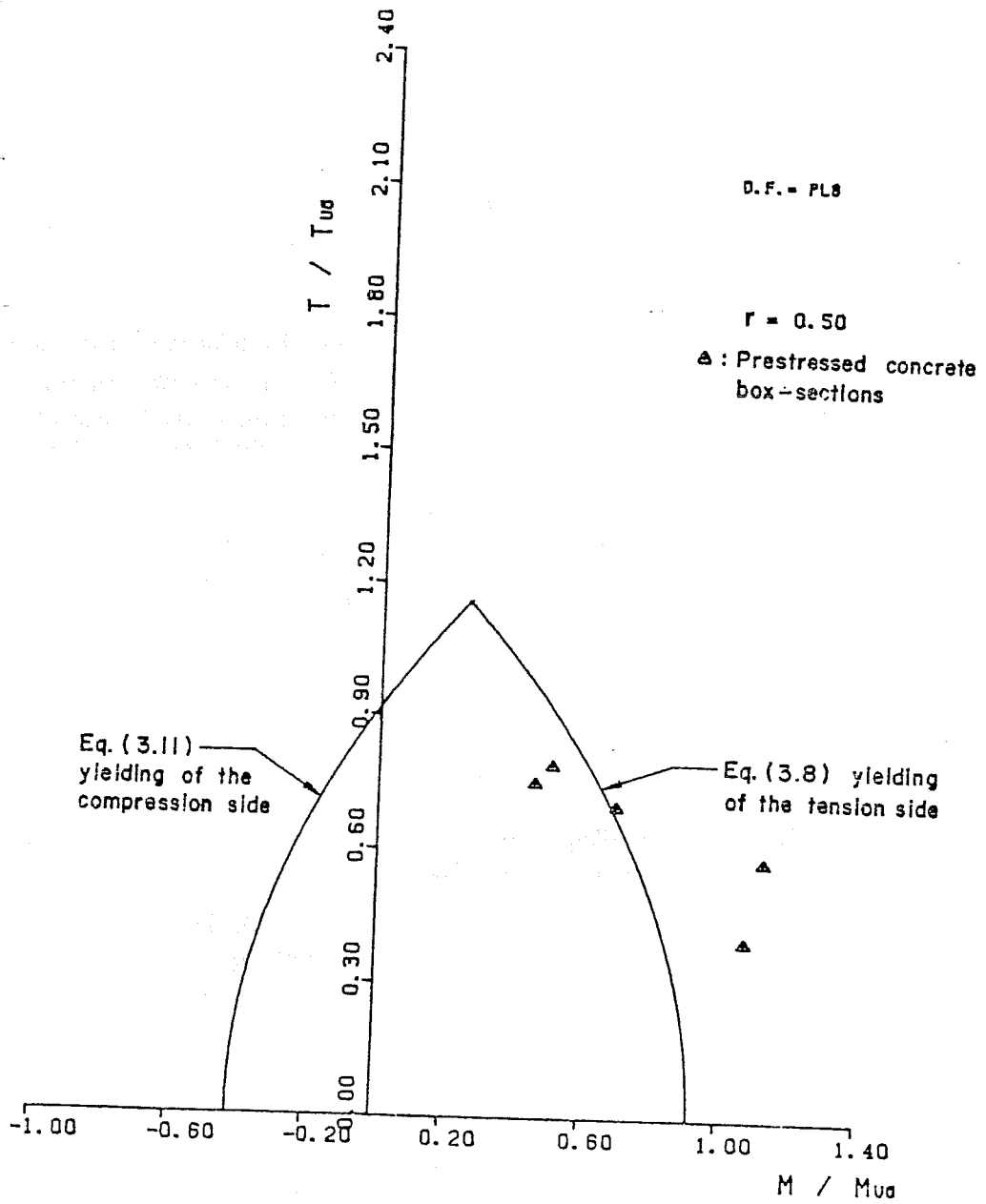
Fig. 3.13  Torsion-bending-shear interaction for
r = 0.50 and $V_u/V_{uo}$ = 0.45
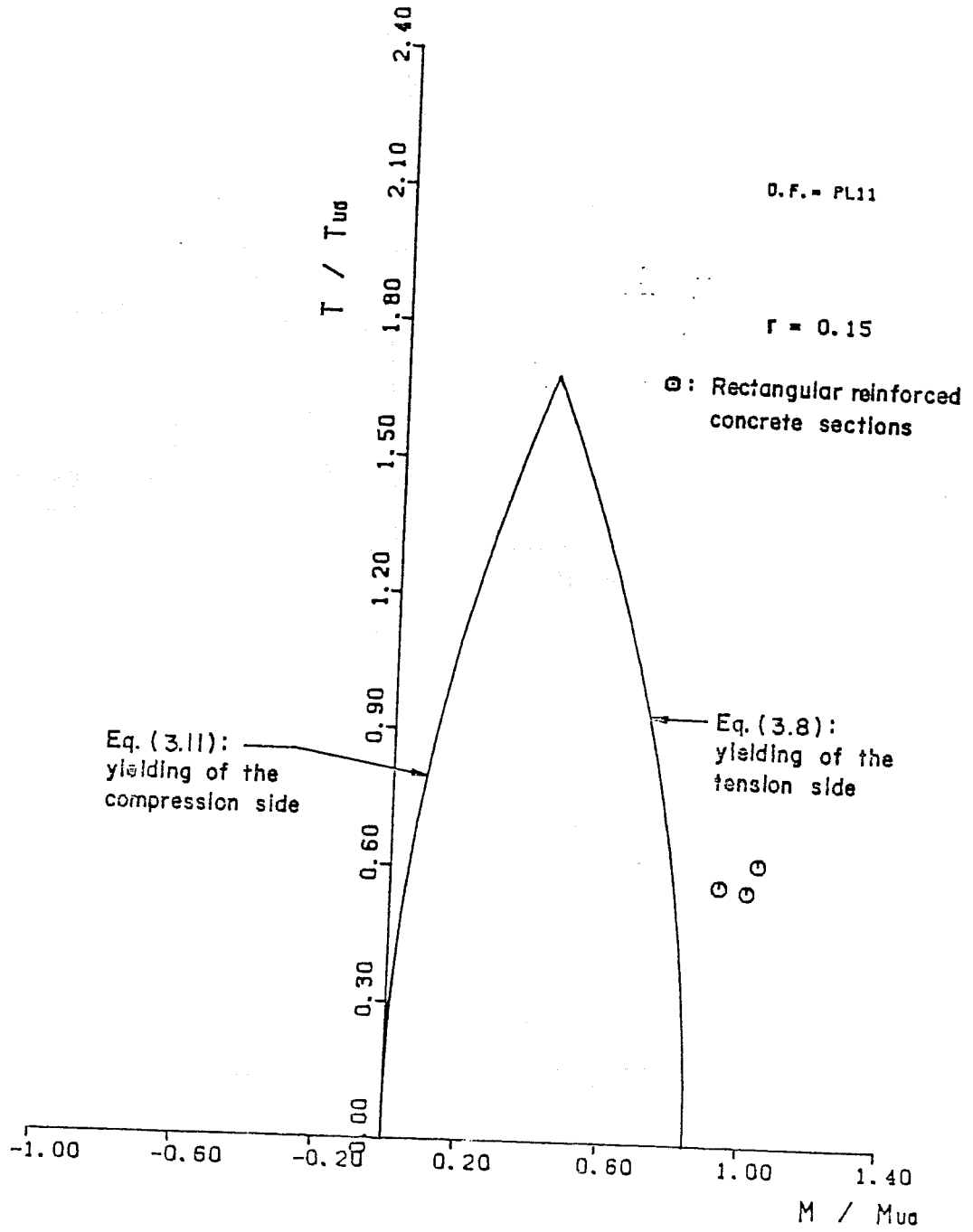
Fig. 3.15   Torsion-bending-shear interaction with
$V_u/V_{uo} = 1.0$

double celled prestressed concrete box sections R3 and R4 from Ref. 161 in Table 3.14 are plotted in Fig. 3.14, together with the interaction Eqs. 3.8 and 3.11 for values of "r" of 0.27 and $V_u/V_{uo}$ of 0.40. Again, there is generally good agreement, although in the case of the double celled prestressed concrete box sections assuming the shear distributed equally on each web, very conservative (I = 1.5) predictions are obtained.

In Figs. 3.15, 3.16, and 3.17, the effect of varying the applied shear ratio is studied using the ultimate test results of the rectangular reinforced concrete specimens A1, A2, A3, A4, A5, B1, B2, B3, B4, and B5 reported in Ref. 133 shown in Table 3.12. All the specimens were of rectangular cross section, had a value of "r" equal to 0.15, and the ratio $V_u/V_{uo}$ varied from 1.0 to 0.45. The results show generally good and conservative agreement with only one specimen slightly inside the interaction curve (I = 0.95).

As a result of the comparison with actual test results carried out in this section, it can be concluded that the truss model can adequately and conservatively represent the ultimate load interaction of both prestressed and reinforced concrete members of various cross sections, provided that the section is underreinforced, and that premature failures due to poor detailing are prevented.

## 3.5 Bending and Shear

In this section the very important case of the ultimate load behavior of reinforced and prestressed concrete members subjected to

shear and flexure as predicted by the truss model is evaluated using test data available in the American literature together with results of recent tests conducted at the Ferguson Laboratory during this research project.

The interaction equation (Eq. 3.68 of Report 248-2), which describes the ultimate load behavior of one-way flexural members subjected to bending and shear was derived as:

$$[M_u/M_{uo}] + [V_u/M_{uo}]^2 = 1 \tag{3.12}$$

Equation 3.12 was obtained from equilibrium conditions of the truss model. $M_u$ and $V_u$ are the ultimate load combination of bending moment and shear force. $M_{uo}$ represents the pure bending capacity of the section.

$$M_{uo} = F_{y1}*z \tag{3.13}$$

where $F_{y1}$ is the yield capacity in tension of the truss chord at the face of the member where the applied moment produces tension; "z" is the distance between the tension and compression chords of the truss model. $V_{uo}$ is the shear capacity of the section, when yielding of the tension chord takes place, if the applied moment $M_u$ is zero.

$$V_{uo} = [2F_{y1} \, S_y \, z/s]^{0.5} \tag{3.14}$$

The terms $F_{y1}$ and "z" are those previously defined. $S_y$ represents the stirrup force $[A_s*f_{ys}]$, "s" is the center-to-center stirrup spacing.

3. Poorly detailed specimens.

Therefore, it was decided that a series of tests on reinforced and prestressed concrete members designed using the truss model approach would be very useful to correctly evaluate the truss model in the area of bending and shear, as well as to illustrate the design procedure based on the truss model.

Schaeffer (153) conducted tests on a series of rectangular reinforced concrete beams specifically designed to illustrate the effect of assuming varied $\alpha$ angles on beam web reinforcement patterns using the truss model. The results of the three specimens failing in shear from that series are shown in Table 3.15.

The term $\rho_v f_y$ tabulated in column (6) represents a measure of the amount of web reinforcement in the member and is given by the web reinforcement ratio $\rho_v = A_v/b_w s$ (where $A_v/s$ is the total area of vertical web reinforcement per inch of stirrup spacing, s, and $b_w$ is the web width) times the yield strength, $f_y$ of the stirrup reinforcement.

Again, as in Secs. 3.3 and 3.4, the dispersion coefficient I, tabulated in column (7) is used as an indicator to measure the accuracy of the truss model ultimate predicted values as given in the case of shear and bending by Eq. 3.12. For the three specimens shown in Table 3.15, the test obtained values are in excellent agreement with the truss predictions. The mean of the dispersion coefficient I is 1.05 and the standard deviation 0.10.

The detailing of the steel reinforcement provided in these members (RL-0.50, RL-1.25, and RH-0.50) is shown in Fig. 3.18. Note the
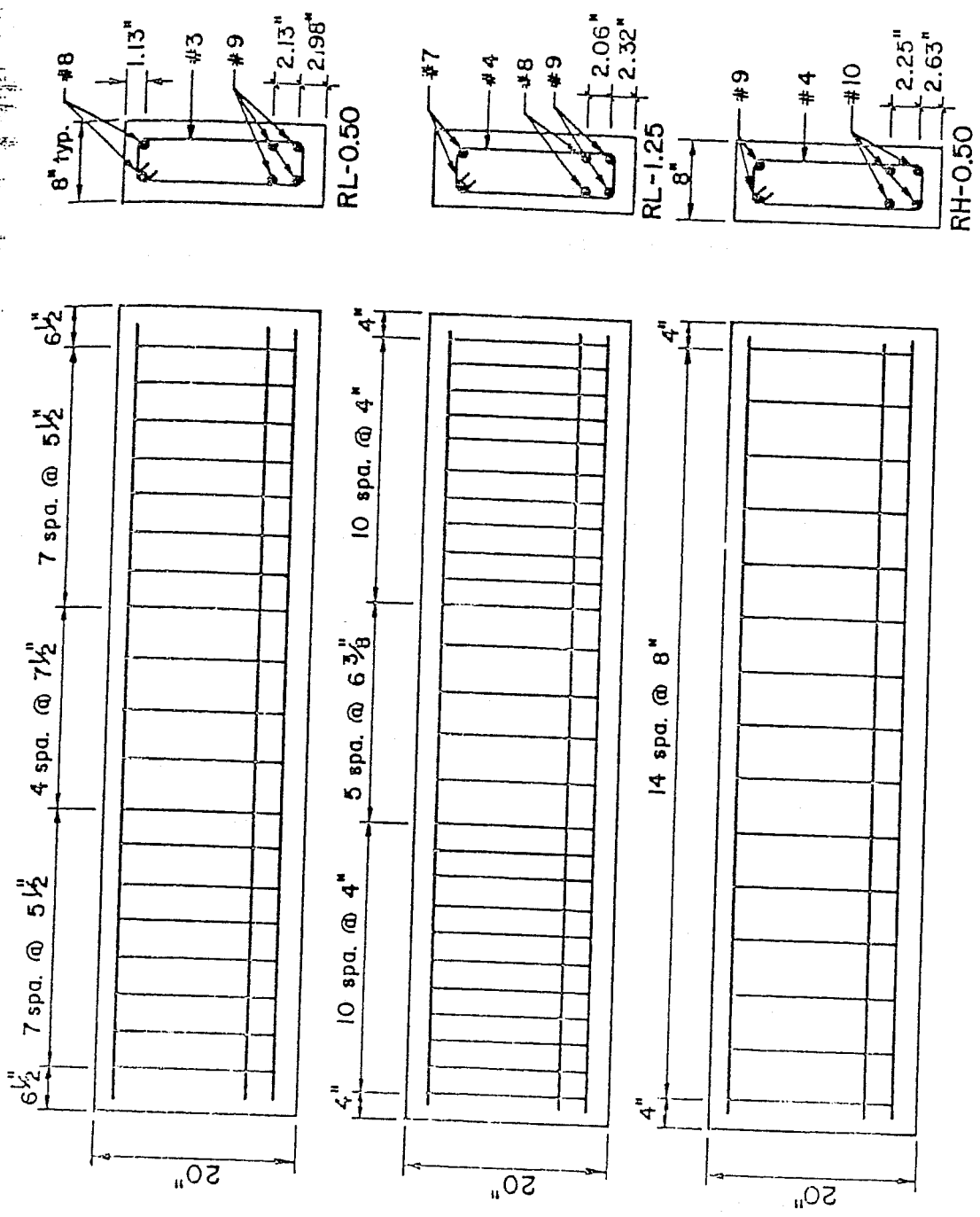
Fig. 3.18  Reinforcing details of members RL-0.50, RL-1.25, and RH-0.50

(a)

(b)

(c)
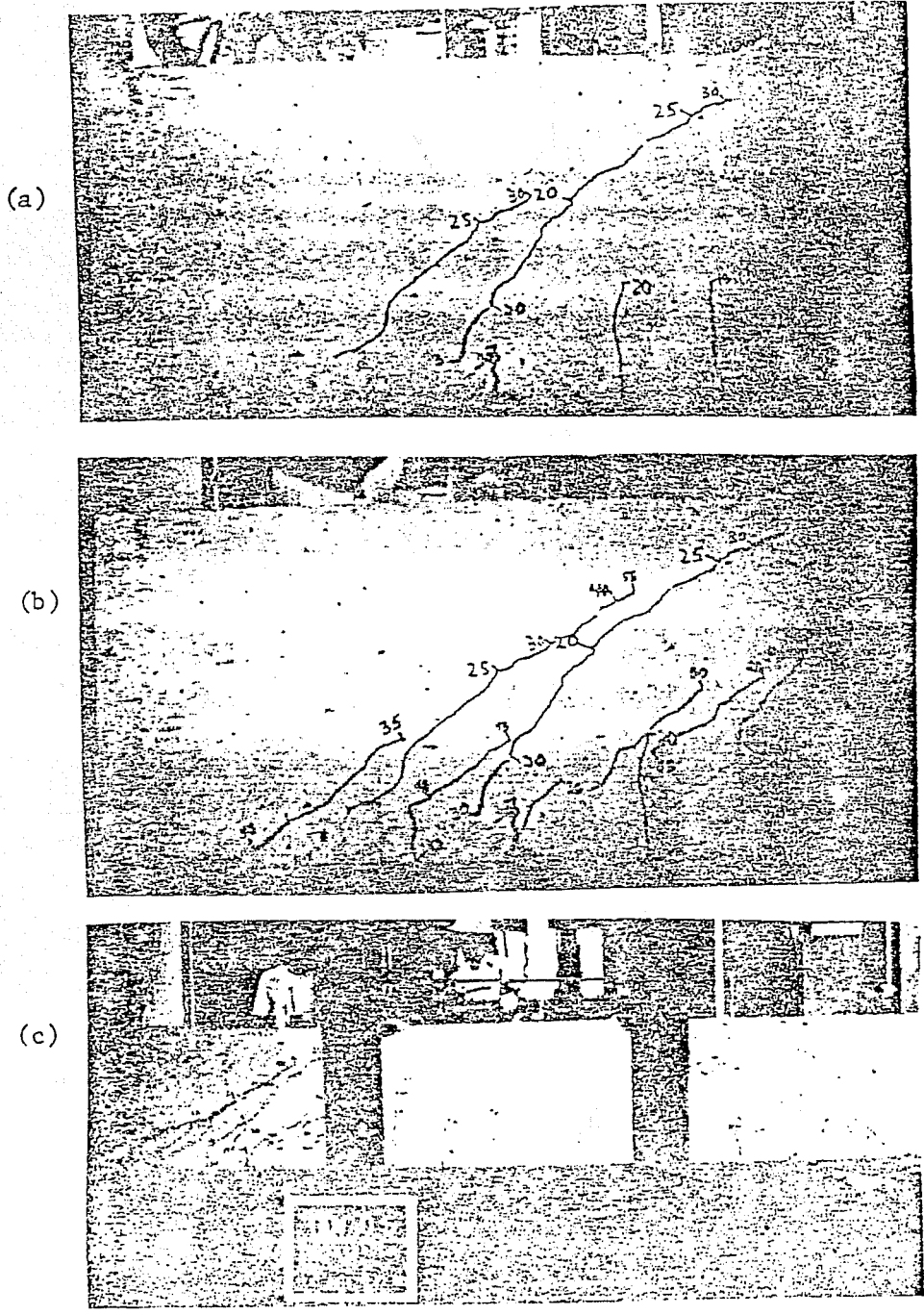
Fig. 3.19   Crack patterns of beam RL-0.50 at load
            stage of 60 kips, 100 kips, and failure
            (top to bottom)

43% of its yield point. Photographs of the crack patterns are shown in Fig. 3.21.

The load-deflection curves for RL-0.50 and RL-1.25 are shown in Fig. 3.22. The load-deflection curve for RH-0.50 is shown in Fig. 3.23.

In Fig. 3.24, a comparison is shown between the predicted ultimate load behavior obtained using the interaction Eq. 3.12 and the ultimate test values of the specimens RL-0.50, RL-1.25 and RH-0.50 given in Table 3.15.

Very good agreement was obtained between the test values and the truss model predictions as shown by the values of the dispersion index I in Table 3.15 and by Fig. 3.24. This good correlation was achieved in spite of the fact that yielding of the longitudinal reinforcement did not occur in two of the members at failure. This suggests that in these cases, provided the member is properly designed such as the ones presented in Table 3.15 and provided either stirrups or longitudinal reinforcement yielded prior to failure the truss model would adequately predict the ultimate load capacity.

A properly designed member should meet the following general requirements:

1. The section must be underreinforced for flexure, i.e. yielding of the longitudinal reinforcement must take place prior to crushing of the concrete in the compression zone.

2. Failures due to web crushing should be avoided by adequately checking the compression stresses in the diagonal strut of the truss model.

3. The angle of inclination of the diagonal strut at failure must be chosen within the prescribed limits $0.5 \leq \tan\alpha \leq 2.0$.
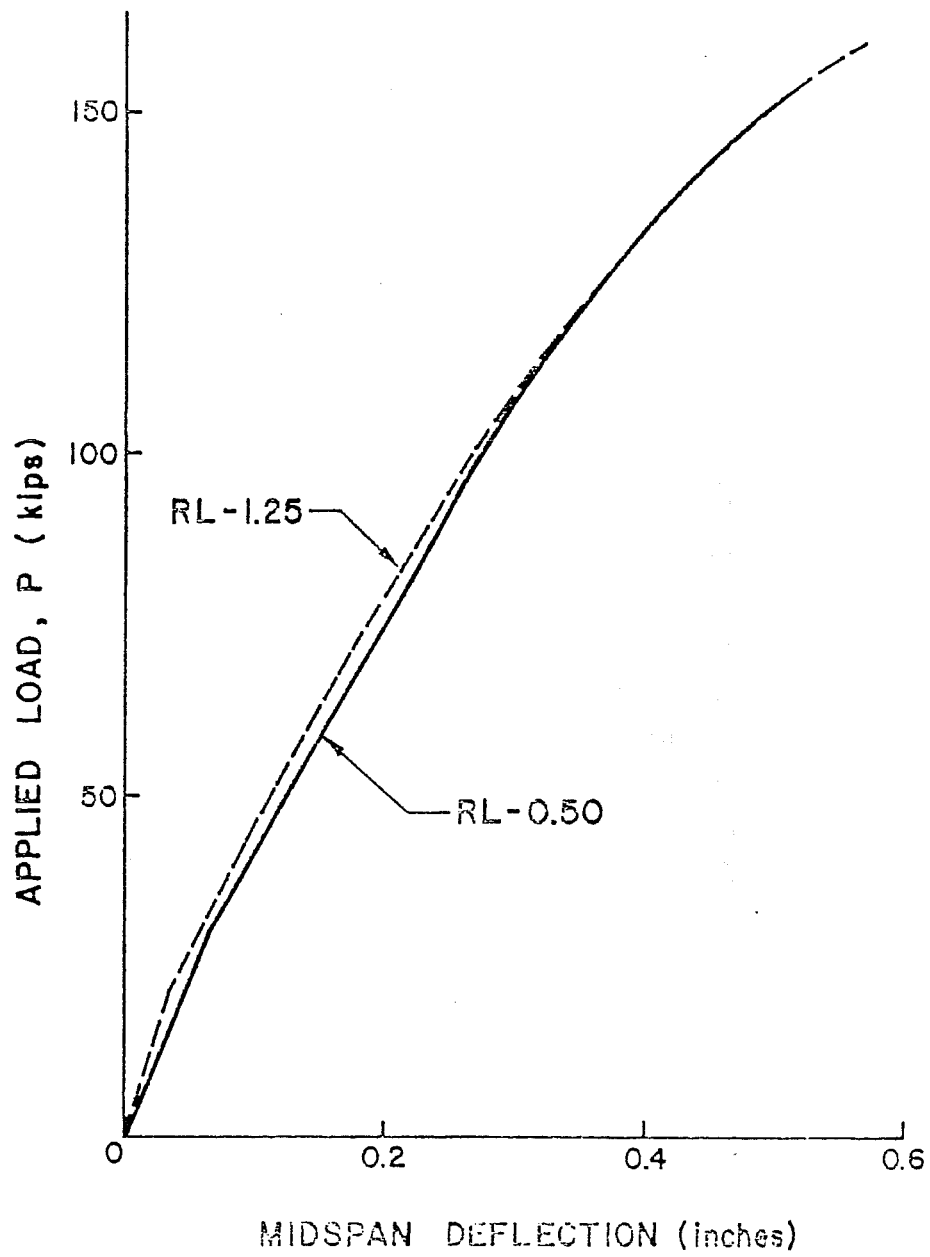
Fig. 3.22  Load-deflection curves of beams RL-0.50
and RL-1.25
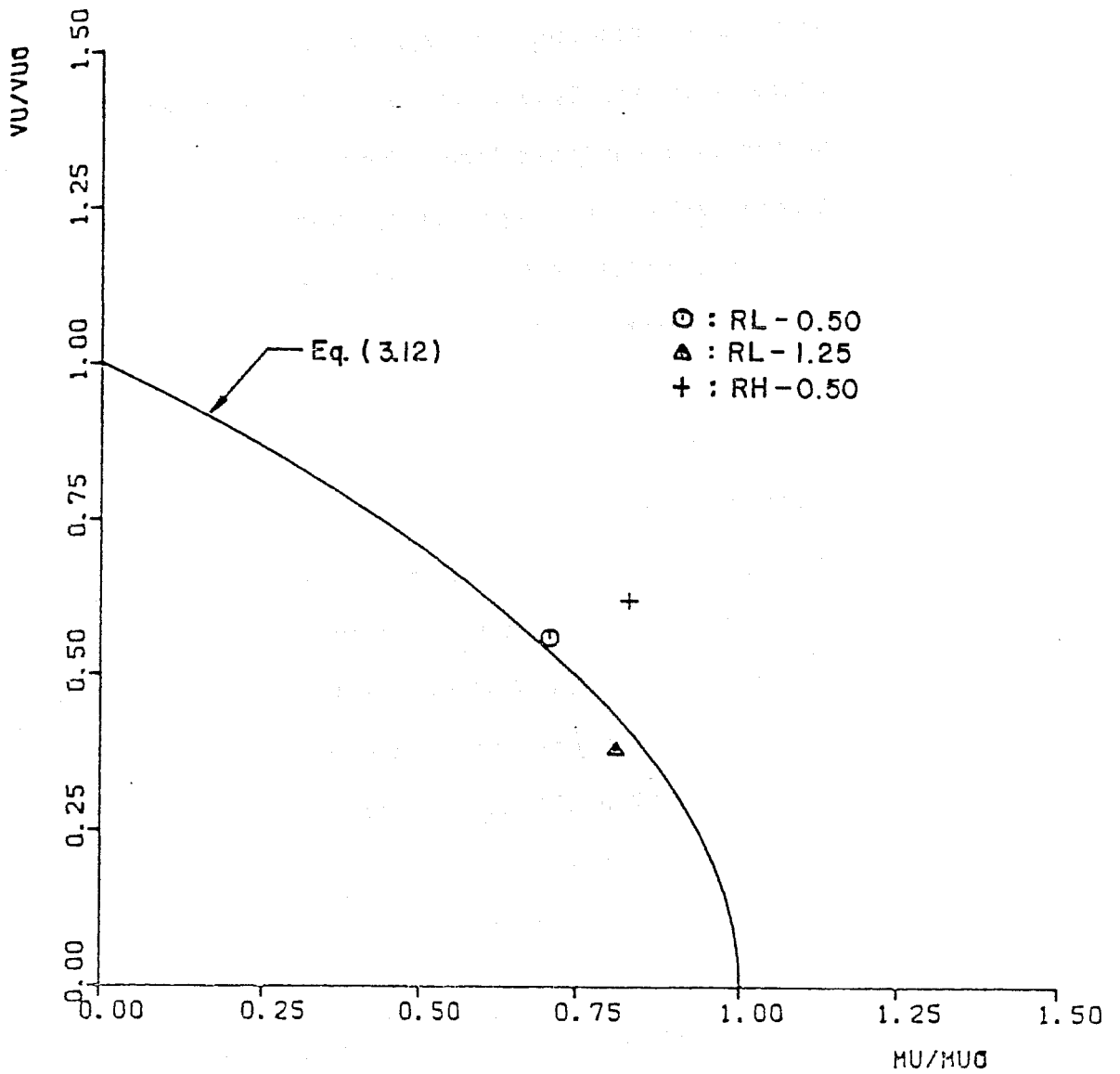
Fig. 3.24   Predicted ultimate bending and shear interaction
using the truss model

SIDE VIEW

END VIEW
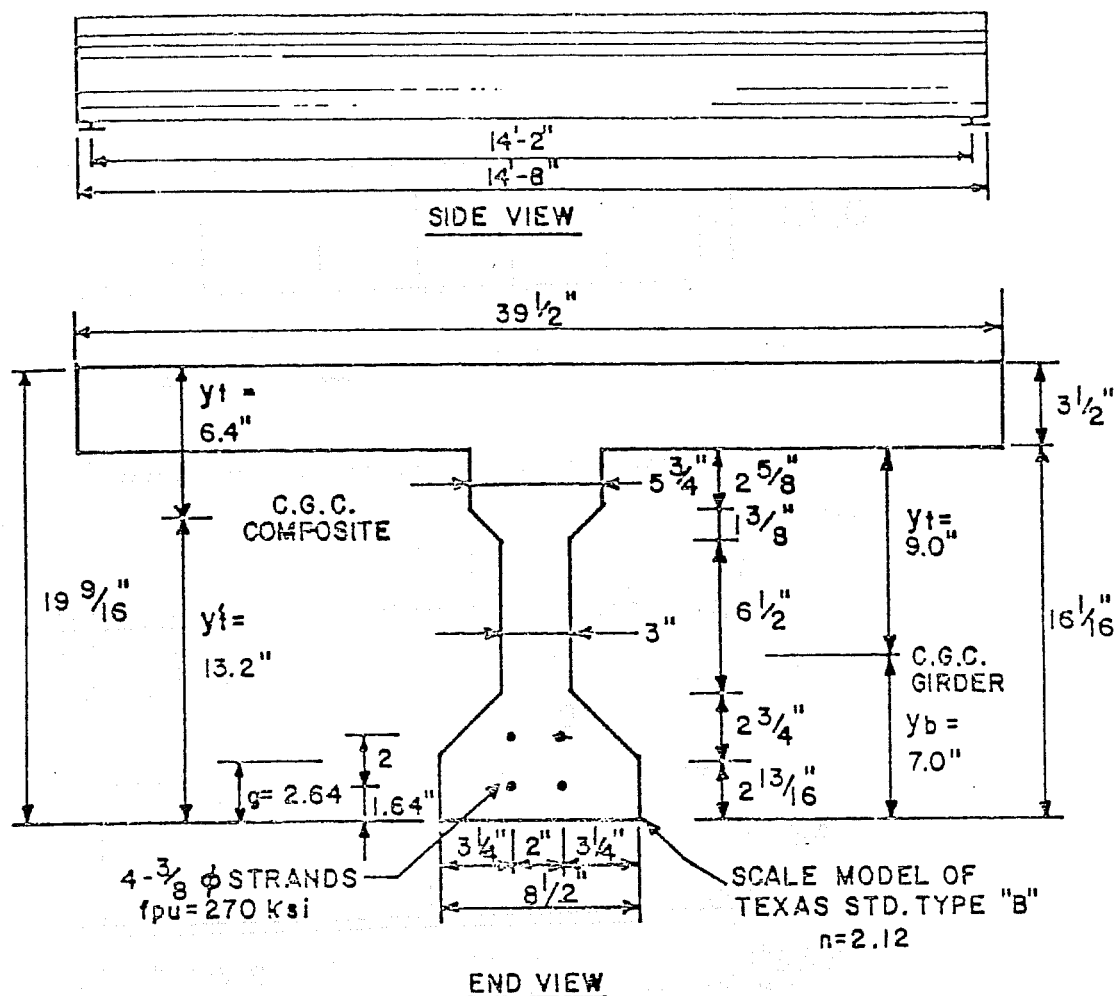
MEMBER PROPERTIES

|  | Girder | Slab | Composite Total | Transformed |
|---|---|---|---|---|
| Area = | 80.3 in$^2$ | 138.2 in$^2$ | 218.5 in$^2$ | 186.7 in$^2$ |
| I = | 2144 in$^4$ | 141 in$^4$ | --------- | 7620 in$^4$ |
| Wt. = | 84 plf | 149 plf | 233 plf | --------- |
| f$_c'$ = | 5000 psi | 3000 psi | --------- | 5000 psi |

Fig. 3.25  Details of the cross section

| (1) Author Reference | (2) Member ID | (3) Section from support (ft) | (4) Vuo (Eq. 3.14) (kips) | (5) Vtest (Kips) | (6) Muo (Eq. 3.13) (in-kip) | (7) Mtest (in-kips) | (8) $\rho_{vfy}$ (ksi) | (9) Level of Prestress $\sigma/f'_c$ |
|---|---|---|---|---|---|---|---|---|
| Castrodale (50) | 0.40A | support | 49.40 | 51.60 | 2232 | 0.0 | 0.18 | 0.10 |
| | | 1.70 | 49.40 | 39.30 | | 926.0 | 0.18 | |
| | | 3.40 | 49.40 | 26.90 | | 1600.0 | 0.18 | |
| | | 5.10 | 45.70 | 14.50 | | 2021.0 | 0.16 | |
| | | | 45.70 | 0.0 | | 2194.0 | 0.16 | |
| | 0.40B | support | 52.50 | 54.80 | 2522 | 0.0 | 0.18 | 0.13 |
| | | 1.75 | 52.50 | 41.20 | | 1008.0 | 0.18 | |
| | | 3.50 | 52.50 | 27.70 | | 1731.0 | 0.18 | |
| | | 5.25 | 48.60 | 14.20 | | 2171.0 | 0.16 | |
| | | | 48.60 | 0.0 | | 2327.0 | 0.16 | |
| | 0.45 | support | 57.70 | 60.0 | 2537 | 0.0 | 0.22 | 0.12 |
| | | 1.56 | 57.70 | 46.80 | | 1003.0 | 3.22 | |
| | | 3.13 | 57.70 | 33.50 | | 1757.0 | 0.22 | |
| | | 4.70 | 52.00 | 20.30 | | 2263.0 | 0.18 | |
| | | 6.26 | 48.60 | 7.00 | | 2518.0 | 0.16 | |
| | | | 48.60 | 0.0 | | 1553.0 | 0.16 | |

Table 3.16   Data from specimens 0.40A, 0.40B, and 0.45
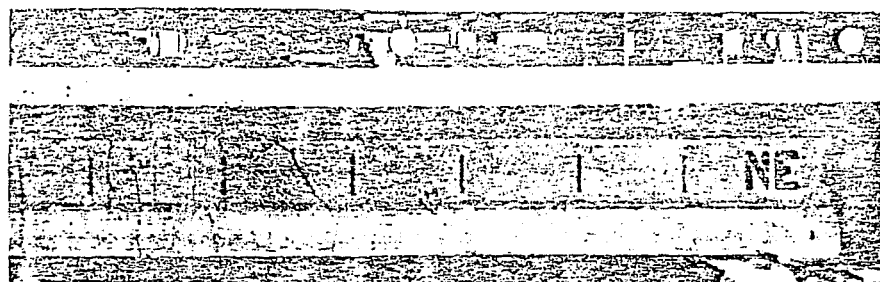
(a)
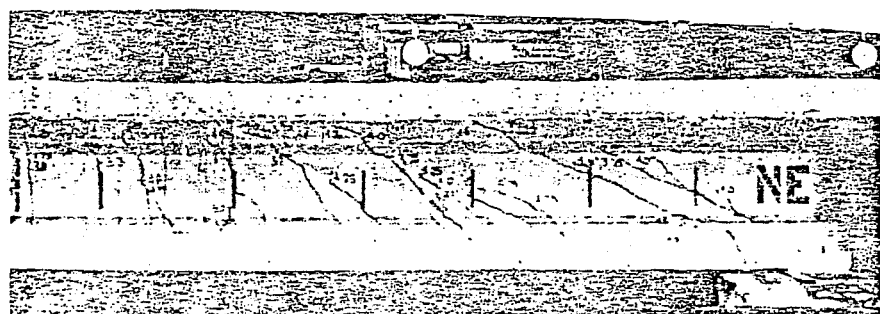


(b)
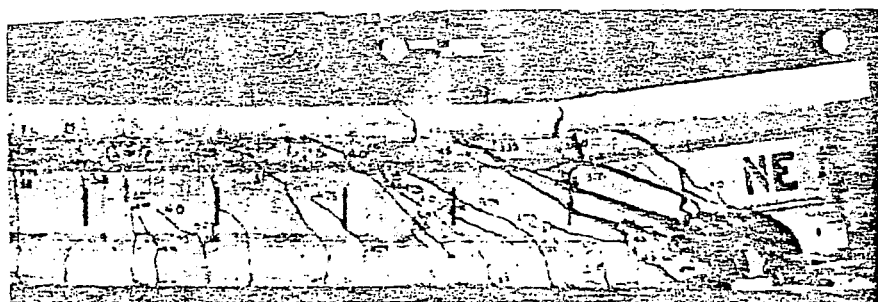


(c)

Fig. 3.27    Crack patterns of beam 0.40A at load stages
             of 4.2 k/f, 6.7 k/f, and failure (top to
             bottom)
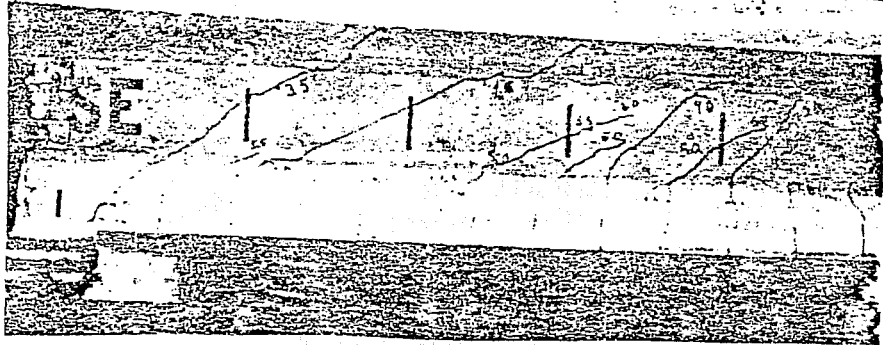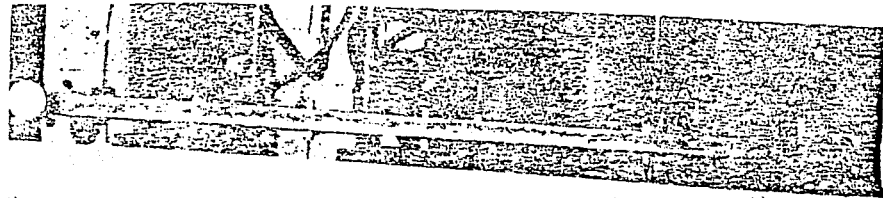
(a)
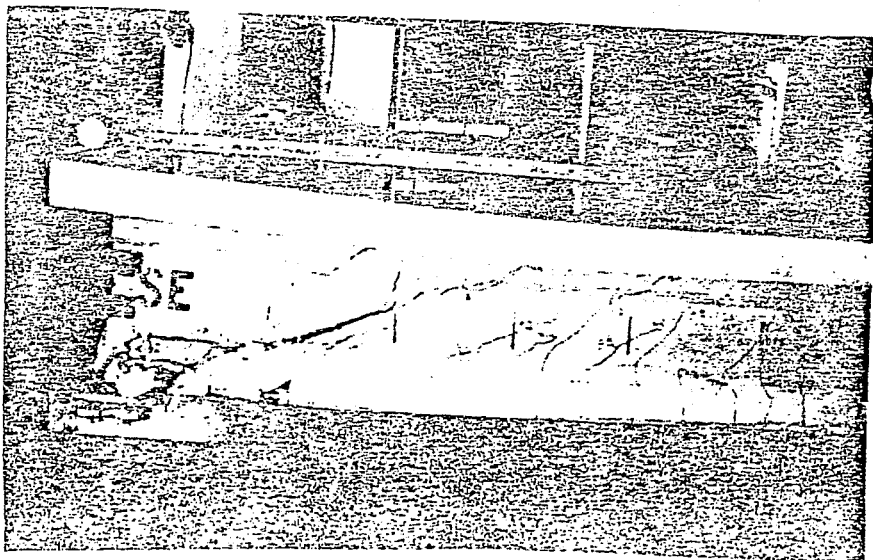
(b)

Fig. 3.28  Crack patterns of beam 0.40B at load stages
of 6.7 k/f and failure (top to bottom)
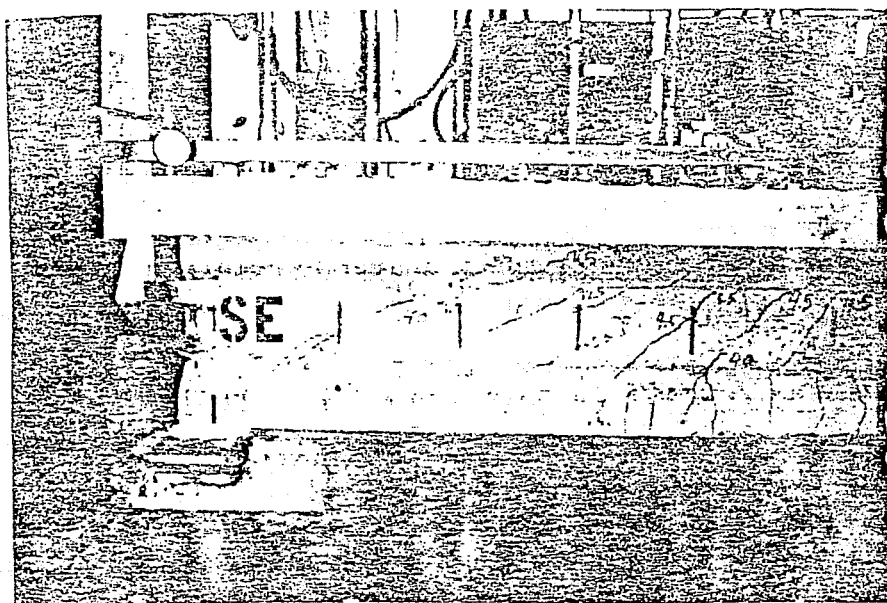
(a)
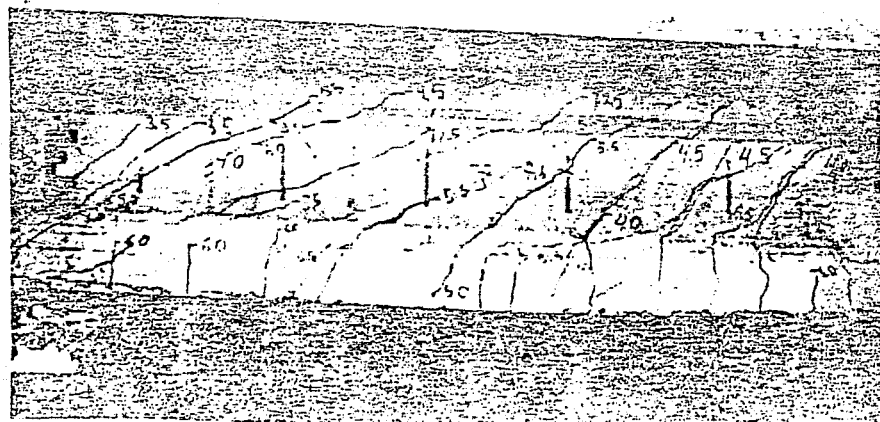


(b)

Fig. 3.29   Crack patterns of beam 0.45 at load stages
of 7.5 k/f and failure (top to bottom)

place prior to failure, the same comments made in the case of specimen 0.40A apply in this case.

The specimen labeled 0.45 was designed assuming a tan of 0.45. The maximum average strain in the transverse reinforcement indicated that first yielding of the stirrup reinforcement in the falure zone was reached at about 88% of the ultimate test load. In the longitudinal nonprestressed tension steel, the maximum average strain recorded in the failure zone indicated yielding of this reinforcement at failure. The stress in the prestressing strands reached 216 ksi, which was 84% of its yield strength. Photographs of the crack patterns are shown in Fig. 3.29.

In specimen 0.45 several significant changes were made. Increasing the design angle of inclination of the diagonal compression strut to a value of $\tan\alpha$ of 0.45 produced a closer stirrup spacing while the longitudinal reinforcement did not have to be increased as compared to specimen 0.40B (see Fig. 3.26). This undoubtedly coused a redistribution of forces in the member. The closer stirrup spacing near the support region forced the critical region away from the support and at the same time caused a more uniform distribution of the diagonal cracks as can be seen in Fig. 3.29b. Furthermore, the increase of transverse reinforcement did not prevent yielding of the stirrups yet at the same time controlled the cracking at the support thus preventing the spalling of concrete at the end support regions of the member.

The load—deflection curves for these three specimens are shown in Fig. 3.30.

In column (6) of Table 3.17 are shown the values of the dispersion index I. The mean of the dispersion coefficient for the three specimens at several different sections was 1.01 and the standard deviation 0.03. This indicates excellent agreement between the predicted ultimate values and the test results.

In Figs. 3.31, 3.32 and 3.33, the ultimate test values shown in Table 3.17 evaluated at different sections using the ultimate test load are compared with the ultimate load interaction predicted by the truss model as obtained from Eq. 3.12.

Figures 3.31, 3.32 and 3.33 confirm the good agreement observed between the test results and the truss model predictions. This agreement was achieved in spite of the fact that the yielding of the longitudinal reinforcement did not occur at failure. Furthermore, the data presented in Table 3.17 in column (4) show that in regions of maximum shear (at the supports $M_u = 0$) the maximum shear capacity in the absence of moment as given by Eq. 3.14 coincide with the value of the shear at failure. Therefore, the results of this series also supports the statement that for sections designed in accordance with the procedures suggested in the truss model would correctly predict their ultimate shear capacity as long as yielding of the stirrups is reached at failure and premature failure due to crushing of the concrete or poor detailing are prevented.

The specimens analyzed in this section were specifically designed to evaluate the truss model analogy and the design procedures suggested for the case of members failing in shear. As suggested, low

VU/VUO

1.50
1.25
1.00
0.75
0.50
0.25
0.00

Eq. (3.12)

◇ : tan α = 0.40A

0.00   0.25   0.50   0.75   1.00   1.25   1.50

MU/MUO
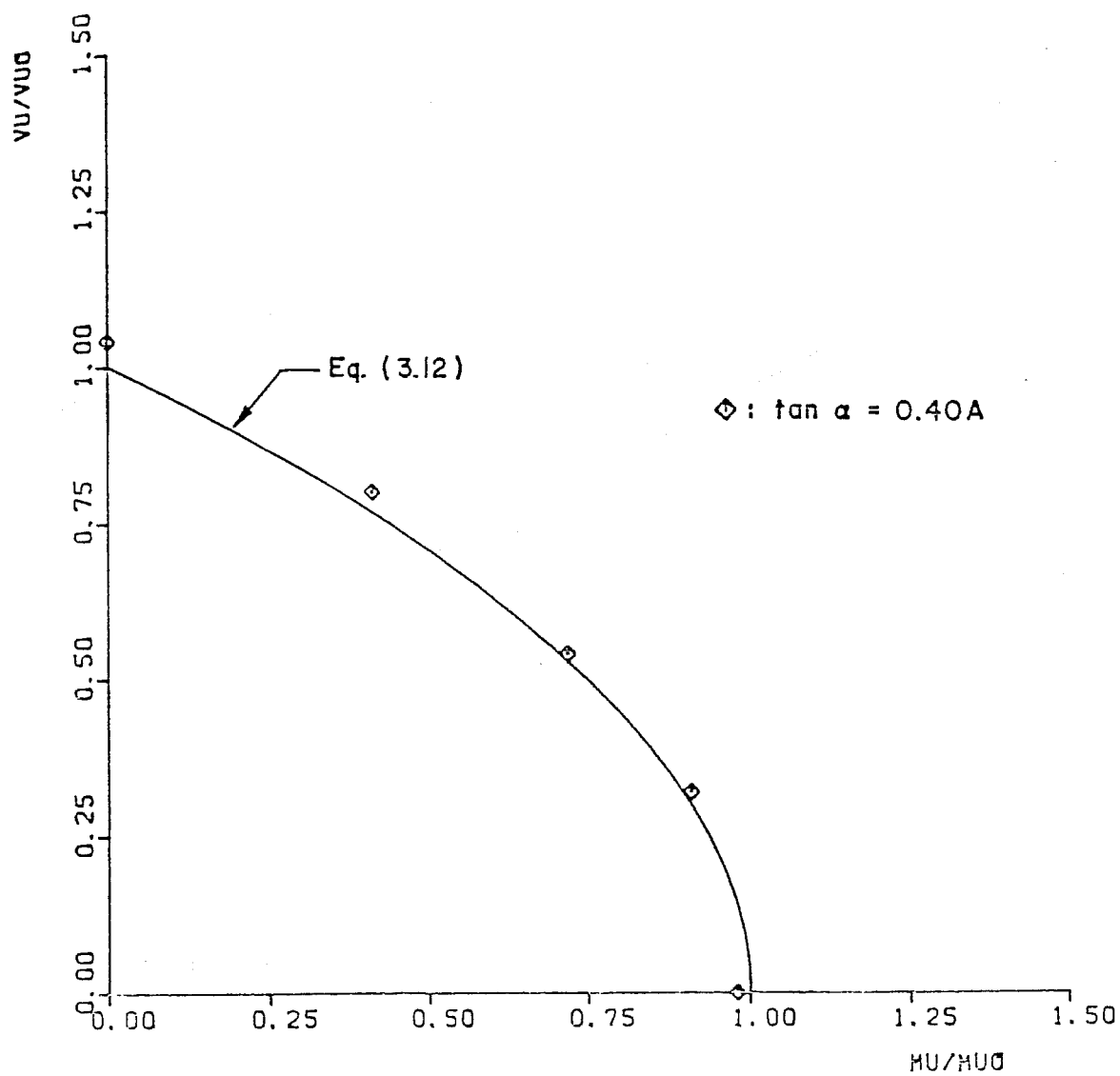
Fig. 3.31   Comparison between the ultimate load interaction
predicted by the truss model and the ultimate
test values at different sections along the span
length for beam 0.40A
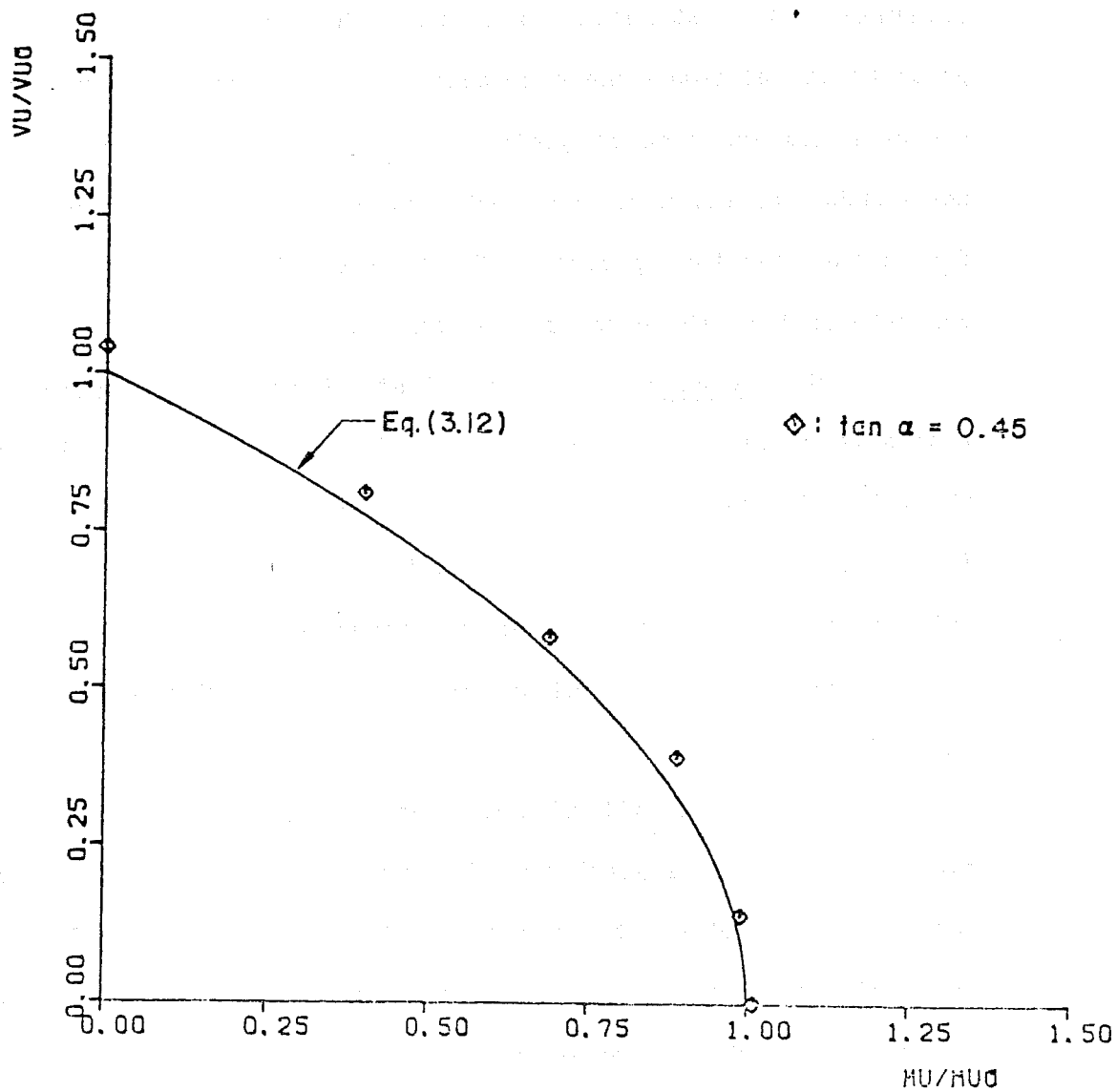
Fig. 3.33  Comparison between the truss model predicted
ultimate load interaction and the results
from beam 0.45

N = Number of specimens

REINFORCED CONCRETE
SHEAR FAILURES
N = 572

$\rho_v f_y$ (psi)

300

250

200

150

100

50

100 200 400 600 800 1000

Fig. 3.34  Tests on reinforced concrete one-way members

web reinforcement percentage $\rho_v * f_y$ is defined as

$$\rho_v f_y = [A_v f_y]/[b_w s] \qquad (3.15)$$

In a later section, members with minimal shear reinforcement (defined as $\rho_v f_y < 100$ psi) will be discussed. The ultimate load as predicted by the truss model for members subjected to bending and shear and containing web reinforcement is presented by the interaction Eqs. 3.12.

In the comparison of the truss model with test results reported in the literature in the area of combined bending and shear, a similar procedure to the one followed in the areas of combined torsion-bending and torsion-bending-shear is used. The index I shown in column (7) of Tables 3.18 thru 3.21 is again used as a measure of the dispersion between data points and the truss model predictions measured along radial lines from the origin (see Fig. 3.36).

The truss model predicted ultimate values are given by the interaction Eq. 3.12. Values I > 1 indicate conservative predictions. Values of I < 1 represent unconservative predictions. The values of the mean (X) and standard deviation (S) of the dispersion index I are also given for both reinforced and prestressed concrete members.

As previously explained, the interaction Eq. 3.12 is derived under the assumption that yielding of the transverse and longitudinal reinforcement is achieved at failure. This situation is almost nonexistent in the case of test data where shear failures were observed. In Sec. 3.5.1 it was shown, however, that as long as the members were

Tests reported by A.P. Clark (53) on reinforced concrete rectangular beams (continuation)

| (1)<br>Member<br>ID | (2)<br>$\frac{M_{test}}{M_{uo}(Eq.3.13)}$ | (3)<br>$\frac{V_{test}}{V_{uo}(Eq.3.14)}$ | (4)<br>$p_v f_y$<br>(psi) | (5)<br>a/d | (6)<br>$\tan\alpha$<br>(Eq.3.16) | (7)<br>I | (8)<br>Level of<br>Prestress<br>$\sigma/f'c$ |
|---|---|---|---|---|---|---|---|
| D1-7 | 0.73 | 0.68 | 170 | 1.96 | 0.36 | 1.13 | 0.0 |
| D1-8 | 0.76 | 0.71 | 170 | 1.96 | 0.35 | 1.19 | 0.0 |
| E1-2 | 0.95 | 0.67 | 260 | 2.02 | 0.47 | 1.30 | 0.0 |
| D2-6 | 0.86 | 0.56 | 220 | 2.42 | 0.51 | 1.14 | 0.0 |
| D2-7 | 0.80 | 0.51 | 220 | 2.42 | 0.56 | 1.04 | 0.0 |
| D2-8 | 0.86 | 0.56 | 220 | 2.42 | 0.51 | 1.13 | 0.0 |
| D4-1 | 0.86 | 0.62 | 180 | 2.42 | 0.41 | 1.19 | 0.0 |
| D4-2 | 0.80 | 0.57 | 180 | 2.42 | 0.45 | 1.09 | 0.0 |
| D4-3 | 0.84 | 0.61 | 180 | 2.42 | 0.42 | 1.16 | 0.0 |
| D5-1 | 0.75 | 0.63 | 130 | 2.42 | 0.36 | 1.10 | 0.0 |
| D5-2 | 0.80 | 0.66 | 130 | 2.42 | 0.34 | 1.17 | 0.0 |
| D5-3 | 0.80 | 0.66 | 130 | 2.42 | 0.34 | 1.17 | 0.0 |
| A1-1 | 0.73 | 0.59 | 180 | 2.34 | 0.41 | 1.06 | 0.0 |
| A1-2 | 0.69 | 0.55 | 180 | 2.34 | 0.43 | 0.99 | 0.0 |
| A1-3 | 0.73 | 0.59 | 180 | 2.34 | 0.41 | 1.06 | 0.0 |
| A1-4 | 1.73 | 0.59 | 180 | 2.34 | 0.41 | 1.06 | 0.0 |

Tests reported by O. Moretto (99) on reinforced concrete rectangular beams ( Point load tests)

| | | | | | | | |
|---|---|---|---|---|---|---|---|
| 1V½1 | 0.59 | 0.79 | 150 | 1.75 | 0.24 | 1.14 | 0.0 |
| 1V½2 | 0.59 | 0.79 | 150 | 1.75 | 0.24 | 1.14 | 0.0 |
| 2V½1 | 0.69 | 0.93 | 150 | 1.75 | 0.20 | 1.33 | 0.0 |
| 2V½2 | 0.68 | 0.92 | 150 | 1.75 | 0.20 | 1.33 | 0.0 |
| 1V3/81 | 0.72 | 0.70 | 290 | 1.75 | 0.38 | 1.15 | 0.0 |
| 1V3/82 | 0.76 | 0.74 | 290 | 1.75 | 0.36 | 1.21 | 0.0 |
| 2V3/81 | 0.75 | 0.74 | 290 | 1.75 | 0.36 | 1.20 | 0.0 |
| 2V3/82 | 0.71 | 0.69 | 290 | 1.75 | 0.38 | 1.13 | 0.0 |
| 1aV½1 | 0.50 | 0.77 | 130 | 1.75 | 0.23 | 1.05 | 0.0 |
| 1aV½2 | 0.51 | 0.78 | 130 | 1.75 | 0.23 | 1.07 | 0.0 |

Overall for Tables 3.18 and 3.19

$X =$ 1.22
$S =$ 0.25

Table 3.19 Data on reinforced concrete rectangular beams failing in shear

Tests reported by Moayer and Regan (33) on prestressed
concrete T-beam (Point load)

| (1) Member ID | (2) $\dfrac{M\,test}{Muo\,(Eq.3.13)}$ | (3) $\dfrac{Vtest}{Vuo\,(Eq.3.14)}$ | (4) $\rho_v f_y$ (psi) | (5) a/d | (6) $\tan\alpha$ (Eq.3.16) | (7) I | (8) Level of Prestress $\sigma/f'c$ |
|---|---|---|---|---|---|---|---|
| P4  | 1.21 | 0.55 | 155 | 3.45 | 0.52 | 1.42 | 0.07 |
| P8  | 0.93 | 0.99 | 104 | 3.64 | 0.12 | 1.55 | 0.14 |
| P13 | 1.11 | 0.98 | 104 | 3.51 | 0.14 | 1.68 | 0.05 |
| P18 | 1.00 | 0.97 | 104 | 3.68 | 0.13 | 1.60 | 0.13 |
| P24 | 1.11 | 0.54 | 155 | 3.51 | 0.49 | 1.33 | 0.05 |
| P25 | 1.19 | 0.79 | 104 | 5.32 | 0.21 | 1.51 | 0.05 |
| P26 | 1.07 | 0.56 | 155 | 3.68 | 0.41 | 1.32 | 0.12 |
| P27 | 1.09 | 0.70 | 104 | 5.57 | 0.18 | 1.43 | 0.13 |
| P28 | 1.00 | 0.59 | 155 | 3.64 | 0.36 | 1.28 | 0.13 |
| P29 | 1.06 | 0.61 | 104 | 5.51 | 0.23 | 1.34 | 0.13 |
| P49 | 0.73 | 0.50 | 155 | 3.61 | 0.37 | 0.98 | 0.16 |
| P50 | 0.89 | 0.44 | 290 | 3.61 | 0.58 | 1.07 | 0.14 |

X = 1.38
S = 0.20

Table 3.21   Data on prestressed concrete T-beams
failing in shear

correctly detailed and premature failures due to crushing of the concrete in the web or in the concrete compression zone were prevented, the truss model adequately predicted the ultimate strength of those members.

The test data used in this section to evaluate the truss model are that of reinforced and prestressed concrete one-way members failing in shear where yielding of the transverse reinforcement was achieved at or previous to failure, unless otherwise indicated. Members where web crushing occurred at failure are examined in Sec. 3.6.

Tables 3.18 and 3.19 show test data for reinforced concrete rectagular one-way members failing in shear. In column (7) are given the values of the dispersion index I. Shown at the bottom of Table 3.19 are the values of the mean (X = 1.22) and the standard deviation (S = 0.25) of the index I for all reinforced concrete beams reported in the data of Tables 3.18 and 3.19. As can be seen from the values of the index I, the truss model is conservative in virtually every case. The excessive conservatism seen in members C1-1, C1-2, C6-2, C6-3, C6-4, and D1-1 of Table 3.18 can be explained by observing the values of $\tan \alpha$ shown in column (6). The value of $\tan \alpha$ is the tangent of the angle of inclination at failure of the diagonal strut (see Eq. 3.64 of Report 248-2).

$$\tan \alpha = [S_y * z]/[V_{TEST} * s] \qquad (3.16)$$

It is determined by the amount of web reinforcement and level of shear present in the member at failure. This corresponds to the angle of

good agreement and in most cases conservative when compared with actual test values.

It is also apparent from the data examined that the truss model predictions once more become very conservative for members with an angle of inclination of the diagonal strut at failure outside the limits suggested in Report 248-2 ($0.5 \leq \tan\alpha \leq 2.0$). For members with an angle $\alpha$ inside the proposed limits the truss model predictions become much more accurate as can be seen from the test data of Ref. 110, beam G20 from Ref. 76, and beams P4 and P50 from Ref. 33.

Finally, the truss model is evaluated using test data from reinforced and prestressed continuous members failing in shear.

Table 3.22 shows the data for two-span continuous reinforced concrete members. The mean of the dispersion index I given in column (7) is 0.96 and the standard deviation 0.14. In general, it can be said that the truss model adequately predicts the strength of those members. The unconservative values predicted for members C3H1, C3H2, C2A1, and C2H1 are explained by the fact that neither the stirrup nor the longitudinal reinforcement had yielded at failure thus indicating a premature type failure due to crushing of the concrete in the web. In the case of specimens E2H1 and E2H2, failure was due to a combination of shear and bond splitting which would indicate poor detailing of the longitudinal tension steel, thus causing a premature failure of the members.

Table 3.23 shows data on continuous prestressed concrete members failing in shear where yielding of the transverse reinforcement was

Tests reported by Mattock and Kaar (111) on continuous prestressed concrete I-beams. (Point load tests)

| (1)<br>Member<br>ID | (2)<br>Mtest<br>$\overline{\text{Muo}}$ (Eq. 3.13) | (3)<br>Vtest<br>$\overline{\text{Vuo}}$ (Eq. 3.14) | (4)<br>ρvfy<br>(psi) | (5)<br>a/d | (6)<br>tanα<br>(Eq. 3.16) | (7)<br>I | (8)<br>Level of<br>Prestress<br>σ/f'c |
|---|---|---|---|---|---|---|---|
| S7 | 1.12 | 1.20 | 282 | 2.0 | 0.21 | 1.89 | 0.15 |
| S13 | 1.08 | 0.84 | 282 | 4.5 | 0.31 | 1.54 | 0.14 |
| S10 | 0.94 | 1.29 | 188 | 2.0 | 0.17 | 1.83 | 0.15 |
| S21 | 0.65 | 1.25 | 188 | 2.0 | 0.17 | 1.62 | 0.14 |
| | | | | X = | | 1.72 | |
| | | | | S = | | 0.17 | |

Table 3.23   Data on continuous prestressed concrete members with I-shape cross section failing in shear

## 3.6 Evaluation of the Compression Strength of the Diagonal Strut

In Sec. 2.3 it was shown that the maximum shear stress $v_{max}$ is achieved when the angle of inclination of the diagonal compression strut is of 45 degrees, and is given by the relation

$$v_{max} = f_d/2 \tag{3.17}$$

where $f_d$ is the compression stress in the diagonal strut of the truss model. It was also suggested that by limiting the compression stress in the diagonal strut $f_d$ to a value equal or less than a maximum allowable compression stress $f_c$ failure due to crushing of the concrete in the diagonal strut would be avoided if the member was designed for an angle of inclination at failure between 26 and 64 degrees.

In this section, test results of beams which failed due to web crushing are examined in order to evaluate proposed limits for the maximum allowable compression stress, $f_c$, in the diagonal strut of the truss model.

Thürlimann (162) on the basis of test evidence and practical experience proposed that the allowable compression stress $f_c$ should be taken as

$$f_c = f_{d\ max} = 0.35f_c' + 696 \leq 2400 \text{ psi} \tag{3.18}$$

where $f_c$ and $f_c'$ are in terms of psi. Thürlimann states that the limit of 2400 psi, which corresponds to $f_c'$ of about 4800 psi, is somewhat arbitrary. It was set at 4800 psi simply because that was the maximum range of $f_c'$ in the tests considered in the evaluation of Eq. 3.18.

Tests reported by Robinson (151) on reinforced concrete rectangular beams

| (1) Member ID | (2) F'c ksi | (3) v(max) Eq.3.21 ksi | (4) $\dfrac{(3)}{v(Eq.3.20)}$ | (5) $\dfrac{(3)}{v(Eq.3.22)}$ | (6) Level of Prestress $\sigma/f'c$ |
|---|---|---|---|---|---|
| NR8 | 2.16 | 0.89 | 1.13 | 1.28 | 0.0 |
| NR10 | 3.44 | 1.66 | 1.66 | 1.89 | |
| NT8-1 | 2.88 | 1.55 | 1.70 | 1.93 | |
| NT8-2 | 2.94 | 1.55 | 1.68 | 1.91 | |
| NT10 | 2.45 | 1.22 | 1.45 | 1.64 | |
| | | | X = 1.52 | X = 1.73 | |
| | | | S = 0.24 | S = 0.28 | |

Tests reported by Leonhardt and Walther (101,102) on reinforced concrete T-beams

| | | | | | |
|---|---|---|---|---|---|
| TA1 | 2.49 | 0.91 | 1.07 | 1.22 | 0.0 |
| TA2 | 2.49 | 0.97 | 1.02 | 1.16 | |
| TA3 | 2.31 | 0.74 | 0.90 | 1.03 | |
| TA13 | 2.87 | 0.94 | 1.03 | 1.17 | |
| TA14 | 2.87 | 0.91 | 1.00 | 1.13 | |
| TA1 | 3.53 | 1.56 | 1.54 | 1.75 | |
| | | | X = 1.09 | X = 1.24 | |
| | | | S = 0.23 | S = 0.26 | |

Tests reported by Bennett and Balasooriya (39) on reinforced concrete I-beams

| | | | | | |
|---|---|---|---|---|---|
| 2B6 | 6460 | 2.01 | 1.47 | 1.67 | 0.0 |

| | | |
|---|---|---|
| Overall for Table 3.24 | X = 1.30 | X = 1.48 |
| | S = 0.31 | S = 0.45 |

Table 3.24  Shear tests on reinforced concrete members experiencing web crushing failure
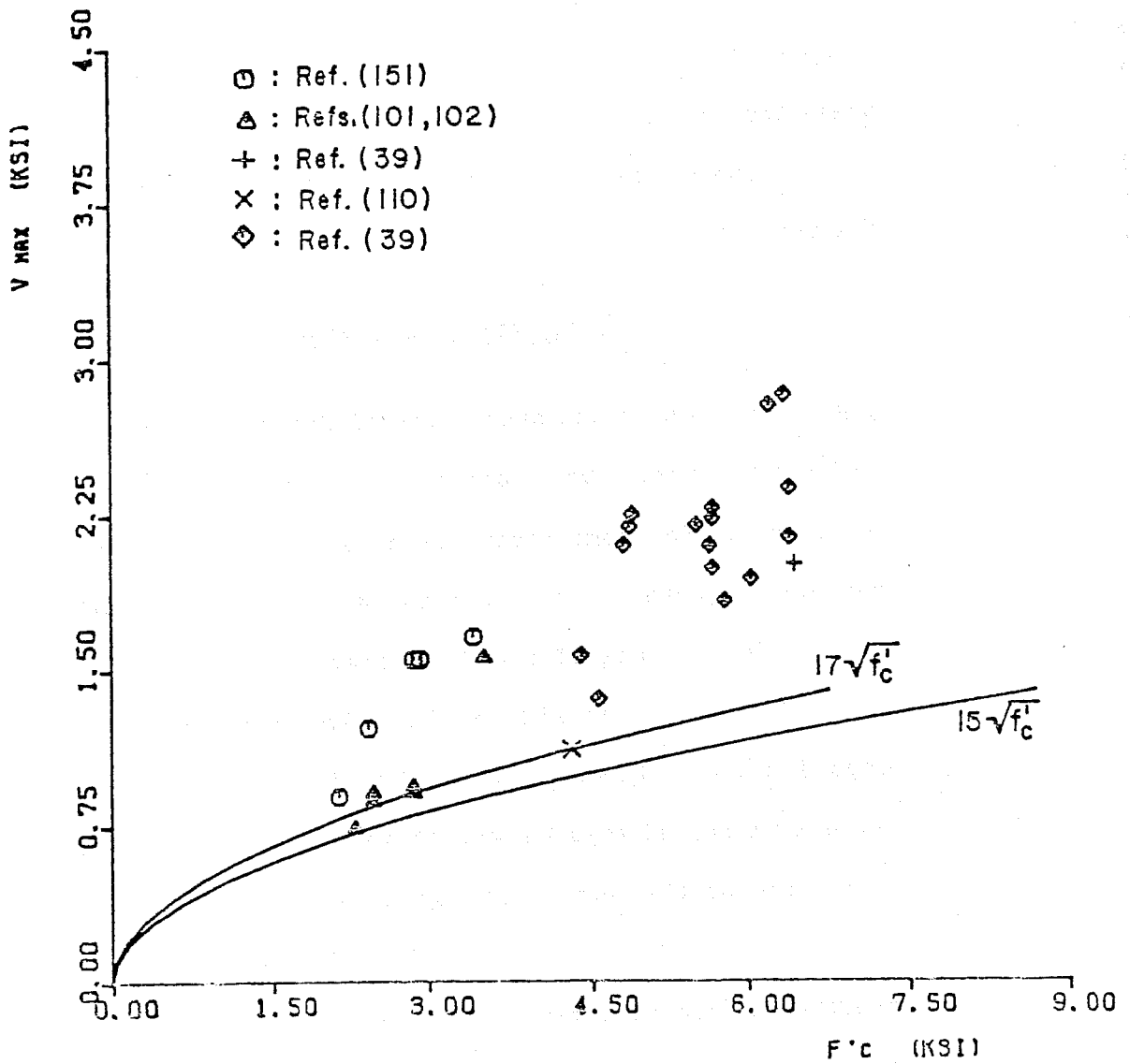
Fig. 3.37  Shear stress at failure vs specified compressive
strength of the concrete $f'_c$ for the case of
reinforced and prestressed concrete beams
failing due to web crushing

Tests reported by Hsu (82) on reinforced concrete rectangular beams

| (1)<br>Member<br>ID | (2)<br>f'c<br>ksi | (3)<br>v(max)<br>Eq.3.23<br>Ksi | (4)<br>(3)<br>$\overline{v(Eq.3.20)}$ | (5)<br>(3)<br>$\overline{v(Eq.3.22)}$ | (6)<br>Level of<br>Prestress<br>$c/f'c$ |
|---|---|---|---|---|---|
| B6 | 4.18 | 2.00 | 1.82 | 2.06 | 0.0 |
| M6 | 4.26 | 2.13 | 1.92 | 2.17 | |
| I6 | 6.64 | 2.80 | 2.01 | 2.28 | |
| J4 | 2.43 | 1.40 | 1.67 | 1.89 | |
| | | | | | |
| G5 | 3.90 | 1.78 | 1.68 | 1.90 | 0.0 |
| K4 | 4.15 | 3.47 | 3.15 | 3.58 | |
| C3 | 3.90 | 0.97 | 0.92 | 1.04 | |
| C4 | 3.94 | 1.28 | 1.20 | 1.36 | |
| C5 | 3.95 | 1.55 | 1.45 | 1.64 | |
| C6 | 4.00 | 2.23 | 2.10 | 2.38 | |
| | | | X = 1.79<br>S = 0.60 | X = 2.03<br>S = 0.69 | |

Tests reported by Wyss, Garland and Mattock (173)
on reinforced concrete I-(I) and rectangular (R) members

| | | | | | |
|---|---|---|---|---|---|
| C6(I) | 6.24 | 4.74 | 3.54 | 4.01 | 0.0 |
| D5(R) | 6.79 | 2.49 | 1.78 | 2.02 | |
| D6(R) | 6.89 | 2.25 | 1.60 | 1.81 | |
| | | | X = 2.31<br>S = 1.07 | X = 2.61<br>S = 1.21 | |

Tests reported by Wyss, Garland and Mattock (173)
on prestressed concrete I-beams

| | | | | | |
|---|---|---|---|---|---|
| A5(I) | 6.00 | 4.05 | 3.07 | 3.48 | 0.19 |
| A6(I) | 6.00 | 4.19 | 3.17 | 3.60 | 0.19 |
| D6(I) | 6.00 | 4.62 | 3.50 | 3.97 | 0.09 |
| C6(I) | 6.0 | 4.95 | 3.75 | 4.25 | 0.09 |
| | | | X = 3.37<br>S = 0.31 | X = 3.83<br>S = 0.35 | |
| Overall for Table 3.26 | | | X = 2.25<br>S = 0.90 | X = 2.56<br>S = 1.02 | |

Table 3.26   Torsion tests on reinforced and prestressed
concrete members experiencing web crushing
failures

Tests reported by Henry and Zia (75) on
prestressed concrete rectnagular beams

| (1) Member ID | (2) $f'c$ ksi | (3) v (max) Eq. 3.21 ksi | (4) $\dfrac{(3)}{v(Eq. 3.20)}$ | (5) $\dfrac{(3)}{v(Eq. 3.22)}$ | (6) Level of Prestress $\sigma/f'c$ |
|---|---|---|---|---|---|
| IV-4 | 5.90 | 2.14 | 1.63 | 1.85 | 0.13 |
| IV-2-5 | 6.04 | 2.62 | 1.98 | 2.25 | 0.13 |
| V-2-3 | 4.90 | 1.93 | 1.62 | 1.84 | 0.21 |
| V-3-4 | 4.48 | 2.44 | 2.78 | 3.15 | 0.23 |
| V-4-5 | 4.29 | 1.69 | 1.52 | 1.73 | 0.25 |
| V-3-6 | 5.08 | 2.10 | 1.74 | 1.97 | 0.20 |
| V-4-6 | 5.08 | 1.44 | 1.19 | 1.35 | 0.20 |
| | | | X = 1.78 | X = 2.02 | |
| | | | S = 0.50 | S = 0.57 | |

Tests reported by McMullen and Woodhead (113) on prestressed concrete
rectangular beams

| | | | | | |
|---|---|---|---|---|---|
| II-4 | 5.78 | 2.23 | 1.73 | 1.96 | 0.12 |
| II-5 | 5.52 | 2.52 | 2.00 | 2.27 | 0.13 |
| III-3 | 6.06 | 2.09 | 1.58 | 1.79 | 0.18 |
| III-5 | 6.58 | 2.60 | 1.88 | 2.14 | 0.18 |
| III-6 | 6.58 | 3.25 | 3.36 | 2.67 | 0.17 |
| V-1 | 5.73 | 2.27 | 1.76 | 1.99 | 0.24 |
| V-2 | 5.73 | 2.02 | 1.57 | 1.77 | 0.21 |
| V-3 | 6.72 | 2.09 | 1.50 | 1.70 | 0.19 |
| V-4 | 6.72 | 2.02 | 1.45 | 1.65 | 0.19 |
| V-5 | 5.52 | 2.27 | 1.80 | 2.04 | 0.23 |
| V-6 | 5.64 | 1.94 | 1.52 | 1.72 | 0.21 |
| V-7 | 5.64 | 2.25 | 1.76 | 1.99 | 0.22 |
| | | | X = 1.74 | X = 1.97 | |
| | | | S = 0.26 | S = 0.29 | |
| Overall for Table 3.27 | | | X = 1.76 | X = 1.99 | |
| | | | S = 0.35 | S = 0.40 | |

Table 3.27   Combined torsion and shear tests on prestressed
concrete members experiencing web crushing

As can be seen from Fig. 3.39, for the case of combined actions both limits (Eqs. 3.20 and 3.22) yield very conservative results. This also supports the assumption that evaluating the maximum applied shear stress when designing for the case of combined shear and torsion by summing the shear stresses due to shear and torsion obtained from Eqs. 3.21 and 3.23 would yield conservative results.

The fact that in Figs. 3.37, 3.38, and 3.39 the computed value of the shear stress at failure for each specimen larger than the possible limiting value $15\sqrt{f_c'}$ indicates that each specimen failed at a higher level of shear stress than that predicted by the web crushing criteria given in Eq. 3.22. Therefore, the requirement that $f_d$ be limited to $30\sqrt{f_c'}$ appears to be very conservative. The lack of ductility in web crushing failures makes it highly desirable to be very conservative in this area.

In Fig. 3.40 the values of the shear stress at failure due to web crushing from shear and/or torsion, are compared with $f_c'$ for each of the specimens of Tables 3.24, 3.25, 3.26 and 3.27. Also shown are the upper limits of $10\sqrt{f_c'}$ for shear and $12\sqrt{f_c'}$ for torsion as given the in current AASHTO Specifications. The proposed new limit of $15\sqrt{f_c'}$ is plotted for comparison.

Figure 3.40 shows that the proposed limit of $15\sqrt{f_c'}$ is a conservative and realistic requirement and is somewhat less restrictive than the current upper limits in the AASHTO Standard Specifications (12,17).

With regard to the proposed limit on the value of $f_c$ as a function of $f'_c$ the test results reviewed in this section indicate that the limit should be extended to include an $f'_c$ of approximately 7000 psi. The new limit of 7000 psi is proposed due to the fact that it is the range covered by the available test data. Further information is required on very high strength concretes although the data trends look generally favorable.

## 3.7 Different Types of Failure

In this section those tests reported in references cited in Secs. 3.2, 3.3, and 3.4, which were excluded from tables and plots in those sections because both longitudinal and transverse reinforcement had not yielded at failure, are evaluated to ascertain the truss model accuracy in predicting the ultimate strength of such members. Theoretically, such members would not be covered by full truss behavior. Also in this section, several members in which the truss model predicted strength was not achieved because of poor detailing are examined.

3.7.1 Torsion. The test data shown in Tables 3.28 and 3.29 include pure torsion tests on reinforced and prestressed concrete beams of rectangular, inverted T and I cross section.

The test data shown in Table 3.28 include those beams in which only longitudinal reinforcement yielded at failure. The mean of the ratio of test to predicted torsional moment is 1.02 with the standard deviation 0.15. Table 3.29 includes data on beams in which only transverse reinforcement yielded prior to failure. The mean of the

Tests reported by Hsu (82) on reinforced concrete rectangular beams

| (1) Member ID | (2) r | (3) Ttest k-in | (4) Tu (Eq.3.1) K-in | (5) α(Eq.3.23) degrees | (6) (3)/(4) | (7) vtest Eq.3.23 Ksi | (8) v(max) Eq.3.22 Ksi | (9) (7)/(8) | (10) Level of Prestress σ/f'c |
|---|---|---|---|---|---|---|---|---|---|
| B10 | 1.0 | 304 | 362 | 23 | 0.84 | 1.09 | 0.93 | 1.17 | 0.0 |
| M3 | | 388 | 387 | 38 | 1.00 | 1.35 | 0.93 | 1.44 | |
| M4 | | 439 | 499 | 38 | 0.88 | 1.57 | 0.93 | 1.69 | |
| M5 | | 493 | 638 | 37 | 0.77 | 1.81 | 0.96 | 1.64 | |
| J3 | | 312 | 370 | 43 | 0.84 | 1.05 | 0.74 | 1.41 | |
| G3 | | 439 | 414 | 43 | 1.06 | 1.05 | 0.94 | 1.12 | |

X = 0.90
S = 0.11

Tests reported by McMullen and Rangan (114) on reinforced concrete rectangular beams

| A1R | 1.0 | 111 | 90 | 44 | 1.23 | 0.52 | 1.10 | 0.47 | 0.0 |

Tests reported by Mitchell and Collins (120) on prestressed concrete rectangular beams

| P5 | 1.0 | 995 | 1098 | 24 | 0.91 | 1.35 | 1.13 | 0.66 | 0.30 |

Tests reported by Wyss, Garland and Mattock (173) on prestressed concrete I-beams

| A4 | 0.29 | 430 | 569 | 26 | 0.76 | 3.64 | 1.16 | 3.13 | 0.19 |
| B5 | 0.33 | 544 | 443 | 47 | 1.23 | 4.60 | 1.16 | 3.96 | 0.09 |

X = 1.0
S = 0.33

Overall for Table 3.29
X = 0.95
S = 0.17

Table 3.29   Data on reinforced and prestressed concrete beams under pure torsion with only yielding of the transverse reinforcement prior to failure

from Sec. 3.6. If this is done, then all the values would be much greater than 1.

It appears that the lack of yielding of either one of the types of reinforcement increases the scatter in the accuracy of the basic truss model predictions. Such lack of yielding can be treated by improved truss model versions which are not as simple for design purposes (180,182).

This scatter is caused by the partial overreinforcement of the member, which induces at failure large tensile stresses in the other reinforcement together with excessive compression stresses in the diagonal strut of the truss model. These large stresses sometimes would lead to premature failures due to crushing of the concrete. These types of failure must be prevented in the truss model design approach.

3.7.2 Torsion-Bending. Shown in Table 3.30 are test data on reinforced and prestressed concrete beams of trapezoidal and rectangular solid and hollow cross sections subjected to combined torsion and bending. The test data from Ref. 86 in Table 3.30 belongs to beams where only the transverse reinforcement yielded at failure. Tests from Ref. 161 and specimen D1 from Ref. 33 belong to beams where only the longitudinal steel yielded prior to failure. In specimens D2 and D3 from Ref. 33, and specimen 1 from Ref. 70, neither yielding of the transverse or the longitudinal reinforcement was reported at failure.

Shown in column (5) of Table 3.30 are the values of the previously explained dispersion index I (see Fig. 3.5), which is used as a measure of the dispersion between test obtained values and truss model

predictions, as given by the proper interaction equations, measured along radial lines from the origin. The mean of the dispersion index I for all the specimens shown in Table 3.30 is 0.88 and the standard deviation 0.14.

It seems that the truss model predictions become unconservative in the case of combined torsion-bending in the case of members where yielding of both reinforcements is not reached at failure. More so in the cases where yielding of the longitudinal reinforcement is not reached prior to failure. However, these apparent unconservative results again can be explained by the effect of partial overreinforcement discussed in the previous section. The large compression stresses induced by the partial overreinforcement eventually lead to failure due to crushing of the concrete in the web such as in the case of member D3 on Table 3.30. In these cases the value of $T_u$ should be based on the web crushing limits suggested in Sec. 3.6. If this is done then the values obtained would be very conservative. Better agreement should be possible if the effective shell thickness is determined as suggested by Marti (182).

3.7.3 Torsion-Bending-Shear. Table 3.31 shows data on prestressed concrete beams of rectangular solid and box sections where only yielding of the transverse reinforcement was reported at failure. The dispersion index I shown in column (6) of Table 3.31 is once again used as a measure of the accuracy of the truss model predictions in the same manner previously explained in Sec. 3.4.

For the data shown in Table 3.31 the mean of the dispersion index I is 1.26 and the standard deviation 0.31. In this case the truss model predictions seem to be overconservative. Very few specimens were under strength. The few which experienced lower values were well within normal scatter. There was considerably more scatter in the dispersion index. This indicates that the lack of yielding of both reinforcements introduced other factors that are not adequately represented by the truss model.

The test data shown in Table 3.32 are for prestressed rectangular beams experiencing only yielding of the longitudinal reinforcement at failure. The very conservative predictions obtained in these cases seem to confirm the assumption that members experiencing only yielding of the longitudinal reinforcement at failure might be in a transition state between the uncracked and the full truss state as far as shear stresses are concerned. This would introduce an additional concrete contribution to the ultimate shear capacity of the member. This would explain the conservative results given by the truss model in such cases.

3.7.4 Failures Due to Inadequate Detailing. During the course of this study it was made clear that adequate detailing is of utmost importance in the design approach using the truss analogy in the case of members subjected to shear, torsion-bending, or combined torsion-bending-shear.

In this section several cases of failure due to inadequate detailing are studied to highlight the importance of adequate detailing

in the design as well as to illustrate how the truss model can be useful to handle the special detailing cases.

Shown in Table 3.33 are data for prestressed concrete inverted T bent caps failing prematurely due to inadequate detailing. Specimens TP43, TP54, and TP63 from Ref. 116 were prestressed concrete inverted T bent caps subjected to pure torsion (see Fig. 3.41a). As reported in Ref. 116, failure of specimens TP43 and TP54 was due to a combination of punching action and bracket action in the bottom flange of the inverted T bent cap. In specimen TP63, failure was entirely due to punching action. Punching action failure of the flange occurred by punching of the concrete along a truncated pyramid around the concentrated load (see Fig. 3.41b). This phenomenon caused the separation of the pyramid from the bottom of the beam without any crushing of the concrete in the compression zone of the flange. The other contributor to the failure mechanism was produced by the flange acting as a short bracket to transmit the load to the web. This phenomenon was analyzed in Sec. 2.2.3 of this study. As previously explained, the truss model can be used to determine the necessary transverse reinforcement in the flange. Supplementary horizontal transverse reinforcement should be distributed as shear friction reinforcement to control cracking along the potential slip plane. If the crack faces are rough and irregular, any slip will be accompanied by a horizontal separation of the crack faces. At ultimate the horizontal crack separation will be sufficient to stress this reinforcement to its yield point.

$P_1$ $P_2$

$\epsilon$ $\epsilon$
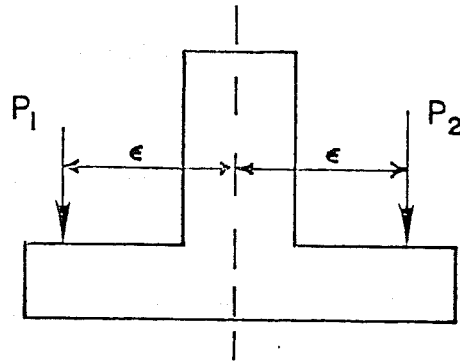
$P_1 > P_2$

$T = ( P_1 - P_2) \epsilon$

(a) Typical cross section

P
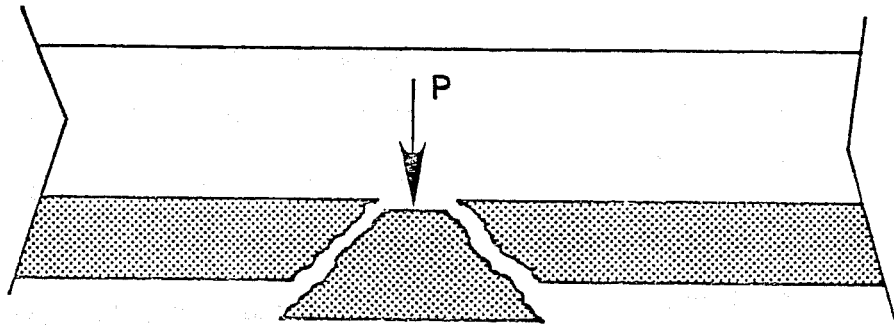
(b) Punching failure (sideview)

P
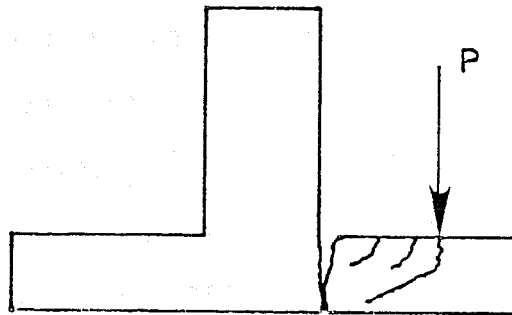
(c) Bracket action

Fig. 3.41  Cross section and types of premature failures
due to improper detailing occurring in
specimens TP43, TP54, and TP63 (from Ref. 116)

beams
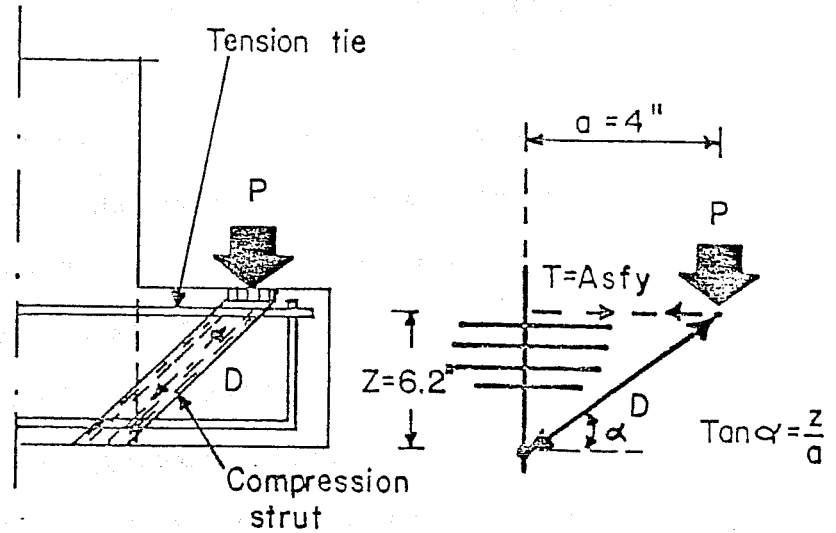
(a) Truss analogy for the flange region together with well distributed horizontal shear reinforcement
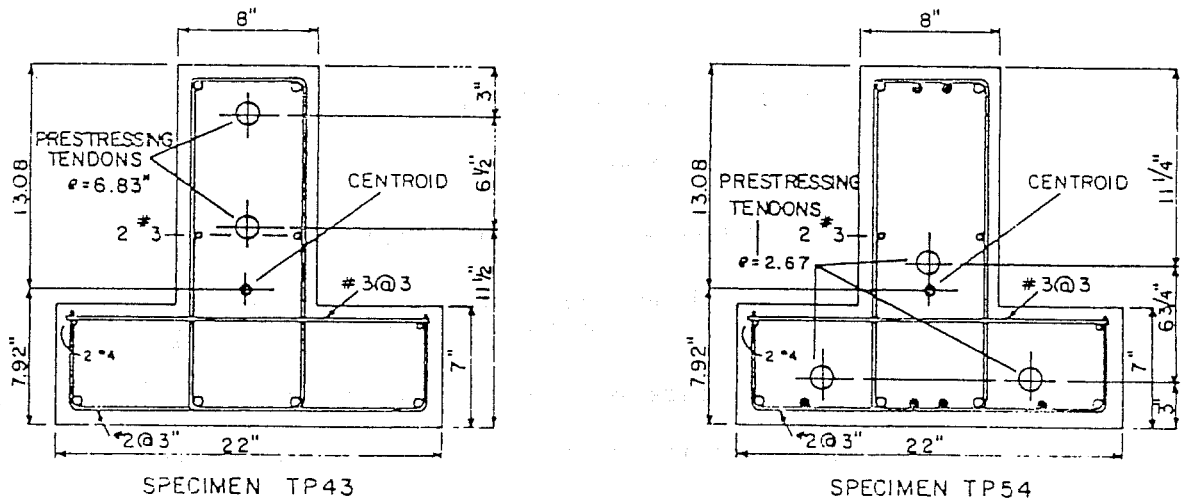


(b) Details of specimens TP43 and TP54 (from Ref. 116)

Fig. 3.42   Truss model and reinforcement details of the web flange connection region of the inverted T-bent cap

The importance of good detailing is shown in the values of the ratio of torsional moment at failure to the predicted torsional capacity shown in Table 3.33. The mean of the ratio was 0.63 and the standard deviation 0.07. This clearly indicates the danger involved in the case of premature failures, i.e. failures where yielding of the steel reinforcement is not reached because of improper detailing of the member.

Table 3.34 shows data on reinforced concrete L-beams under combined torsion-bending-shear which failed prematurely due to inadequate detailing. Specimens 3LS-4 and 3LS-7 from Ref. 104 failed locally at the supporting diaphragms. Unfortunately in this case, no more information was available in regard to the actual causes of failure. Although beam 3LS-4 shows unconservative results, beam 3LS-7 seemed to yield reasonable results. However, without more information no further conclusions can be drawn from these two specimens.

Shown in Table 3.35 are data for specimen 0.5B from Ref. 50. This specimen was a prestressed concrete I-beam with web reinforcement and a composite slab cast on top. Beam 0.5B was about a one-half scale model of the Texas Standard Type B girder. This member was subjected to a uniformly distributed load. Specimen 0.50B was tested in a different phase of this research project. Details of all the specimens as well as the loading scheme are reported by Castrodale (50).

Figure 3.43 shows details of the cross section at the end regions of the member. Figures 3.44a and 3.44b illustrate the premature failure that took place during the testing of this specimen.

STIRRUP (TYP)
PRESTRESSING STRAND
(TYP)
NON-PRESTRESSED
REINFORCEMENT (TYP)

ADDED BAR OVER
BEARINGS
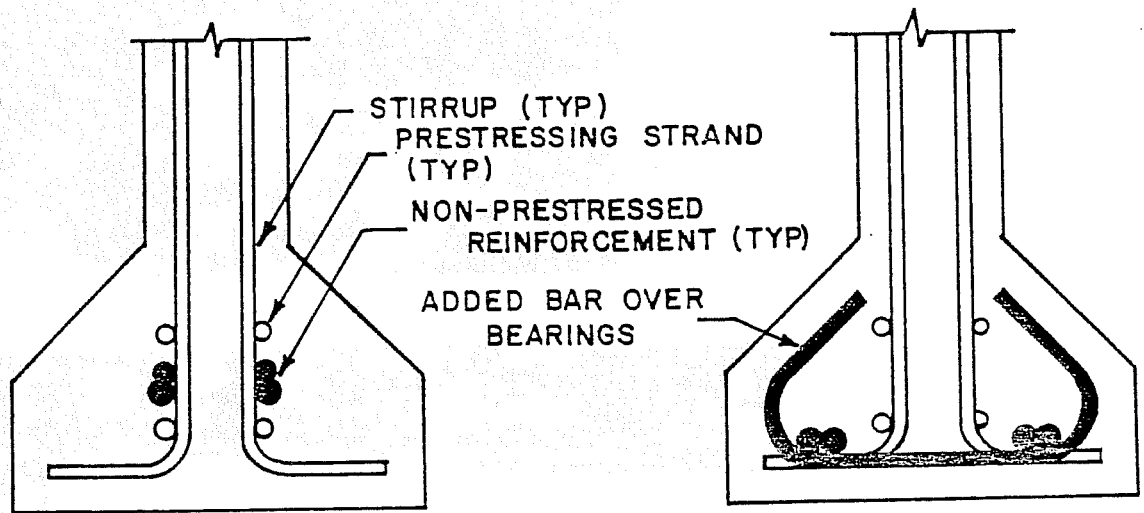
(a) Specimen 0.5B (also
Specimens 0.5A and
0.4A)

(b) Revised cross section
for Specimens 0.4B and
0.45

Fig. 3.43   Revision in reinforcement detailing at the end
region due to premature failure of specimen 0.5B

As can be seen from Fig. 3.44a there was a complete separation of the bottom flange from the vertical web of the member at the bearing. The mechanisms involved in this premature failure due to improper detailing are examined with the aid of the truss model.

Figure 3.45a from Ref. 56 illustrates the fanning effect of the diagonal compression struts of the truss model at the end regions of the member. This fanning effect, previously explained in Sec. 2.2.2, results in high diagonal compression stresses which in the case of flange sections are directly transmitted through the vertical web of the member.

The concentration of diagonal compression stresses can be attenuated by adequately detailing the longitudinal steel reinforcement at the end regions of the member. As shown in Figs. 3.45b and 3.45c from Ref. 56, the attenuation of the diagonal compression stresses is achieved by distributing the horizontal component of the diagonal compression strut over the entire end region of the members by means of end distribution plates, as shown in Fig. 3.45b, or by the uniform distribution of the longitudinal reinforcement, as shown in Fig. 3.45c.

The large concentration of diagonal compression stresses induced by the improper detailing at the end regions of beam 0.50B was the major cause of the premature failure of this specimen. As can be seen from Fig. 3.43a, the concentration of all the longitudinal reinforcement at one particular location failed to adequately distribute the diagonal compression stresses and caused an excessive concentration of these over the bearing area, as shown in Fig. 3.45a.

This large concentration of diagonal compression forces caused extreme deformation of the neoprene bearing pad. These deformations induced tensile splitting stresses between the web and the bottom flange. Closed stirrups at the end of the girder had been omitted. The lack of horizontal reinforcement across this failure plane allowed the crack to grow without control and finally caused separation of the bottom flange from the web as shown in Figs. 3.44a and 3.44b. In order to prevent this type of failure in subsequent specimens the detailing of the cross section at the end region was changed as shown in Fig. 3.43b. The longitudinal steel was more evenly distributed across the entire tension flange and additional reinforcement to hold the flanges and vertical web together was added over the bearing area. The revised design performed very satisfactorily.

The data shown in Table 3.35 are plotted in Fig. 3.46. The ratios of tested vs predicted values are plotted for different sections along the span of the member. Fig. 3.46 together with the values of the dispersion index I of Table 3.35 for different sections along the span-length of the member clearly illustrate the unconservative results caused by the premature failure of specimen 0.50B due to inadequate detailing.

The examples of premature failures due to improper detailing examined in this section help to illustrate the danger involved from poor detailing procedures. They also help to show how the truss model can be utilized to first spot the problematic regions and then to

adequately detail the member so that its ultimate strength is fully attained.

### 3.8 Evaluation of the Additional Concrete Contribution in the Uncracked and Transition States

In Sec. 2.5 it was suggested that three well-defined failure states could be distinguished in the case of reinforced and prestressed concrete beams subjected to shear and/or torsion. The first is the uncracked state. This failure state is characterized by a shear failure when first inclined cracking of the web occurs. Then there is a transition state for the section at which failure might be in between the uncracked state and its ultimate full truss state. Failure occurs sometime after initial inclined cracking but before full development of the truss state.

In Sec. 2.5 it was also suggested that in the uncracked and transition states the concrete in the web contributes an additional shear resistance. In the uncracked state this concrete contribution is equal to the shear stress necessary to produce initial diagonal cracking in the web of the member, $v_{cr}$, and is taken equal to

$$v_{cr} = 2 \sqrt{f'_c} \qquad (3.24)$$

where $f'_c$ is the specified compressive strength of the concrete, psi.

It should be noted that the a/d or $M/V_d$ effect is not included in the $v_{cr}$ expression. The reason is that the a/d ratio influences the ultimate strength of the member, but it has no bear on the shear stress required to produce initial diagonal cracking.

Figure 3.47 shows the proposed concrete contribution in the uncracked and transition states for the case of reinforced concrete members. Since only underreinforced sections are being considered and premature failures due to either crushing of the concrete or poor detailing are avoided, the presence of prestress will only influence the cracking load and will not influence the ultimate load of prestressed concrete members (162,165,166) in the full truss state.

Consider the case of a prestressed concrete member prior to cracking subjected to a bending moment and a shear force. The Mohr circle for an element at the neutral axis of the member is shown in Fig. 3.48.

From Fig. 3.48, it becomes apparent that since the resulting principal tension stress is smaller than the applied shear stress the cracking load for the member is increased by a factor K due to the presence of prestressing where

$$K = [1 + (f_{ps}/f_t)]^{0.5} \tag{3.25}$$

The term $f_{ps}$ is the compression stress at the neutral axis of the member due to the effective prestress force $F_{se}$ and can be expressed as:

$$f_{ps} = F_{se}/A_c \tag{3.26}$$

where $A_c$ is the gross area of the prestressed concrete member. The term $f_t$ is the principal tensile stress required to produce diagonal cracking of the concrete member, and will be taken equal to $v_{cr}$ from Eq. 3.24. Thus, in the case of prestressed concrete members the concrete

contribution in the uncracked state is taken equal to $K*v_{cr}$. By assuming continuously diminishing resistance function due to the K term, the Swiss Code (156) suggests that the concrete contribution in the transition state varies linearly between the uncracked shear strength of the prestressed concrete member, $K*v_{cr}$ at the beginning of the transition state to a value of zero when the applied shear stress is equal to $(2 + K)*v_{cr}$. However, while $K = \sqrt{1 + f_{ps}/f_t}$ the Swiss code imposes a strict limit of 1 on K in those regions of the member where the resulting extreme fiber tensile stress at ultimate exceeds twice the cracking shear stress $v_{cr}$. Figure 3.49 shows the additional concrete contribution for the case of prestressed concrete members.
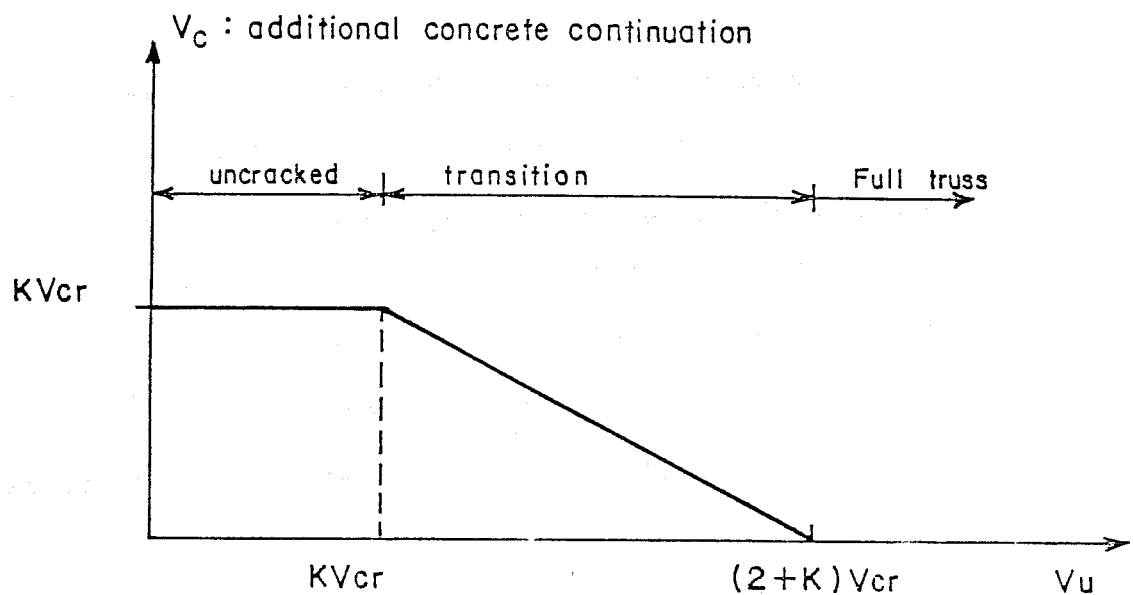


Fig. 3.49  Additional concrete contribution for the case of prestressed concrete members (156, 162)

Transition study

Reinforced (non-prestressed)

| (1) Author | (2) Member ID | (3) vtest Eq.3.21 (ksi) | (4) vcr (ksi) | (5) $\rho vfy$ (psi) | (6) f'c (ksi) | (7) a/d | (8) $\dfrac{vutest}{vcr}$ |
|---|---|---|---|---|---|---|---|
| Richart series 1911 | 291.1 | 0.18 | 0.08 | 0 | 1.69 | 2.4 | 2.25 |
| | 291.2 | 0.16 | 0.08 | | | | 2.00 |
| | 291.3 | 0.19 | 0.08 | | | | 2.38 |
| | 294.1 | 0.18 | 0.08 | | 1.49 | | 2.25 |
| | 294.2 | 0.14 | 0.08 | | | | 5.75 |
| | 294.3 | 0.17 | 0.08 | | | | 2.13 |
| | 293.4 | 0.19 | 0.09 | | 2.35 | | 2.38 |
| Richart series 1917 | 16B20.1 | 0.22 | 0.14 | 0 | 4.77 | 4.8 | 1.57 |
| | 16B20.2 | 0.21 | | | | | 1.50 |
| | 16B1.1 | 0.22 | | | | | 1.57 |
| | 16B1.2 | 0.20 | | | | | 1.43 |
| | 16B2.1 | 0.19 | | | | | 1.36 |
| | 16B2.2 | 0.21 | | | | | 1.50 |
| Richart and Jensen series 1931 | 1 | 0.48 | 0.14 | 0 | 4.76 | 1.52 | 3.43 |
| | 2 | 0.53 | 0.14 | | 4.62 | | 3.79 |
| | 3 | 0.50 | 0.13 | | 4.29 | | 3.85 |
| | 4 | 0.45 | 0.12 | | 3.86 | | 3.75 |
| | 5 | 0.35 | 0.09 | | 2.23 | | 3.89 |
| | 6 | 0.39 | 0.10 | | 2.63 | | 3.90 |
| Moretto 1945 | 1N1 | 0.39 | 0.12 | 0 | 3.55 | 1.75 | 3.25 |
| | 1N2 | 0.49 | 0.12 | | 3.62 | | 4.08 |
| | 2N1 | 0.43 | 0.13 | | 4.34 | | 3.31 |
| | 2N2 | 0.50 | 0.14 | | 4.64 | | 3.57 |
| Clark 1951 | AO-1 | 0.18 | 0.11 | 0 | 3.13 | 2.34 | 1.64 |
| | AO-2 | 0.22 | 0.12 | | 3.77 | 2.34 | 1.83 |
| | BO-1 | 0.25 | 0.12 | | 3.42 | 1.95 | 2.08 |
| | BO-2 | 0.19 | 0.12 | | 3.47 | 1.95 | 1.58 |
| | BO-3 | 0.26 | 0.12 | | 3.41 | 1.95 | 2.17 |
| | CO-3 | 0.34 | 0.12 | | 3.42 | 1.56 | 2.83 |
| | DO-1 | 0.45 | 0.12 | | 3.75 | 1.17 | 3.75 |
| | DO-3 | 0.45 | 0.12 | | 3.765 | 1.17 | 3.75 |

mean = X = 2.6

Standard deviation = S = 0.95

Table 3.36   Test data on beams with no web reinforcement failing in shear (from Ref. 99)

Transition study                                    Reinforced (non-prestressed)

| Author | Member ID | vutest Eq.3.21 (ksi) | vcr (ksi) | ρvfy (psi) | f'c ksi | a/d | $\dfrac{vutest}{vcr}$ |
|--------|-----------|----------------------|-----------|------------|---------|-----|------------------------|
| Moody  |           |                      |           |            |         |     |                        |
|        | 24a       | 0.50                 | 0.10      | 0          | 2.58    | 1.52 | 5.00                  |
| series | 24b       | 0.51                 | 0.11      |            | 2.99    |     | 4.64                   |
| III    | 25a       | 0.45                 | 0.12      |            | 3.53    |     | 3.75                   |
|        | 25b       | 0.49                 | 0.10      |            | 2.50    |     | 4.9                    |
| 1953   | 26a       | 0.71                 | 0.11      |            | 3.14    |     | 6.45                   |
|        | 26b       | 0.67                 | 0.11      |            | 2.99    |     | 6.09                   |
|        | 27a       | 0.59                 | 0.11      |            | 3.10    |     | 5.36                   |
|        | 27b       | 0.60                 | 0.12      |            | 3.32    |     | 5.05                   |
|        | 28a       | 0.51                 | 0.12      |            | 3.38    |     | 4.25                   |
|        | 28b       | 0.58                 | 0.12      |            | 3.25    |     | 4.83                   |
|        | 29a       | 0.76                 | 0.11      |            | 3.15    |     | 6.00                   |
|        | 29b       | 0.74                 | 0.12      |            | 3.62    |     | 6.17                   |

$X$ = mean   =                          5.20
$S$ = st. dev. =                        0.83

Table 3.38   Test data on beams with no web reinforcement
             failing in shear (from Ref. 99)

| | | | failing in Shear | | | Reinforced (non-prestressed) | |
|---|---|---|---|---|---|---|---|
| Transition study | | | | | | | |
| (1) Author | (2) Member ID | (3) vutest Eq.3.21 Ksi | (4) vcr ksi | (5) $\rho_v f_y$ psi | (6) f'c ksi | (7) a/d | (8) $\dfrac{\text{vutest}}{\text{vcr}}$ |
| | 26-1 | 0.29 | 0.15 | 79 | 5.82 | 4.0 | 1.93 |
| Krefeld | 29a-1 | 0.22 | 0.15 | 53 | 5.63 | | 1.47 |
| & | 29b-1 | 0.22 | 0.15 | 53 | 5.46 | | 1.47 |
| Thurston | 213.5-1 | 0.21 | 0.15 | 35 | 5.64 | | 1.40 |
| (90) | 29a-2 | 0.30 | 0.15 | 62 | 5.39 | | 2.00 |
| | 29b-2 | 0.28 | 0.15 | 62 | 6.00 | | 1.87 |
| rectang. | 29c-2 | 0.22 | 0.12 | 62 | 3.50 | | 1.83 |
| sections | 29d-2 | 0.23 | 0.13 | 62 | 4.41 | | 1.77 |
| | 29e-2 | 0.29 | 0.17 | 62 | 7.03 | | 1.71 |
| | 29g-2 | 0.21 | 0.10 | 62 | 2.28 | | 2.10 |
| | 213.5a-2 | 0.22 | 0.15 | 42 | 5.36 | | 1.47 |
| | 218a-2 | 0.23 | 0.15 | 31 | 5.45 | | 1.53 |
| | 29-3 | 0.25 | 0.14 | 40 | 4.97 | | 1.79 |
| | 318-1 | 0.31 | 0.15 | 93 | 5.81 | | 2.07 |
| | 321-1 | 0.23 | 0.15 | 79 | 5.62 | | 1.53 |
| | 318-2 | 0.25 | 0.15 | 64 | 5.65 | | 1.67 |
| | 321-2 | 0.23 | 0.15 | 55 | 5.51 | | 1.53 |
| | 313.5-3 | 0.30 | 0.16 | 65 | 6.19 | | 1.88 |
| | 318-3 | 0.24 | 0.16 | 48 | 6.24 | | 1.50 |
| | 321-3 | 0.20 | 0.16 | 42 | 6.24 | | 1.25 |
| Palaskas | #2 | 0.16 | 0.14 | 0 | 4.75 | 4.14 | 1.14 |
| Attiogbe | A00 | 0.14 | 0.14 | 0 | 4.74 | 3.92 | 1.00 |
| and | A25 | 0.19 | 0.14 | 32 | 4.72 | 3.97 | 1.36 |
| Darwin | A25a | 0.20 | 0.14 | 32 | 4.79 | 4.00 | 1.43 |
| (134) | A50 | 0.25 | 0.12 | 74 | 3.81 | 3.96 | 2.08 |
| T-beams | A50a | 0.24 | 0.13 | 75 | 4.06 | 3.94 | 1.85 |
| | A75 | 0.30 | 0.14 | 97 | 4.67 | 3.92 | 2.14 |
| | B00 | 0.15 | 0.14 | 0 | 4.64 | 3.88 | 1.07 |
| | B25 | 0.17 | 0.13 | 32 | 4.47 | 3.93 | 1.31 |
| | B50 | 0.23 | 0.13 | 76 | 4.39 | 3.96 | 1.77 |
| | C00 | 0.13 | 0.13 | 0 | 4.27 | 3.96 | 1.00 |
| | C25 | 0.18 | | 32 | 4.10 | 3.98 | 1.38 |
| | C50 | 0.29 | | 76 | 4.30 | 3.94 | 2.23 |
| | | | | | | X | 1.62 |
| | | | | | | S | 0.34 |

Table 3.40  Test data on reinforced concrete beams with no
or very light web reinforcement failing in
shear (from Refs. 90, 134)
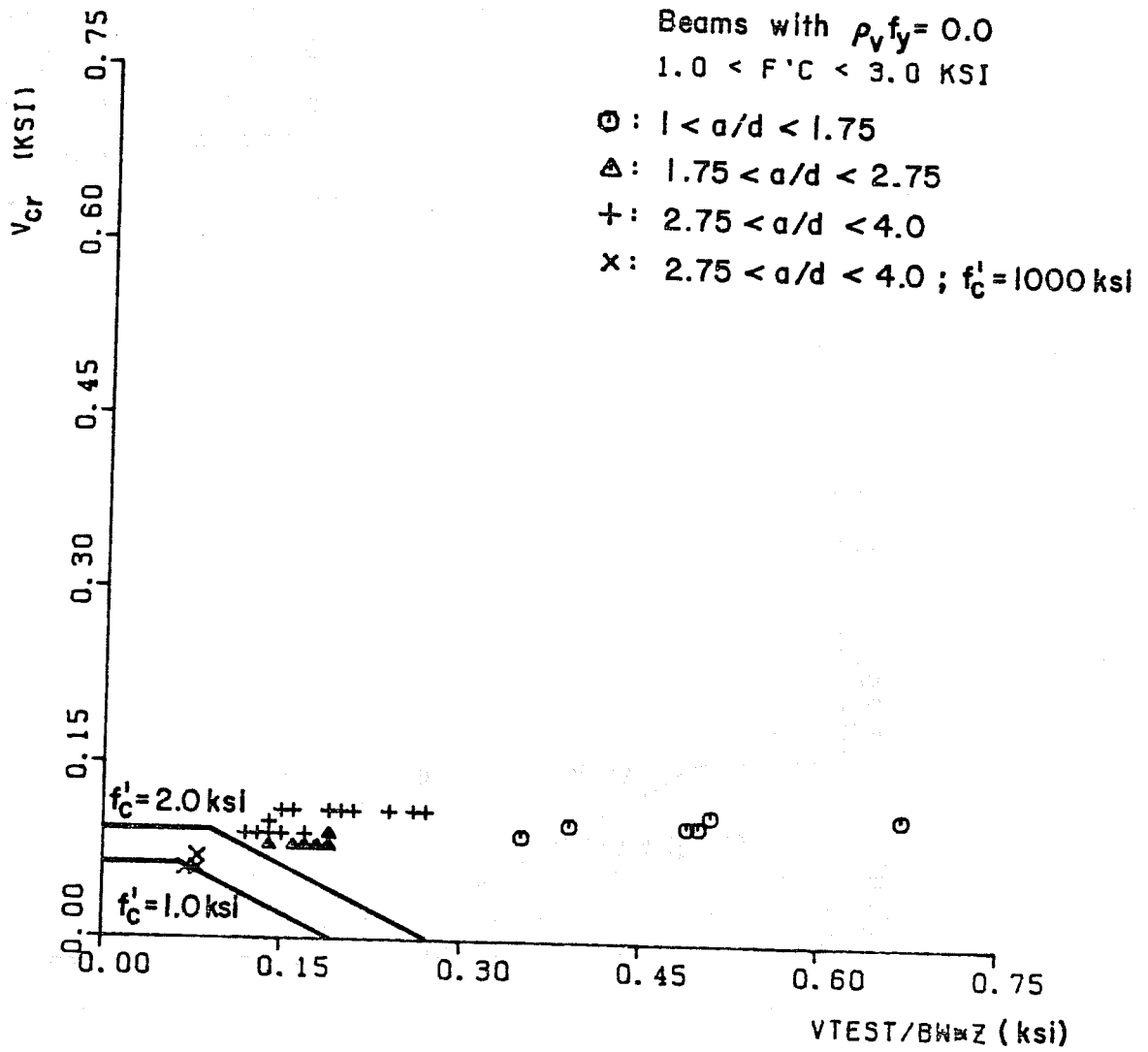
Fig. 3.50   Evaluation of the concrete contribution in
the case of reinforced concrete beams
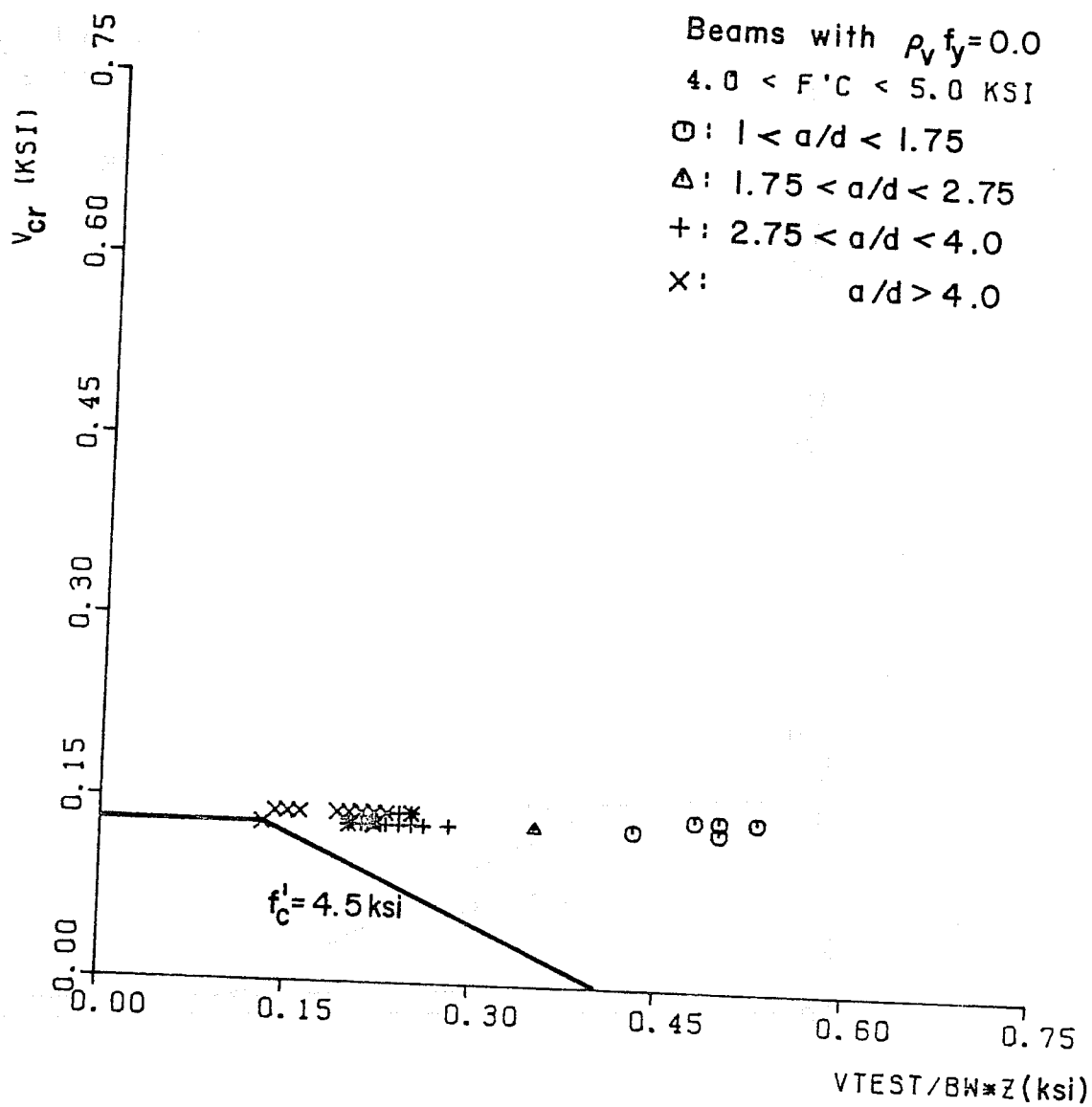
Fig. 3.52    Evaluation of the concrete contribution in
reinforced concrete beams failing in shear

expressions. However, the contribution at this term is relatively small for all except deep beams when shear reinforcement is pre-cut and the resulting complication in design has led many to question its usefulness (108).

The data shown in Table 3.40 for reinforced concrete beams failing in shear containing no or very light amounts of web reinforcement are plotted in Fig. 3.54. The beams shown in Table 3.40 were all tested using an a/d ratio larger than 3.5. Figure 3.54 shows a plot of the data for different values of the concrete compressive strength $f_c'$. Again, the proposed concrete contribution shows to be a safe lower bound. For these larger a/d ratios, the gross conservatism evident in some at the previous plots has vanished.

Tables 3.41 through 3.43 include test data (152) for 90 simply supported prestressed concrete beams. All beams, except four which were tested over a 7 ft. span, had 9 ft. spans and were subjected to bending and shear by means of concentrated loads. Only straight prestressed longitudinal reinforcement was used. The beams were either pretensioned or post-tensioned and grouted. The series included 43 rectangular beams (identified by the first letter A), 33 I-beams with 1.75 inch thick webs (letter C). The term K in Tables 3.41 through 3.43 is computed using Eq. 3.25 but in no case was taken greater than 2.0. The different a/d ratios, together with their respective $f_c'$ were identified for each specimen.

Table 3.41 through 3.43 and Figs. 3.55 through 3.62 show a comparison between the test ultimate shear stresses from column (2) and

Transition study                                                    Prestressed Data

| (1) Author | (2) Member ID | (3) vutest Eq. 3.21 (ksi) | (4) K Actual value | (5) K but<2 | (6) Kvcr (ksi) | (7) ρvfy (psi) | (8) f'c (ksi) | (9) a/d | (10) vutest/Kvcr |
|---|---|---|---|---|---|---|---|---|---|
| Sozen | A.11.43 | 0.28 | 2.37 | 2.0 | 0.31 | 0 | 5.87 | 6.55 | 0.90 |
| | A.11.51 | 0.15 | 2.15 | 2.0 | 0.22 | | 2.96 | 6.40 | 0.68 |
| | A.11.53 | 0.22 | 2.46 | 2.0 | 0.26 | | 4.15 | 6.72 | 0.85 |
| Zwoyer | A.11.96 | 0.21 | 2.82 | 2.0 | 0.21 | | 2.77 | 6.42 | 1.00 |
| Siess | A.12.23 | 0.27 | 1.87 | 1.87 | 0.30 | 0 | 6.27 | 3.86 | 0.90 |
| | A.12.31 | 0.29 | 2.14 | 2.0 | 0.28 | | 4.73 | 4.17 | 1.04 |
| (152) | A.12.34 | 0.38 | 2.22 | 2.0 | 0.34 | | 7.37 | 4.39 | 1.12 |
| | A.12.36 | 0.22 | 1.96 | 1.96 | 0.25 | | 4.18 | 3.92 | 0.88 |
| | A.12.42 | 0.35 | 2.23 | 2.0 | 0.32 | | 6.28 | 4.34 | 1.09 |
| | A.12.46 | 0.32 | 2.42 | 2.0 | 0.26 | | 4.36 | 4.39 | 1.23 |
| | A.12.53 | 0.27 | 2.29 | | 0.22 | | 3.02 | 4.19 | 1.23 |
| | A.12.56 | 0.29 | 2.37 | | 0.26 | | 4.36 | 4.19 | 1.12 |
| | A.12.69 | 0.29 | 2.38 | | 0.24 | | 3.47 | 4.43 | 1.21 |
| | A.12.73 | 0.32 | 2.55 | | 0.23 | | 3.35 | 4.27 | 1.39 |
| | A.12.31 | 0.26 | 2.56 | | 0.22 | | 2.93 | 4.16 | 1.18 |
| | A.14.39 | 0.33 | 2.00 | 2.00 | 0.23 | 0 | 3.44 | 2.87 | 1.43 |
| | A.14.44 | 0.36 | 2.20 | | 0.21 | | 2.80 | 2.82 | 1.71 |
| | A.14.55 | 0.41 | 2.28 | | 0.24 | | 3.66 | 2.81 | 1.71 |
| | A.14.68 | 0.34 | 2.44 | | 0.18 | | 2.13 | 2.85 | 1.89 |
| | A.21.29 | 0.10 | 1.47 | 1.47 | 0.17 | 0 | 3.53 | 6.39 | 0.59 |
| | A.21.39 | 0.12 | 1.65 | 1.65 | 0.17 | | 2.66 | 6.03 | 0.71 |
| | A.21.51 | 0.20 | 1.88 | 1.88 | 0.28 | | 5.77 | 6.65 | 0.71 |
| | A.22.20 | 0.17 | 1.47 | 1.47 | 0.19 | 0 | 4.20 | 4.26 | 0.89 |
| | A.22.24 | 0.16 | 1.46 | 1.46 | 0.16 | | 2.91 | 4.09 | 1.00 |
| | A.22.27 | 0.16 | 1.51 | 1.51 | 0.17 | | 3.35 | 4.30 | 0.94 |
| | A.22.28 | 0.14 | 1.41 | 1.41 | 0.17 | | 3.77 | 4.11 | 0.82 |
| | A.22.31 | 0.18 | 1.70 | 1.70 | 0.20 | | 3.37 | 4.47 | 0.90 |
| | A.22.34 | 0.16 | 1.62 | 1.62 | 0.19 | | 3.53 | 4.33 | 0.84 |
| | A.22.36 | 0.17 | 1.65 | 1.65 | 0.21 | | 3.94 | 4.31 | 0.81 |
| | A.22.39 | 0.12 | 1.35 | 1.35 | 0.14 | | 2.88 | 4.09 | 0.86 |
| | A.22.40 | 0.31 | 1.89 | 1.89 | 0.28 | | 5.44 | 4.39 | 1.11 |
| | A.22.49 | 0.27 | 1.78 | 1.78 | 0.25 | | 4.91 | 4.39 | 1.08 |

Table 3.41   Data on prestressed concrete beams with no web
reinforcement failing in shear (from Ref. 152)

Transition Study                                                         <span>Prestressed Data</span>

| (1) Author | (2) Member (ID) | (3) vutest Eq. 3.21 (ksi) | (4) K Actual value | (5) K | (6) Kvcr | (7) $\rho_{vfy}$ (psi) | (8) f'c (ksi) | (9) a/d | (10) vutest / Kvcr |
|---|---|---|---|---|---|---|---|---|---|
| Sozen | B.32.11 | 0.20 | 1.0 | 1.0 | 0.14 | 0 | 5.00 | 3.46 | 1.43 |
|  | B.32.19 | 0.19 |  |  | 0.14 |  | 4.58 | 3.53 | 1.36 |
|  | B.32.31 | 0.14 |  |  | 0.10 |  | 2.62 | 3.53 | 1.40 |
|  | B.32.34 | 0.18 |  |  | 0.10 |  | 2.62 | 3.53 | 1.40 |
|  | B.32.41 | 0.29 |  |  | 0.10 |  | 2.36 | 3.56 | 1.80 |
| Zwoyer | B.32.54 | 0.27 |  |  | 0.10 |  | 2.57 | 3.47 | 2.70 |
| Siess | C.12.09 | 0.49 | 1.74 | 1.74 | 0.27 |  | 6.22 | 3.26 | 1.81 |
|  | C.12.18 | 0.61 | 2.09 | 2.0 | 0.26 |  | 4.38 | 3.72 | 2.35 |
| (152) | C.12.19 | 0.70 | 2.13 | 2.0 | 0.31 |  | 5.89 | 3.56 | 2.26 |
|  | C.12.32 | 0.51 | 2.61 |  | 0.17 |  | 1.88 | 3.65 | 3.00 |
|  | C.12.33 | 0.76 | 2.67 |  | 0.29 |  | 5.39 | 3.57 | 2.62 |
|  | C.12.40 | 0.41 | 2.28 |  | 0.22 |  | 2.89 | 3.72 | 1.86 |
|  | C.12.44 | 0.44 | 2.28 |  | 0.25 |  | 3.99 | 3.79 | 2.76 |
|  | C.12.50 | 0.57 | 2.76 |  | 0.22 |  | 3.10 | 3.60 | 2.59 |
|  | C.12.57 | 0.81 | 2.99 |  | 0.22 |  | 3.10 | 3.63 | 2.62 |
|  | C.22.29 | 0.28 | 1.59 | 1.59 | 0.15 | 0 | 2.27 | 3.46 | 1.87 |
|  | C.22.31 | 0.37 | 1.71 | 1.71 | 0.21 |  | 3.65 | 3.31 | 1.76 |
|  | C.22.36 | 0.33 | 1.88 | 1.88 | 0.23 |  | 3.60 | 3.52 | 1.43 |
|  | C.22.39 | 0.23 | 2.03 | 2.0 | 0.13 |  | 1.03 | 3.54 | 1.77 |
|  | C.22.40 | 0.59 | 2.48 | 2.0 | 0.27 |  | 4.54 | 3.65 | 2.19 |
|  | C.22.46 | 0.41 | 2.02 | 2.0 | 0.23 |  | 3.44 | 3.56 | 1.78 |
|  | C.22.62 | 0.35 | 1.91 | 1.91 | 0.19 |  | 2.51 | 4.00 | 1.84 |
|  | C.22.73 | 0.44 | 2.43 | 2.0 | 0.20 |  | 2.46 | 3.63 | 2.20 |
|  | C.32.11 | 0.30 | 1.0 | 1.0 | 0.17 | 0 | 6.87 | 3.25 | 1.76 |
|  | C.32.22 | 0.33 |  |  | 0.13 |  | 3.92 | 3.60 | 2.54 |
|  | C.32.37 | 0.29 |  |  | 0.12 |  | 3.63 | 3.60 | 2.42 |
|  | C.33.42 | 0.25 |  |  | 0.10 |  | 2.61 | 3.56 | 2.50 |
|  | C.32.50 | 0.31 |  |  | 0.11 |  | 2.82 | 3.37 | 2.82 |
|  | C.32.80 | 0.34 |  |  | 0.11 |  | 3.25 | 3.60 | 3.09 |

* Specimens A.12.48, A.12.60, A.22.26, A.32.08, A.32.11, A.32.17, V.11.07, V.12.07, V.13.07 failed in flexure

Combined of Tables 3.41, 3.42 and 3.43          X = 1.55
                                                S = 0.63

Table 3.43   Data on prestressed concrete beams with no web
             reinforcement failing in shear (from Ref. 152)
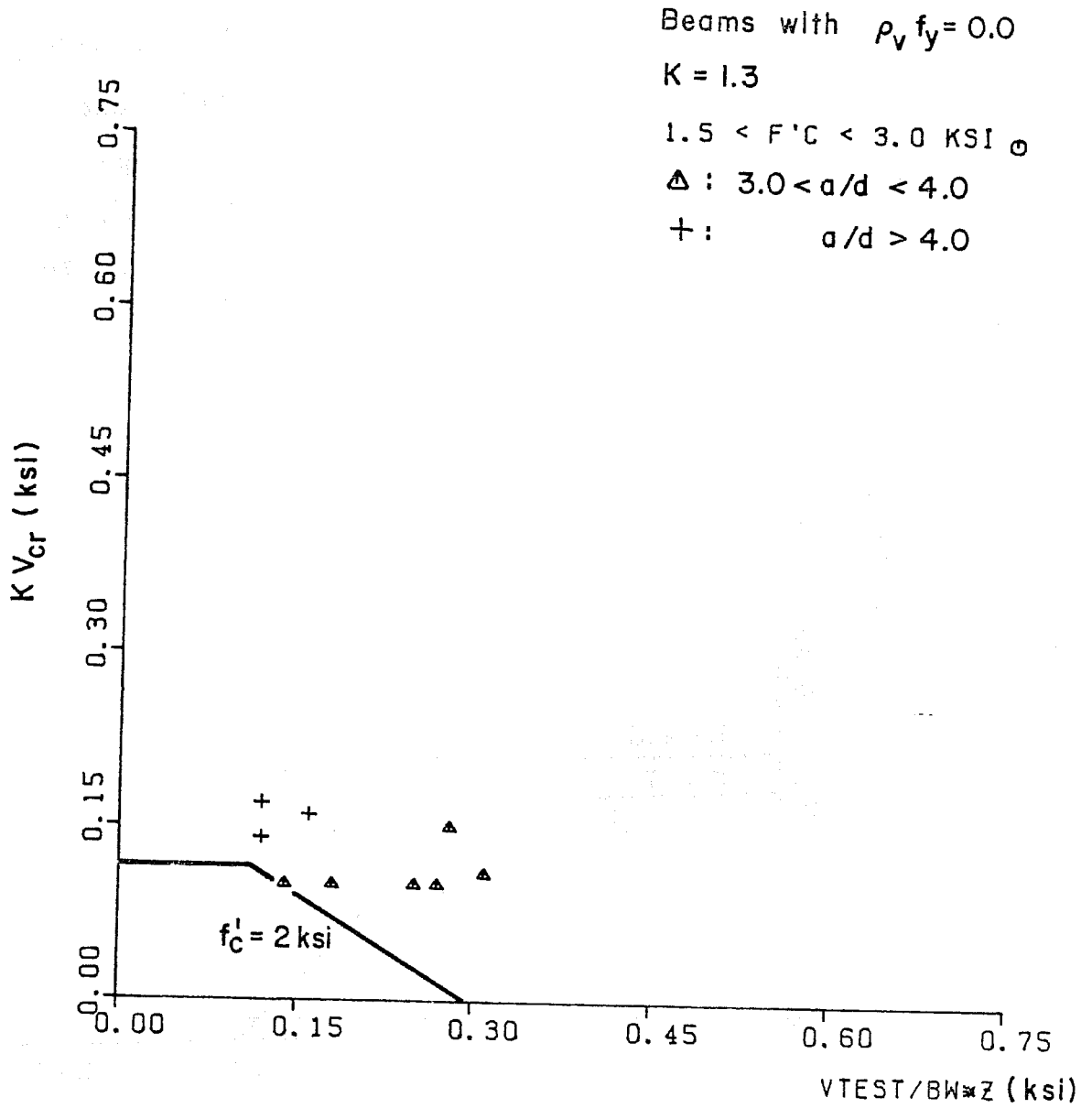
Fig. 3.56 Evaluation of the concrete contribution in
prestressed concrete members failing in
shear with K = 1.3
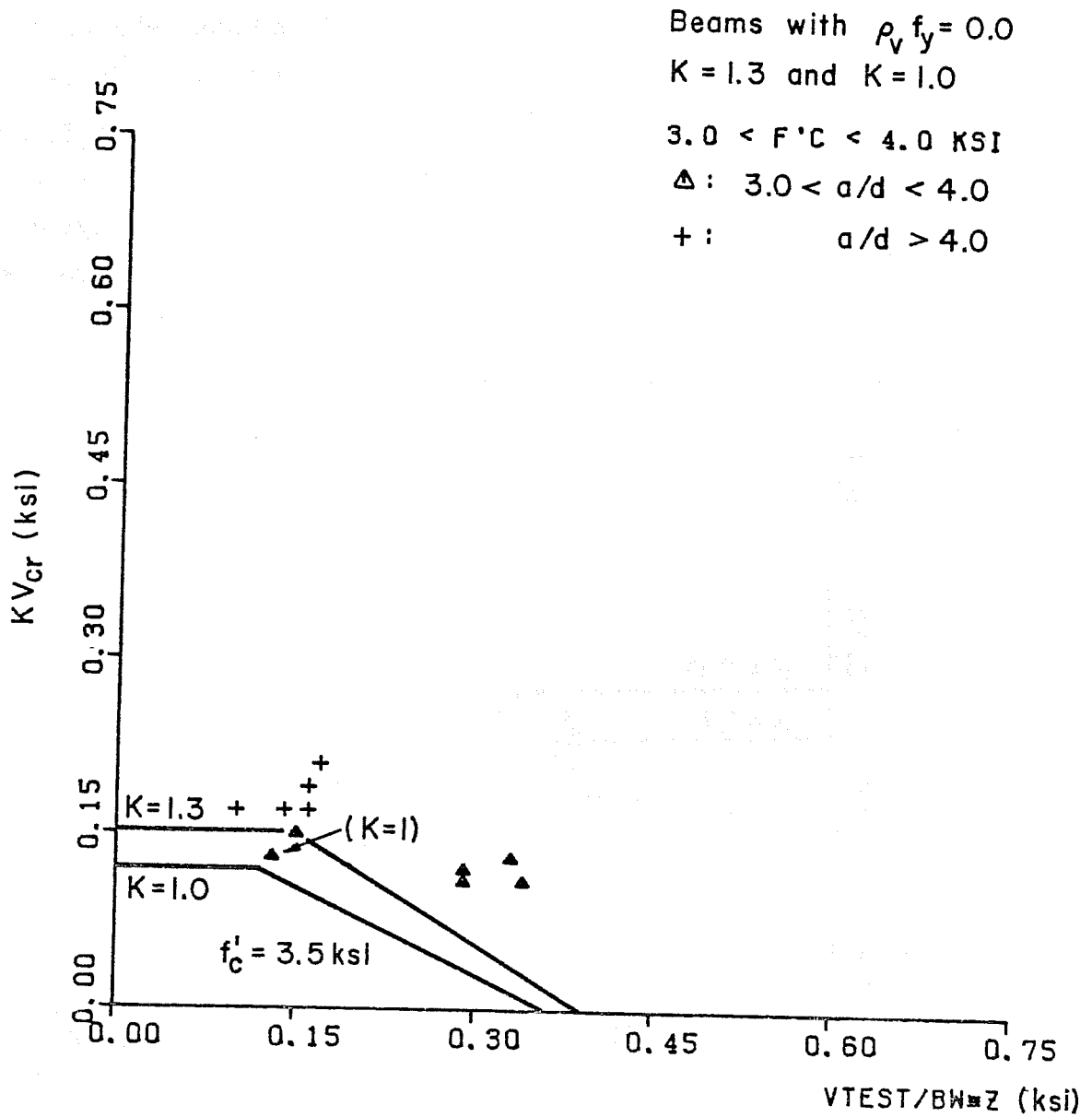
Fig. 3.58 Evaluation of the concrete contribution in
prestressed concrete beams failing in shear
with values of K = 1.3 and K = 1.0

Beams with $\rho_v f_y = 0.0$

$4.0 < F'C < 5.0$ KSI

$K = 1.0$ and $K = 1.3$

$\triangle : 3.0 < a/d < 4.0 ; K = 1.0$

$+ : \quad\quad a/d > 4.0 ; K = 1.3$

$KV_{cr}$ (ksi)

K=1.3

K=1.0

$f'_c = 4.5$ ksi

VTEST/BW*Z (ksi)
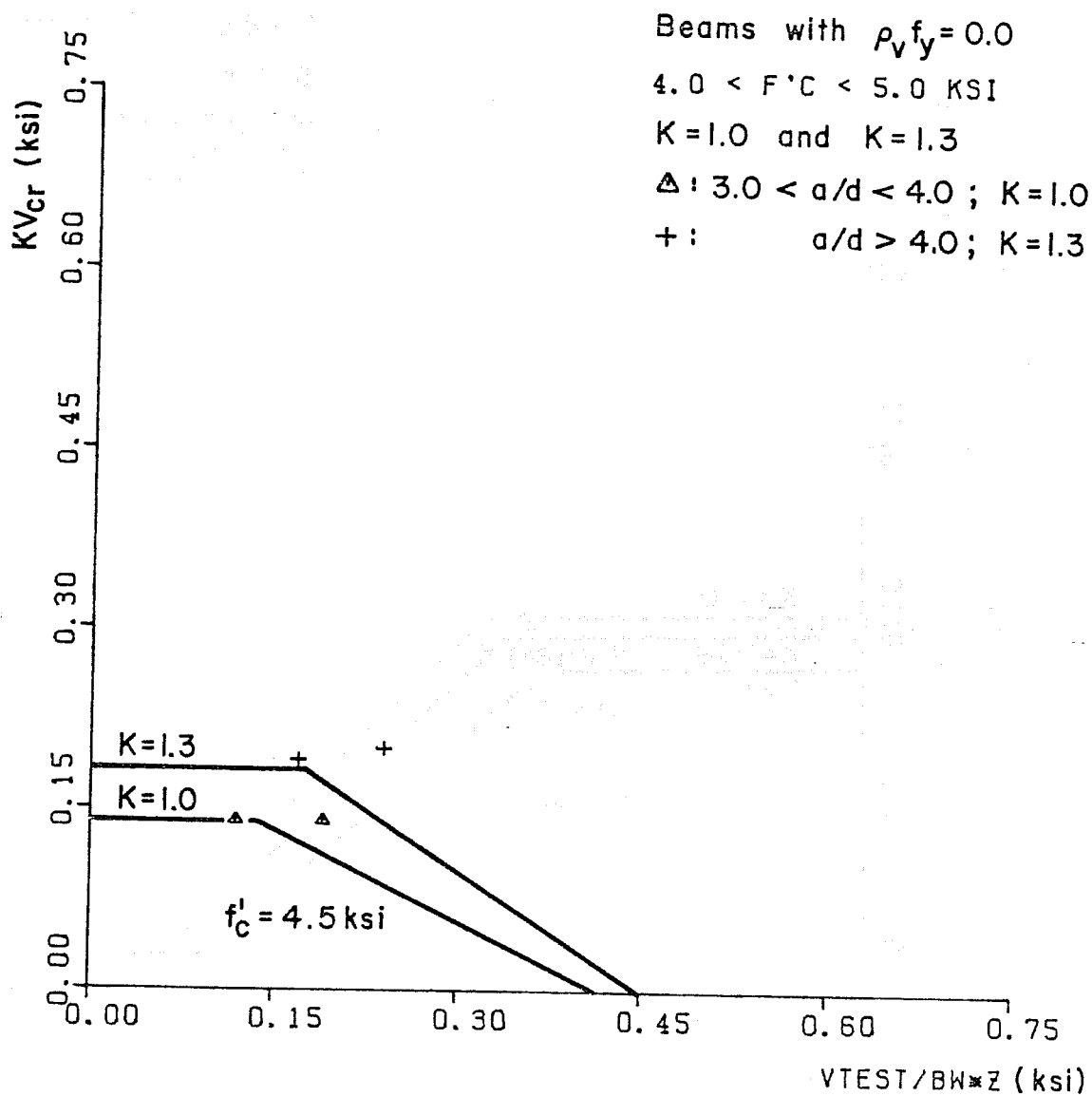
Fig. 3.60   Evaluation of the contrete contribution in
prestressed concrete beams failing in shear
with values of K = 1.3 and K = 1.0
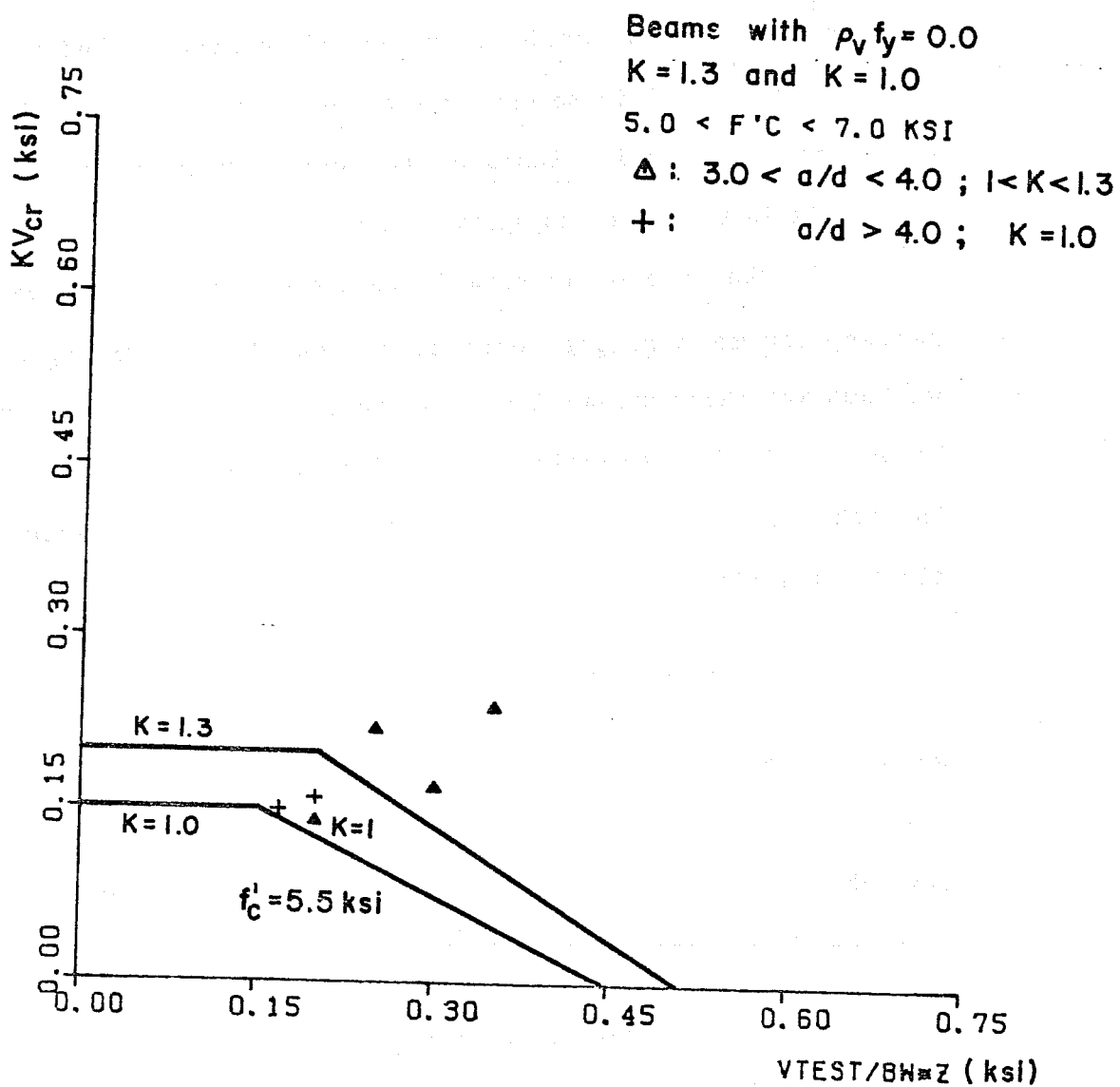
Fig. 3.62  Evaluation of the concrete contribution in
prestressed concrete beams failing in shear
with values of K = 1.3 and K = 1.0
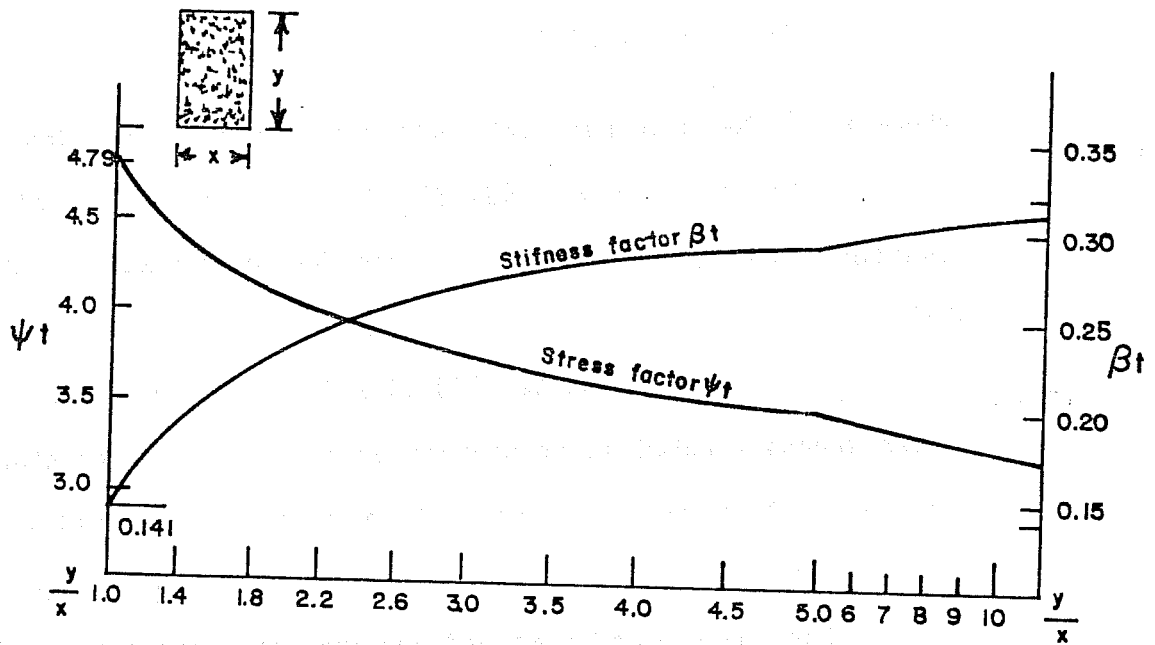
Fig. 3.63  Stiffness and strength factor for rectangular
section subjected to torsion (from Ref. 135)

torsional strength of a plain concrete section will be between the
values predicted by the plastic and elastic theories.  In light of this
fact, The ACI Committee 438 (34) proposed that the ultimate shear stress
induced by torsion in plain concrete be evaluated as

$$v_T = 3T_u/[x^2 y]$$

(3.30)

where $x < y$.  The value of 3 for $\psi_t$ is a minimum for the elastic theory
and a maximum for the plastic theory (see Fig. 3.63 and Eq. 3.29).  In

plotted experimental points (33) were found to be respectively

$$v_V = 2.68 \sqrt{f_c'} \text{ (psi)} \tag{3.33}$$

and

$$v_T = 4.8 \sqrt{f_c'} \text{ (psi)} \tag{3.34}$$

ACI 318-77 (24) suggests that the nominal shear stress be taken as $2\sqrt{f_c'}$ for the case of shear, and $2.4\sqrt{f_c'}$ for the case of torsion. This relatively small difference between the shear and torsion values seems to be an unnecessary complication for combined actions since minimum web reinforcement should always be present in combined actions states.

In light of the previous discussion it is suggested that the concrete contribution in the uncracked and transition states for reinforced beams subjected to torsion and/or shear be taken the same as shown in Fig. 3.47 with the value of $v_{cr}$ assumed as $2\sqrt{f_c'}$.

Shown in Table 3.44 are data from reinforced concrete rectangular beams with no web reinforcement subjected to pure torsion. Fig. 3.64 shows an evaluation of the proposed concrete contribution. As can be seen from this plot, the proposed concrete contribution for the case of members under pure torsion constitutes a safe lower bound.

In the case of prestressed concrete members subjected to torsion, the concrete contribution shown in Fig. 3.49 is evaluated using the test data shown in Table 3.45. The data in Table 3.45 are plotted for comparison in Figs. 3.65 through 3.67. As can be seen from these plots, the proposed concrete contribution in the uncracked and transition states for the case of prestressed concrete members
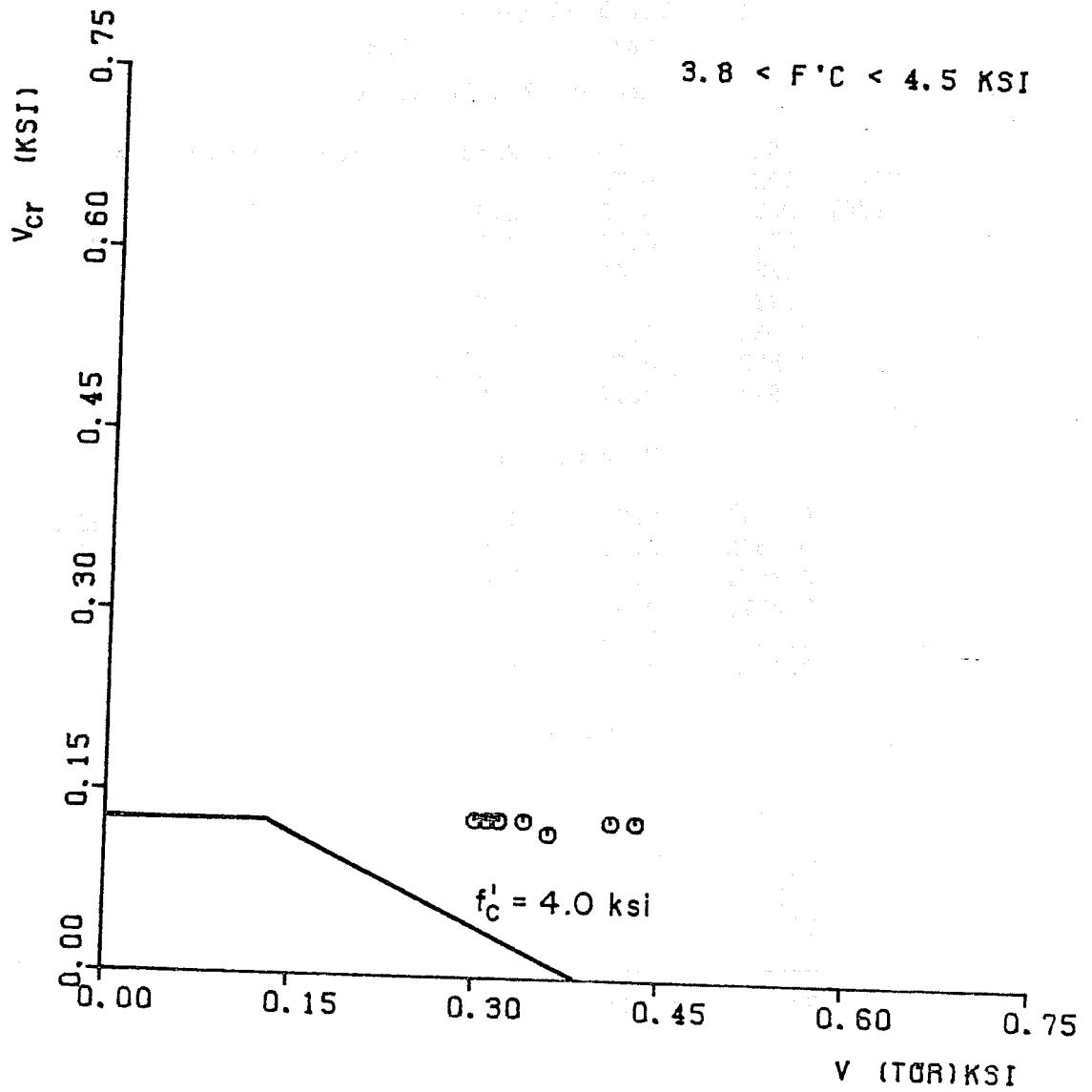
Fig. 3.64   Evaluation of the concrete contribution in
reinforced concrete rectangular members
under pure torsion

$8.0 < F'C < 8.55$ KSI
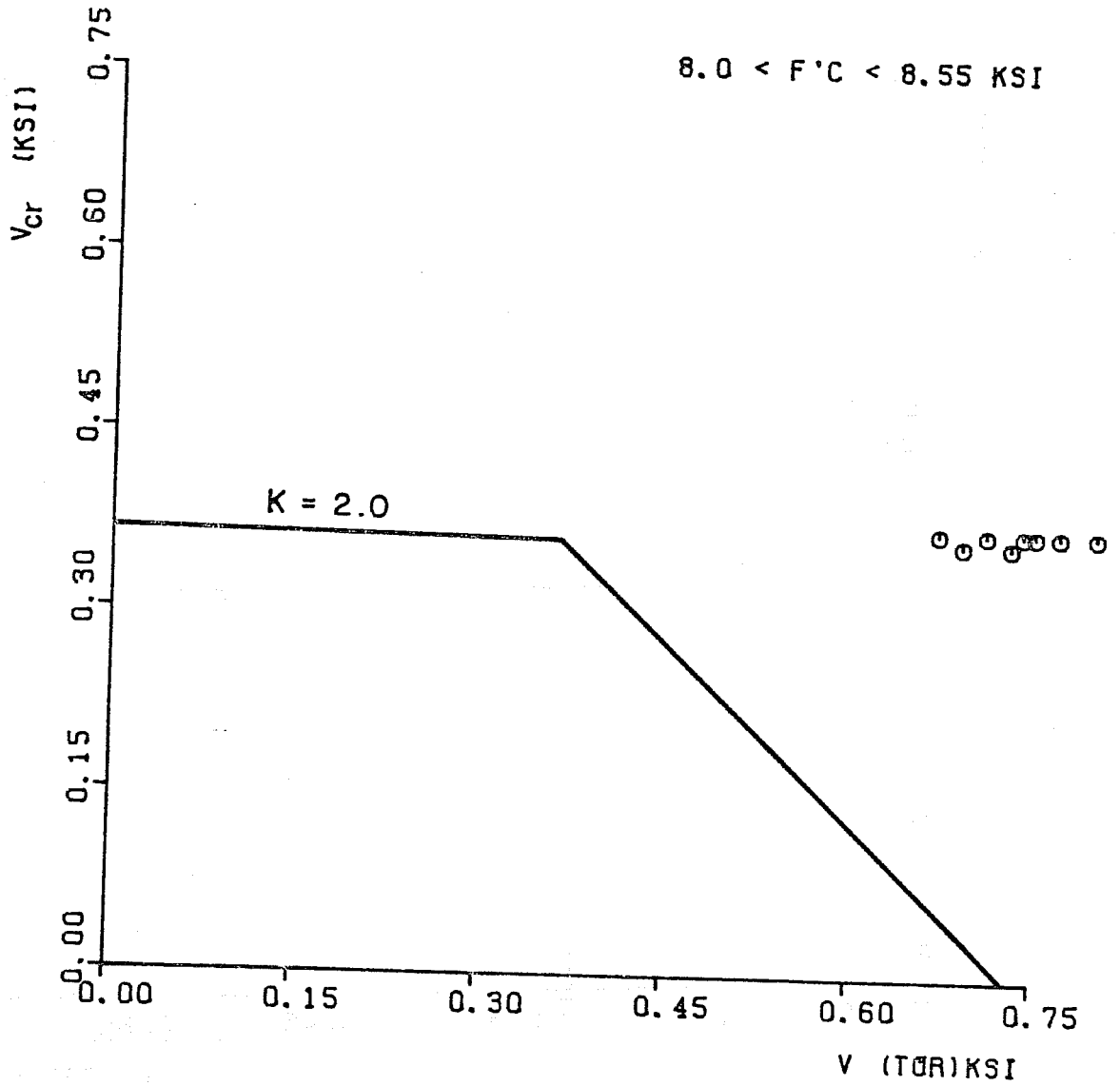


Fig. 3.65 Evaluation of the concrete contribution in prestressed concrete rectangular members subjected to torsion with K = 2.0

4. 75 < F'C< 6. 30 KSI

K = 2.0
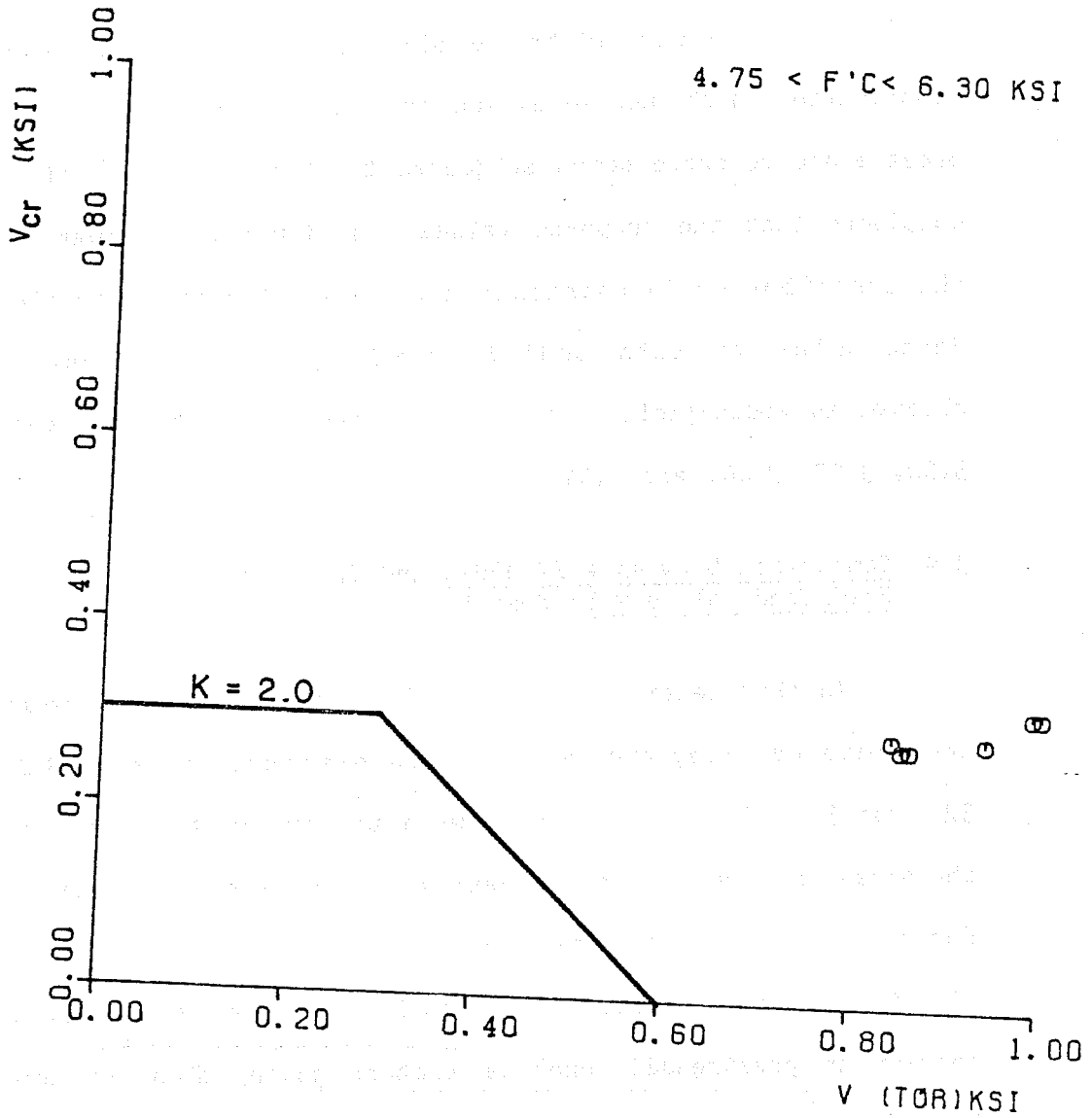
Fig. 3.67    Evaluation of the concrete contribution in prestressed concrete I-beams subjected to torsion with K = 2.0

3.9.1 <u>Torsion.</u> In the case of pure torsion the ACI/AASHTO ultimate strength is evaluated in accordance with the guidelines given in Refs. 24 and 12 discussed in Sec. 2.4 of Report 248-2.

Shown in Tables 3.46 through 3.50 are data on reinforced concrete rectangular, L, and I-beams subjected to pure torsion previously examined in Sec. 3.2. Specimens B6, M6, I6, J4, G5, K4, C3, C4, C5, and C6 from Ref. 82 and D5, D6, and C6 from Ref. 173 failed in a web crushing mode and have already been used in Sec. 3.6 to compare the proposed upper limit for the diagonal compression stress with the current ACI/AASHTO upper limits to prevent web crushing, and thus are not included in this section. Figure 3.68 shows a comparison between the ACI/AAHSTO and Truss Model predicted ultimate strength using the data from Tables 3.46 through 3.50. As can be seen from Fig. 3.68, the Truss Model predictions are in generally better agreement with the test results and show significantly less scatter than the ACI/AASHTO predicted values.

3.9.2 <u>Torsion-Bending.</u> In the case of combined torsion-bending the ACI/AASHTO ultimate strength is evaluated following the requirements given in Refs. 24 and 12. The comparison between the ACI/AASHTO and Truss Model approaches in the case of combined actions has to be conducted in a different manner than the one followed in the case of single actions (pure torsion). Since the ACI/AASHTO design procedures do not consider the interaction between bending and torsion directly in the design, both ultimate predicted strengths (pure torsion and pure bending) are computed separately.

Tests reported by Hsu (82) on reinforced concrete rectangular beams

| (1) Member ID | (2) r | (3) $\dfrac{T_{test}}{T_{ACI/AASHTO}}$ | (4) $\dfrac{T_{test}}{T_u}$ Eq. 3.1 | (5) $\alpha$(Eq.3.2) degrees |
|---|---|---|---|---|
| G4 | 1.0 | 1.12 | 1.07 | 43 |
| G6 | | 0.99 | 1.09 | 45 |
| G7 | | 1.01 | 1.06 | 44 |
| G8 | | 1.27 | 1.08 | 44 |
| N1 | | 1.06 | 0.94 | 49 |
| N1a | | 1.05 | 0.93 | 49 |
| N2 | | 1.12 | 0.93 | 49 |
| N2a | | 1.02 | 0.85 | 49 |
| N3 | | 1.06 | 0.84 | 49 |
| N4 | | 1.28 | 0.70 | 50 |
| K1 | | 1.06 | 1.35 | 44 |
| K2 | | 1.12 | 1.25 | 44 |
| K3 | | 1.38 | 1.15 | 43 |
| C1 | | 1.04 | 1.23 | 44 |
| C2 | | 1.00 | 0.94 | 44 |
| Overall for Tables 3.45 and 3.46 | X | 1.07 | 1.01 | |
| | S | 0.17 | 0.15 | N = 43 |

\* Specimens B6,M6,I6,I4,G5,K4,C3,C4,C5,C6
  are compared in Table 3.56.

Table 3.47   Data on reinforced concrete beams with web
            reinforcement subjected to pure torsion

Tests reported by Liao and Ferguson (104) on reinforced concrete L-beams

| (1) Member ID | (2) r | (3) $\dfrac{T_{test}}{T_{ACI/AASHTO}}$ | (4) $\dfrac{T_{test}}{T_u (Eq.3.1)}$ | (5) $\alpha$(Eq.3.2) degrees |
|---|---|---|---|---|
| PT1 | 1.0 | 1.42 | 0.92 | 9 |
| PT2 | | 1.66 | 0.96 | 16 |
| PT7 | | 1.08 | 1.11 | 31 |
| PT8 | | 1.61 | 1.03 | 16 |
| | X | 1.44 | 1.01 | N = 4 |
| | S | 0.26 | 0.08 | |

Tests reported by Rajagopalan and Ferguson (140) on reinforced concrete L-beams

| | | | | |
|---|---|---|---|---|
| R7 | 1.0 | 1.68 | 1.21 | 18 |
| R8 | | 1.86 | 1.38 | 12 |
| R17 | | 1.68 | 1.18 | 24 |
| R19 | | 1.95 | 1.35 | 17 |
| | X | 1.79 | 1.28 | N = 4 |
| | S | 0.14 | 0.10 | |
| Overall for Table 3.49 | X | 1.62 | 1.14 | N = 8 |
| | S | 0.27 | 0.17 | |

Table 3.49   Data on reinforced concrete L-beams with web reinforcement subjected to pure torsion

(a) ACI/AASHTO
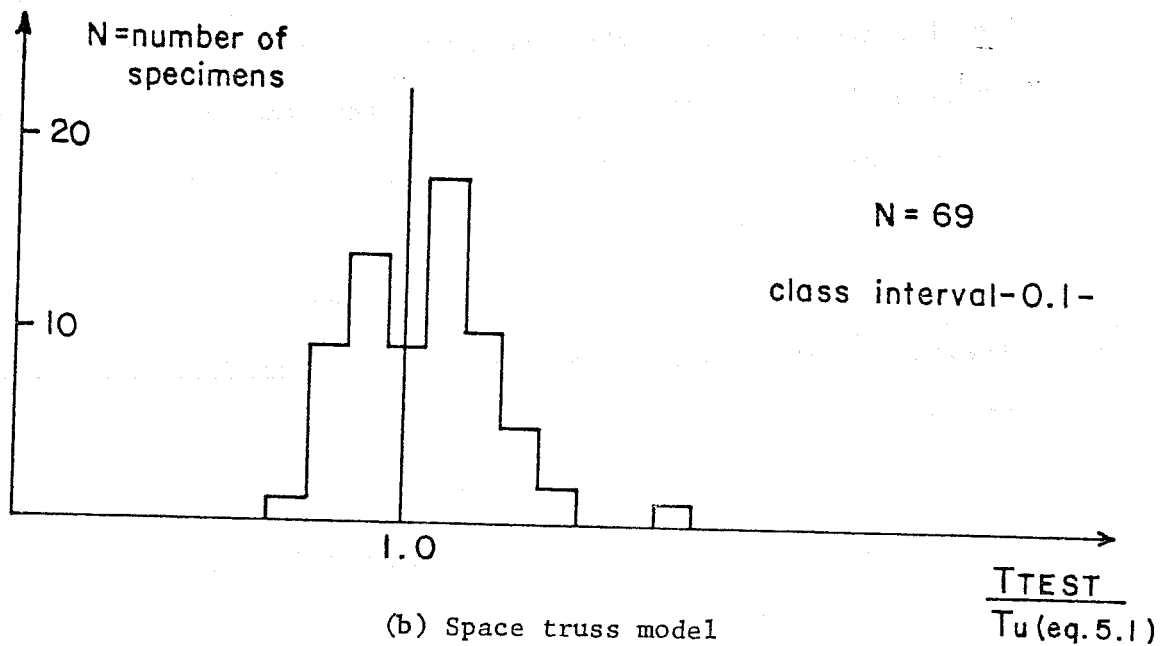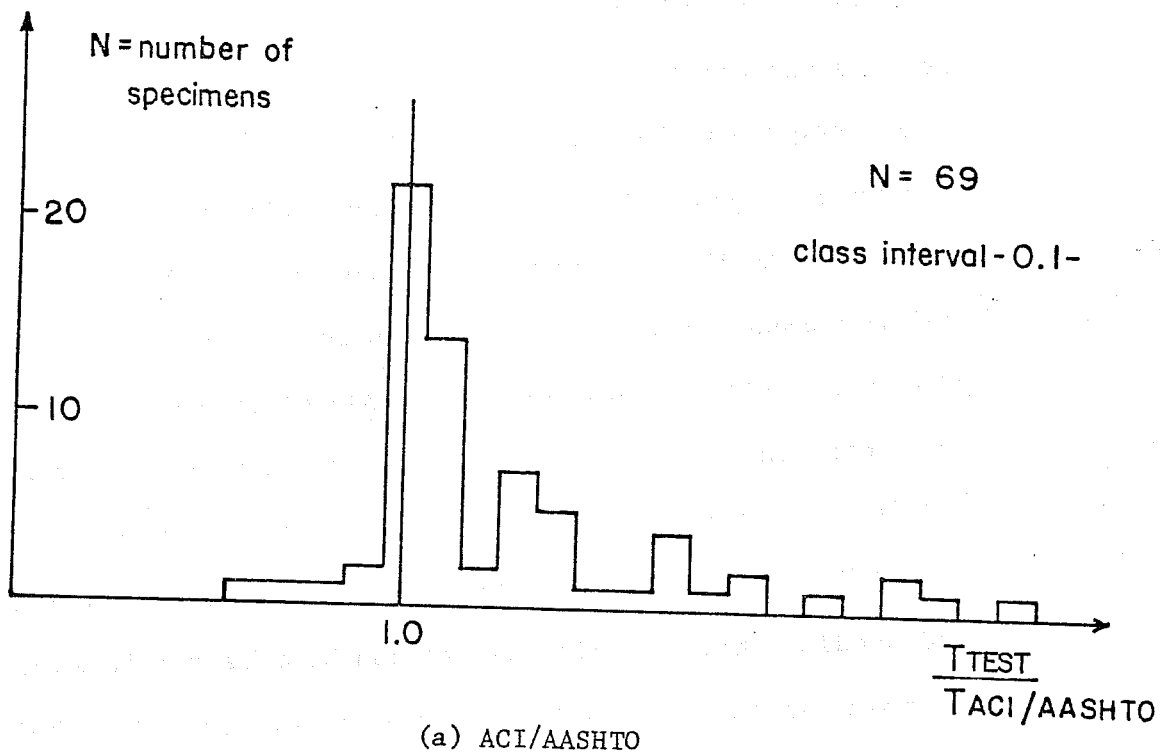


(b) Space truss model

Fig. 3.68  Comparison between the ACI/AASHTO and space truss model predictions with test results of reinforced concrete beams under pure torsion

Tests reported by Gesund, Schuetter, Buchanan, and Gray [76]
on reinforced concrete rectangular beams.

| (1) | (2) | (3) | (4) | (5) | (6) |
|---|---|---|---|---|---|
| Member ID | r | I (space truss) | $\dfrac{M_{TEST}}{M_{ACI}/AASHTO}$ | $\dfrac{T_{TEST}}{T_{ACI}/AASHTO}$ | Mode of failure (ACI/AASHTO) |
| 1 | 0.7 | 0.97 | 0.43 | 1.20 | T |
| 2 | 0.7 | 0.94 | 0.55 | 0.82 | T |
| 3 | 0.7 | 0.81 | 0.66 | 0.90 | T |
| 4 | 0.7 | 0.90 | 0.73 | 0.55 | M |
| 5 | 0.7 | 1.04 | 0.80 | 0.77 | M |
| 6 | 0.7 | 1.01 | 0.92 | 0.47 | M |
| 7 | 0.7 | 0.93 | 0.93 | 0.64 | M |
| 8 | 0.7 | 0.98 | 0.94 | 0.35 | M |
| 9 | 0.7 | 1.18 | 0.42 | 1.04 | T |
| 10 | 0.7 | 1.03 | 0.62 | 0.80 | T |
| 11 | 0.7 | 0.98 | 0.48 | 0.75 | T |
| 12 | 0.7 | 1.03 | 0.75 | 0.60 | M |
| x | | 0.98 | 0.69 | 0.74 | N=12 |
| s | | 0.09 | 0.19 | 0.24 | |

Table 3.51  Data on reinforced concrete rectangular beams
with web reinforcement subjected to combined
bending torsion

Tests reported by Pandit and Warwaruk [33]
on reinforced concrete rectangular beams.

| (1) | (2) | (3) | (4) | (5) | (6) |
|---|---|---|---|---|---|
| Member ID | r | I (space truss) | $\frac{M_{TEST}}{M_{ACI/AASHTO}}$ | $\frac{T_{TEST}}{T_{ACI/AASHTO}}$ | Mode of failure |
| B2 | 0.5 | 1.13 | 0.81 | 0.74 | M |
| B3 | 0.5 | 1.03 | 0.45 | 0.88 | T |
| C1 | 0.5 | 1.14 | 0.89 | 0.64 | M |
| C2 | 0.5 | 1.04 | 0.62 | 0.87 | T |
| D1 | 0.34 | 0.87 | 0.74 | 0.82 | T |
| D2 | 0.34 | 0.80 | 0.45 | 1.34 | T |
| D3 | 0.34 | 0.65 | 0.23 | 1.32 | T |
| E1 | 1.0 | 1.23 | 0.80 | 0.63 | M |
| E2 | 1.0 | 1.16 | 0.45 | 0.83 | T |
| | x | 1.01 | 0.60 | 0.90 | N=9 |
| | s | 0.19 | 0.22 | 0.26 | |

Table 3.52   Data on reinforced concrete rectangular beams
with web reinforcement subjected to combined
bending torsion

3.9.3  Torsion-Bending-Shear.  In the case of combined torsion-bending-shear the ACI/AASHTO ultimate predicted values are evaluated in accordance with the requirements given in Refs. 24 and 12 and previously discussed in Report 248-2.

Since the current ACI/AASHTO design recommendations do not directly consider the interaction between torsion and bending the comparison has to be carried out as in the case of combined torsion-bending.  However, since the ACI/AASHTO design procedures do consider the interaction between torsion and shear, in this case the value of the torsional moment computed to evaluate the ratio of column (5) of Tables 3.53 and 3.54 do reflect the level of shear force present at ultimate in the member.

Shown in Tables 3.53 and 3.54 are data on reinforced concrete rectangular and L-beams subjected to combined torsion-bending-shear. Once more the dominant mode of failure for each specimen given in column (7) is selected by choosing the largest of the two ratios given in columns (4) and (5) for each specimen.

Figure 3.70 shows a comparison between the Space Truss and the ACI/AASHTO predicted values with the data from Tables 3.53 and 3.54.  As can be seen from Fig. 3.70 the Truss Model is as good as the current ACI/AASHTO procedures for the case of failures controlled by flexure. In the case of failures controlled by torsion (Fig. 3.70c), the Truss Model predicted values (see Fig. 3.70a) show a much better agreement with test results greatly reducing the scatter between the predicted and observed ultimate values.

Tests reported by Osburn, Mayoglou, and Mattock [133]
on rectangular (R) and L-beams (L)

| (1)<br>Member ID | (2)<br>r | (3)<br>I<br>(space truss) | (4)<br>$\frac{M_{TEST}}{M_{ACI/AASHTO}}$ | (5)<br>$\frac{T_{TEST}}{T_{ACI/AASHTO}}$ | (6)<br>$V_{TEST}$<br>(k) | (7)<br>Mode of<br>failure |
|---|---|---|---|---|---|---|
| A1(R) | 0.15 | 1.31 | 1.17 | 0.96 | 13.2 | M |
| A2(R) | 0.15 | 1.27 | 1.07 | 0.93 | 14.2 | M |
| A3(R) | 0.15 | 1.19 | 1.10 | 0.92 | 15.6 | M |
| A4(R) | 0.15 | 1.03 | 1.07 | 0.88 | 17.2 | M |
| A5(R) | 0.15 | 0.91 | 1.06 | 0.99 | 20.2 | M |
| B1(R) | 0.15 | 1.24 | 1.09 | 1.20 | 8.72 | T–S |
| B2(R) | 0.15 | 1.15 | 1.05 | 1.16 | 9.1 | T–S |
| B3(R) | 0.15 | 1.15 | 1.09 | 1.18 | 10.4 | T–S |
| B4(R) | 0.15 | 1.07 | 0.98 | 1.11 | 11.2 | T–S |
| B5(R) | 0.15 | 1.04 | 1.06 | 1.09 | 12.8 | T–S |
| C1(R) | 0.10 | 1.14 | 1.10 | 0.93 | 10.0 | M |
| C2(R) | 0.12 | 0.94 | 0.95 | 0.80 | 10.55 | M |
| C3(R) | 0.13 | 1.03 | 1.04 | 0.87 | 13.4 | M |
| C4(R) | 0.10 | 0.94 | 1.00 | 0.94 | 16.1 | M |
| D1(L) | 0.10 | 1.26 | 1.10 | 1.00 | 10.8 | M |
| D2(L) | 0.12 | 1.12 | 1.00 | 0.94 | 12.3 | M |
| D3(L) | 0.13 | 0.92 | 0.96 | 0.90 | 13.4 | M |
| D4(L) | 0.10 | 0.93 | 0.87 | 0.90 | 15.9 | T–S |
| E1(L) | 0.10 | 1.24 | 1.09 | 0.99 | 10.7 | M |
| E2(L) | 0.12 | 1.02 | 0.93 | 0.85 | 11.4 | M |
| E3(L) | 0.13 | 1.00 | 0.93 | 0.85 | 12.97 | M |
| E4(L) | 0.10 | 0.80 | 0.76 | 0.77 | 13.9 | T–S |
| x̄ | | 1.08 | 1.02 | 0.96 | N=22 | |
| s | | 0.14 | 0.09 | 0.12 | | |

Table 3.54   Data on reinforced concrete rectangular and
L-beams with web reinforcement subjected to
combined torsion-bending-shear

3.9.4 <u>Bending</u> <u>and</u> <u>Shear</u>. In this section the data examined in Sec. 3.5 on reinforced and prestressed concrete beams with web reinforcement failing in shear are utilized to compare the Truss Model predictions and the ACI/AASHTO ultimate expected values.

The ACI/AASHTO predicted ultimate strength is evaluated in accordance with the requirements given in Refs. 24 and 12, and previously discussed in Report 248-2.

In computing the concrete contribution in the case of AASHTO/ACI predicted values, the formula $1.9\sqrt{f_c'} + 2500 \, \rho_w \, V_d/M$ is used; where $\rho_w$ is a ratio of longitudinal reinforcement defined as $A_s/[b_w d]$, $A_s$ being the area of longitudinal tension reinforcement, V and M are the ultimate test values, and "d" is the distance between the extreme compression fiber and the centroid of the longitudinal tension reinforcement.

Shown in Tables 3.55 through 3.57 are data from simply supported reinforced concrete rectangular beams failing in shear. Given in column (5) of Tables 3.55 through 3.57 is the ratio of the test value to the ACI/AASHTO predicted value. In column (4) the dispersion index "I" of the Truss Model, previously explained in Sec. 3.5, is given.

In Fig. 3.71 the values of columns (4) and (5) from Tables 3.55 through 3.57 are shown to compare the truss model predictions and the ACI/AASHTO expected ultimate load values with data from reinforced concrete beams failing in shear. As can be seen from Fig. 3.71, the Truss Model predictions, although conservative, show much better agreement with the actual test values. They significantly reduce the scatter of the test to predicted shear ratio.

Tests reported by A.P. Clark (53) on reinforced concrete rectangular beams

| (1) Member ID | (2) $\rho_{vfy}$ psi | (3) $\tan \alpha$ Eq.3.16 | (4) Ispace truss | (5) $\dfrac{V_{test}}{V_{ACI/AASHTO}}$ | (6) Level of Prestress $\sigma/f'c$ |
|---|---|---|---|---|---|
| B1-1 | 180 | 0.30 | 1.23 | 1.58 | 0.0 |
| B1-2 |  | 0.34 | 1.14 | 1.41 |  |
| B1-3 |  | 0.30 | 1.25 | 1.60 |  |
| B1-4 |  | 0.32 | 1.17 | 1.50 |  |
| B1-5 |  | 0.36 | 1.06 | 1.32 |  |
| B2-1 | 350 | 0.58 | 1.13 | 1.10 |  |
| B2-2 |  | 0.54 | 1.19 | 1.16 |  |
| B2-3 |  | 0.52 | 1.24 | 1.21 |  |
| C1-1 | 170 | 0.29 | 1.50 | 1.63 |  |
| C1-2 |  | 0.25 | 1.70 | 1.84 |  |
| C1-3 |  | 0.33 | 1.34 | 1.45 |  |
| C1-4 |  | 0.28 | 1.56 | 1.64 |  |
| C3-1 |  | 0.36 | 1.21 | 1.43 |  |
| C3-2 |  | 0.40 | 1.09 | 1.29 |  |
| C3-3 |  | 0.43 | 1.02 | 1.20 |  |
| C2-1 | 330 | 0.56 | 1.33 | 1.12 |  |
| C2-2 |  | 0.53 | 1.39 | 1.17 |  |
| C2-4 |  | 0.56 | 1.33 | 1.10 |  |
| C4-1 | 170 | 0.27 | 1.27 | 1.75 |  |
| C4-2 |  | 0.19 | 1.73 | 2.11 |  |
| C6-3 |  | 0.18 | 1.78 | 2.18 |  |
| C6-4 |  | 0.19 | 1.75 | 2.09 |  |
| D1-1 | 220 | 0.35 | 1.55 | 1.51 |  |
| D1-3 |  | 0.41 | 1.32 | 1.29 |  |
| D3-1 | 440 | 0.55 | 1.24 | 1.19 |  |
| D2-1 | 290 | 0.49 | 1.37 | 1.20 |  |
| D2-2 |  | 0.46 | 1.47 | 1.27 |  |

Table 3.56   Data on simply supported reinforced concrete rectangular beams failing in shear

N=number of
specimens

N= 58

class interval-0.1-

(a) space truss

I (space truss)

N

N = 58

class interval-0.1-
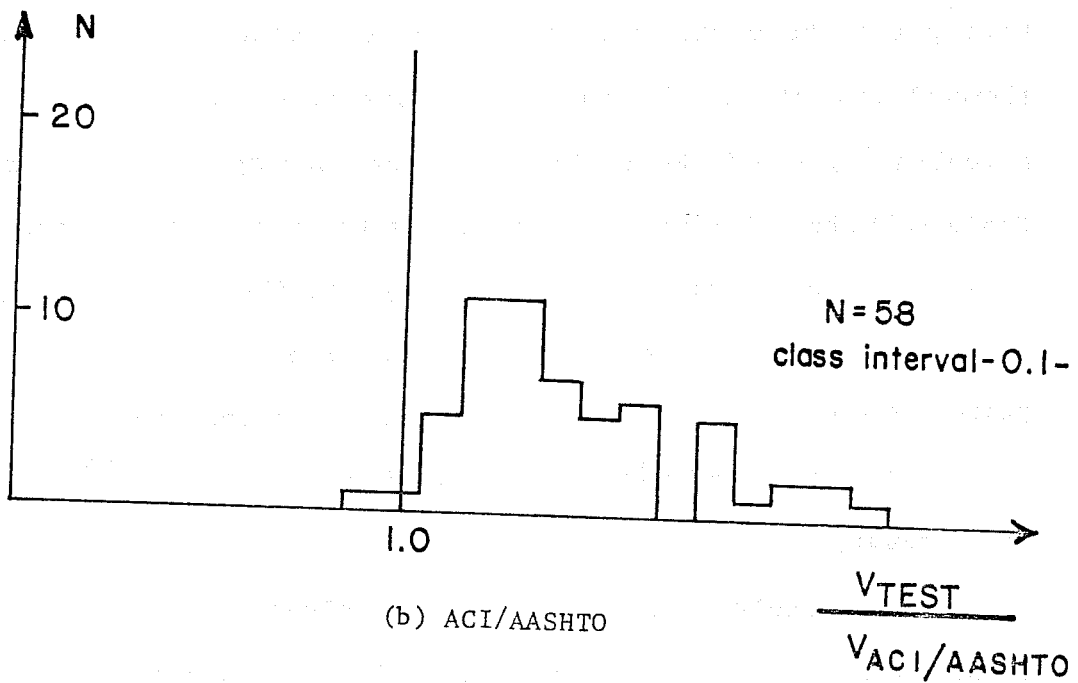
(b) ACI/AASHTO

$$\frac{V_{TEST}}{V_{ACI/AASHTO}}$$
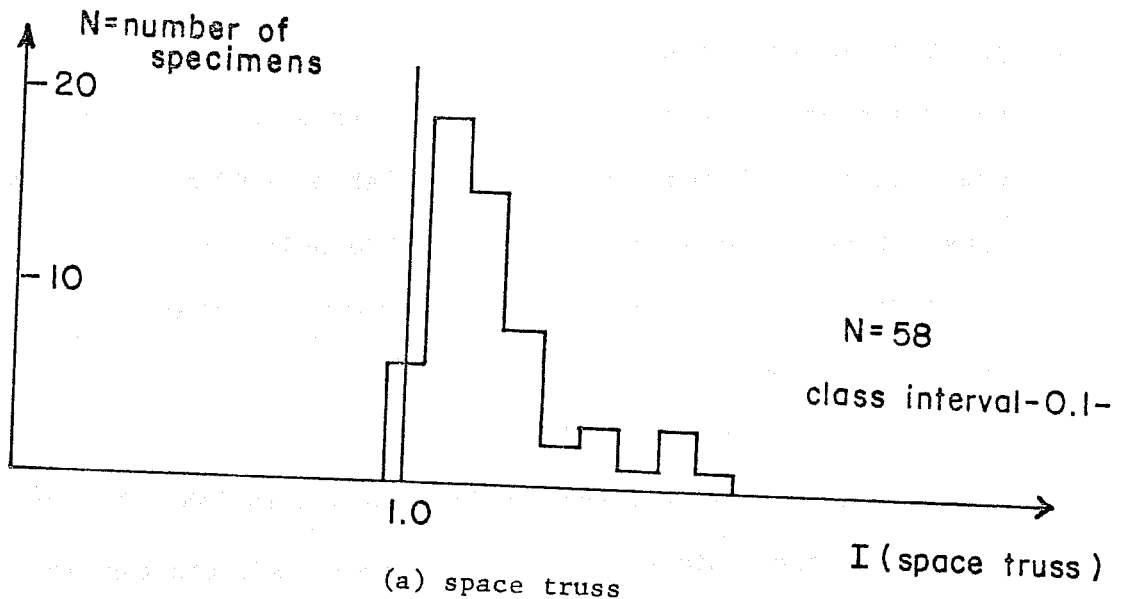
Fig. 3.71 Comparison between the ACI/AASHTO and space truss
model predictions with test results of reinforced
concrete beams where shear failures were observed

### Tests reported by Moayer and Regan (33) on prestressed concrete T-Beams

| (1) Member ID | (2) $\rho_{vfy}$ psi | (3) $\tan \alpha$ Eq.3.16 | (4) Ispace truss | (5) $\dfrac{V_{test}}{V_{ACI/AASHTO}}$ | (6) Level of Prestress $\sigma/f'c$ |
|---|---|---|---|---|---|
| P4  | 155 | 0.52 | 1.42 | 1.05 | 0.07 |
| P8  | 104 | 0.12 | 1.55 | 1.60 | 0.14 |
| P13 | 104 | 0.14 | 1.68 | 1.65 | 0.05 |
| P18 | 104 | 0.13 | 1.60 | 1.50 | 0.13 |
| P24 | 155 | 0.49 | 1.33 | 1.03 | 0.05 |
| P25 | 104 | 0.21 | 1.51 | 1.45 | 0.05 |
| P26 | 155 | 0.41 | 1.32 | 1.04 | 0.12 |
| P27 | 104 | 0.18 | 1.43 | 1.37 | 0.13 |
| P28 | 155 | 0.36 | 1.28 | 1.15 | 0.13 |
| P29 | 104 | 0.23 | 1.34 | 1.40 | 0.13 |
| P49 | 155 | 0.37 | 0.98 | 1.15 | 0.16 |
| X | | | 1.38 | 1.28 | N = 2 |
| S | | | 0.20 | 0.24 | |

### Tests reported by Castrodale (50) on prestressed concrete I-beams under distributed loadings

| | | | | | |
|---|---|---|---|---|---|
| 0.40A | 180 | 0.17 | 1.04 | 1.84 | 0.10 |
| 0.40B | 180 | 0.17 | | 2.00 | 0.13 |
| 0.45  | 220 | 0.19 | | 2.00 | 0.12 |
| | | X | 1.04 | 1.95 | N = 3 |
| | | S | 0.0 | 0.09 | |
| Overall for Table 3.58 | | X | 1.31 | 1.41 | N = 15 |
| | | S | 0.23 | 0.35 | |

Table 3.58  Data on simply supported prestressed concrete T and I beams failing in shear

N = number of
   specimens

10

N=23
class interval-0.1-

1.0

I (space truss)

(a) Space truss

N

10

N=23
class interval-0.1-

1.0

$\dfrac{V\,Test}{V\,ACI/AASHTO}$
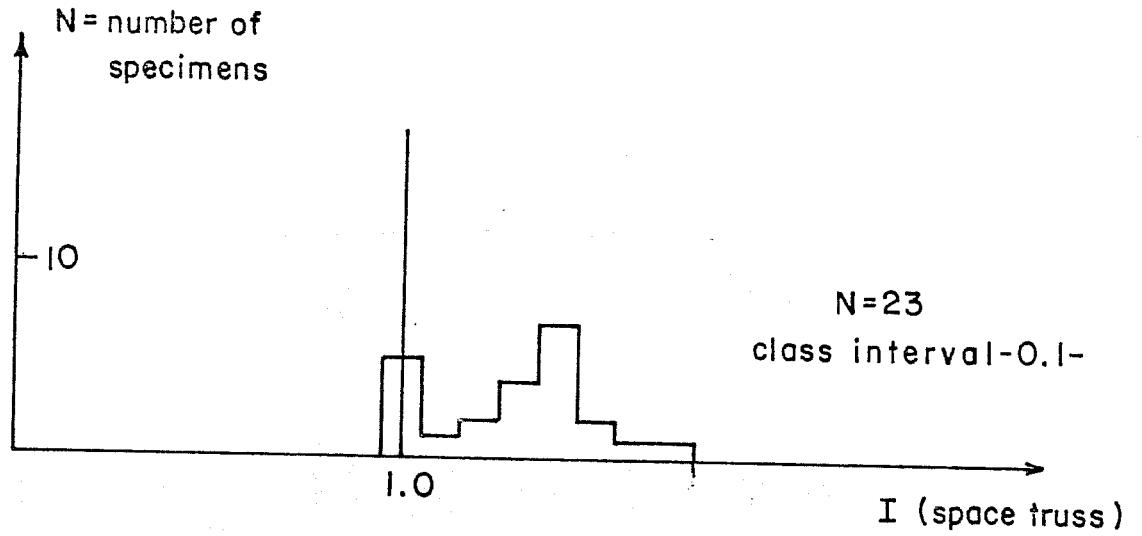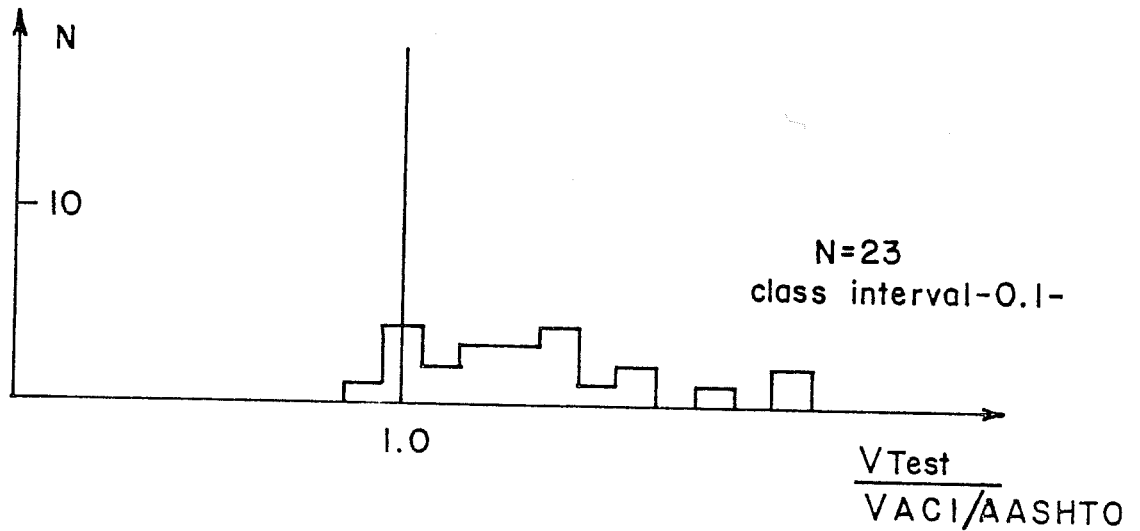
(b) ACI/AASHTO

Fig. 3.72   Comparison between the space truss model and the
ACI/AASHTO predictions with test results of
prestressed concrete beams failing in shear

Tables 3.61 and 3.62 show data for reinforced and prestressed concrete continuous beams failing in shear. Figure 3.73 shows a comparsion between the ACI/AASHTO and Space Truss Model predictions with test data from Tables 3.61 and 3.62 on continuous beams failing in shear. It is apparent that the Truss Model tends to yield reasonable predicted values; however, it is slightly more unconservative than the current ACI/AASHTO design procedures. The shaded portion of the space truss values in Fig. 3.73 are specimens in which $\tan\alpha$ falls significantly outside the space truss limits, these should not be considered in judging the accuracy of the design procedure.

After comparing both procedures with test results it can be concluded that:

1. In the cases of pure torsion, combined torsion-bending and torsion-bending-shear the Truss Model yields conservative results and is in better agreement with observed test values than the current ACI/AASHTO procedures.

2. In the case of bending and shear the Truss Model again is in better agreement with test results than the current ACI/AASHTO procedures. However, it seems to yield more conservative predictions than in the case of combined actions.

Tests reported by Mattock and Kaar (111) on semi-continuous
prestressed concrete I-beams.

| (1)<br>Member<br>ID | (2)<br>ρvfy<br>psi | (3)<br>tanα<br>Eq.3.16 | (4)<br>I space<br>truss | (5)<br>Vtest<br>V(ACI/AASHTO) | (6)<br>Level of<br>prestress<br>$\sigma/f'c$ |
|---|---|---|---|---|---|
| S7 | 282 | 0.21 | 1.89 | 2.07 | 0.15 |
| S13 | 282 | 0.31 | 1.54 | 1.53 | 0.14 |
| S10 | 188 | 0.17 | 1.83 | 2.18 | 0.15 |
| S21 | 188 | 0.17 | 1.62 | 2.08 | 0.14 |
| | | X = | 1.72 | 1.97 | |
| | | | | | N = 4 |
| | | S = | 0.17 | 0.29 | |

Table 3.62  Data on semicontinuous prestressed
concrete I beams failing in shear

C H A P T E R   4

CONCLUSIONS

4.1  Summary

In this report a complete evaluation of the truss model in the areas of shear, torsion, and shear and torsion, has been conducted by careful comparison with several hundred experimental results.

A comparison of the variable angle truss model predicted ultimate values with test results of reinforced and prestressed concrete one-way flexural members where failure produced yielding of the longitudinal and web reinforcement was carried out. This comparative study showed that the truss model predicted ultimate strength is in very good agreement with observed ultimate values of members where yielding of the reinforcement at failure was reported.

In Sec. 3.2 it was pointed out that the basic truss model used herein does not include the effects of warping torsion. This type of torsion becomes significant in the case of open-ended members formed by three or more walls, where the torsional warping of the cross section is restrained. In these cases, the basic truss model tends to underestimate the torsional capacity of those members. More advanced truss models have been proposed for cases where warping torsion is important.

It was also shown that the truss model interaction equations very adequately represent the ultimate load interaction of reinforced

281

## 4.2 Recommendations

With the general interaction behavior and expected failure capacities confirmed by test results, the general procedures derived from the truss model are translated in Report 248-4F into design recommendations and draft AASHTO requirements. A review of some of the current design procedures available in other codes is also given in Report 248-4F. In that report, the design procedures based on the truss model are applied through a series of design examples. A parallel design using the current AASHTO design procedures, wherever available, is conducted and a comparison of the results of the two design procedures is presented.

# REFERENCES

1. American Association of State Highway Officials, _Standard Specifications for Highway Bridges_, American Association of State Highway Officials, 1935.

2. American Association of State Highway Officials, _Standard Specifications for Highway Bridges_, American Association of State Highway Officials, 1941.

3. American Association of State Highway Officials, _Standard Specifications for Highway Bridges_, American Association of State Highway Officials, 1944.

4. American Association of State Highway Officials, _Standard Specifications for Highway Bridges_, American Association of State Highway Officials, 1949.

5. American Association of State Highway Officials, _Standard Specifications for Highway Bridges_, American Association of State Highway Officials, 1953.

6. American Association of State Highway Officials, _Standard Specifications for Highway Bridges_, American Association of State Highway Officials, 1957.

7. American Association of State Highway Officials, _Standard Specifications for Highway Bridges_, American Association of State Highway Officials, 1961.

8. American Association of State Highway Officials, _Standard Specifications for Highway Bridges_, American Association of State Highway Officials, 1965.

9. American Association of State Highway Officials, _Standard Specifications for Highway Bridges_, American Association of State Highway Officials, 1969.

Reinforced Concrete (ACI 318-63), American Concrete Institute, 1963.

22. American Concrete Institute, Commentary on Building Code Requirements for Reinforced Concrete (ACI 318-63), American Concrete Institute, 1965.

23. American Concrete Institute, Building Code Requirements for Reinforced Concrete (ACI 318-71), American Concrete Institute, 1971.

24. American Concrete Institute, Building Code Requirements for Reinforced Concrete (ACI 318-77), American Concrete Institute, 1977.

25. American Concrete Institute, ``Tentative Recommendations for Prestressed Concrete (ACI 323),'' ACI Journal, Vol. 29, No. 7, Jan.1958, pp. 545-578.

26. ACI-ASCE Committee 326, ``Shear and Diagonal Tension,'' ACI Journal, Vol. 59, Jan.,Feb. 1962, pp. 3-30, 277-333.

27. ACI-ASME Committee 359, Code for Concrete Reactor Vessels and Containments (ACI 359-74),ASME Boiler and Pressure Vessel Code,Section III, Div.2, American Society of Mechanical Engineers, 1975.

28. ACI-ASCE Committee 426, ``The Shear Strength of Reinforced Concrete Members,'' Journal of the Structural Division, ASCE, Vol. 99, No. St6, June 1973, pp. 1091-1187.

29. ACI-ASCE Committee 426, Suggested Revisions to Shear Provisions for Building Codes, American Concrete Institute, Detroit, 1977, pp. 99.

30. American Concrete Institute, Analysis of Structural Systems for Torsion, Publication SP-35, Detroit, 1973, .

31. ACI Committee 438, Torsion in Concrete, American Concrete Institute Bibliography, Detroit, 1978, .

32. American Concrete Institute, Shear in Reinforced Concrete, ACI Publication SP-42, Detroit, 1974, .

33. American Concrete Institute, Torsion of Structural Concrete, Publication SP-18, Detroit, 1974, .

34. ACI Committee 438, ``Tentative Recommendations for the Design of Reinforced Concrete Members to Resist Torsion,'' Journal of

46. Campbell,T.I., Chitnuyanondh,L., and Batchelor,B. de V., ``Rigid-plastic Theory vs. Truss Analogy Method for Calculating the Shear Strength of Reinforced Concrete Beams,'' _Magazine of Concrete Research_, Vol. 32, No. 110, March 1980, pp. 39-44.

47. Campbell,T.I., Batchelor, B. de V., and Chitnuyanoudh,I., ``Web Crushing in Prestressed Concrete Girders with Ducts in the Webs,'' _PCI Journal_, Vol. 24, No. 5, September,October. 1979, pp. 70-88.

48. Caflish,R., Krauss,R., and Thürlimann,B., ``Biege-und Schubversuche an Teilweise Vorgespannten Betonbalken, Serie C.,'' Bericht 6504-3, Institut fur Baustatik, ETH Zurich, February, 1971.

49. Canadian Standards Association, ``Canadian Code Draft-Clause 11 Shear and Torsion'', Draft #9, unpublished.

50. Castrodale,R.W., ``A Comparison of Design for Shear in Prestressed Concrete Bridge Girders'', Thesis,University of Texas at Austin,unpublished.

51. Christophe,P., _Le Beton Arme et ses Applications_, Libraire Polytechnique, 1902, 2nd edition.

52. Chana,P.S., ``Some Aspects of Modelling the Behavior of Reinforced Concrete Under Shear Loading,'' Technical Report 543, Cement and Concrete Association, July 1981.

53. Clark,A.P., ``Diagonal Tension in Reinforced Concrete Beams,'' _ACI Journal_, Vol. 48, No. 2, October 1951, pp. 145-156.

54. Clarke,J.L., Taylor,H.P.J., ``Web Crushing-A Review of Research,'' Technical Report, Cement and Concrete Association, August 1975.

55. Comite Euro-International du Beton, ``Shear, Torsion, and Punching,'' Bulletin D'Information, , 1982, Number 146

56. Collins,M.P., and Mitchell,D., ``Shear and Torsion Design of Prestressed and Non-Prestressed Concrete Beams,'' _PCI Journal_, Vol. 25, No. 5, September, October 1980, pp. 32-100.

57. Collins,M.P., ``Towards a Rational Theory for RC Members in Shear,'' _Journal of the Structural Division,ASCE_,, Vol. 104, No. ST4, April 1978, pp. 649-666.

58. Collins,M.P., ``Investigating the Stress-Strain Characteristics of Diagonally Cracked Concrete,'' _IABSE Colloquium on_

70.  Gesund.H., Schuete,F.J., Buchanan,G.R., and Gray,G.A., ``Ultimate Strength in Combined Bending and Torsion of Concrete Beams Containing both Longitudinal and Transverse Reinforcement,'' _ACI Journal_, Vol. 611, No. 12, December 1964, pp. 1509-1522.

71.  Grob,J., ``Ultimate Strength of Beams with Thin Walled Open Cross-Sections,'' Bericht 56, Institut fur Baustatik und Konstruktion ETHZ, 1970, Birkhauser Verlag Basel und Stuttgart.

72.  Grob,J., and Thürlimann,B., _Ultimate Strength and Design of Reinforced Concrete Beams Under Bending and Shear_, IABSE, Zurich, 1976, pp. 15, Publication No.36 II.

73.  Hanson,J.M., _Ultimate Shear Strength of Prestressed Concrete Beams With No Web Reinforcement_, PhD dissertation, Lehigh University, 1964.

74.  Henley, H.G., ``Report of the Committee on Laws an Ordinances,'' _National Association of Cement Users_, Vol. 4, 1908, pp. 233-239.

75.  Henry, R.L.,and Zia, P., ``Behavior of Rectangular Prestressed Concrete Beams Under Combined Torsion Bending and Shear,'' Report, University of North Carolina State, University at Raleigh, April 1971.

76.  Hernandez, G., _Strength of Prestressed Concrete Beams With Web Reinforcement_, PhD dissertation, University of Illinois, Urbana., May 1958.

77.  Hicks, A.B., ``The Influence of Shear Span and Concrete Strength Upon the Shear Resistance of a Pretensioned Concrete Beam,'' _Magazine of Concrete Research_, November 1958, pp. 115-121, University of London, Imperial College of Science and Technology.

78.  Hognestad, E., ``What Do We Know About Diagonal Tension and Web Reinforcement In Concrete?,'' Circular Series 64, University of Illinois Engineering Experiment Station, March 1952.

79.  Hsu, T.C., and Kemp, E.L., ``Background and Practical Application of Tentative Design Criteria for Torsion,'' _Journal of the American Concrete Institute_, Vol. 66, No. 1, January 1969, pp. 12-23.

80.  Hsu, T.C., ``Torsion of Structural Concrete-Plain Concrete Rectangular Sections,'' Bulletin D134, Portland Cement Association, September 1968.

of Reinforced Concrete Beams in Torsion and Bending,'' *IABSE*, No. 31-I, October 1971, pp. 107-131, Publication. Zurich.

94. Lampert, P., and Collins, M.P., ``Torsion, Bending, and Confusion — An Attempt to Establish the Facts,'' *Journal of the American Concrete Institute*, August 1972, pp. 500-504.

95. Lampert, P., and Thürlimann, B., ``Torsionsversuche an Stahlbetonbalken,'' Bericht 6506-2, Institut fur Banstatik ETH, June 1968.

96. Lampert, P., and Thürlimann, B., ``Torsions-Biege-Versuche an Stahlbetonbalken,'' Bericht 6506-3, Institut fur Banstatik ETH, January 1969, Zurich.

97. Lampert, P., *Postcracking Stiffness of Reinforced Concrete Beams in Torsion and Bending*, American Concrete Institute, Detroit, SP-35-12 , 1973.

98. Laupa, A., *The Shear Strength of Reinforced Concrete Beams*, PhD dissertation, The University of Illinois, Urbana, September 1953, Thesis.

99. Laupa, A., Siess, C.P., and Newmark, N.M., ``Strength in Shear of Reinforced Concrete Beams,'' Bulletin 428, University of Illinois Engineering Experiment Station, March 1955, Volume 52.

100. Leonhardt, F.,, ``Shear and Torsion in Prestressed Concrete,'' *FIP Symposium*, 1970, pp. 137-155, Session IV, Prague.

101. Leonhardt, F., and Walther, R., ``Tests on T-Beams Under Severe Shear Load Conditions,'' Bulletin 152, Deutscher Ausschuss fur Stahlbeton, 1962, Berlin.

102. Leonhardt, F., and Walther, R., ``Shear Tests on T-Beam with Varying Shear Reinforcement,'' Bulletin 156, Deutscher, Ausschuss fur Stahlbeton, 1962, Berlin.

103. Lessig, N.N., ``Determination of Load Bearing Capacity of Reinforced Concrete Elements with Rectangular Cross Section Subject to Flexure with Torsion,'' Foreign Literature Study 371, Concrete and Reinforced Concrete Institution, 1959, Translated from Russian, PGA Research and Development Lab., Skokie, Ill.

104. Liao, H.M., and Ferguson, P.M., ``Combined Torsion in Reinforced Concrete L-Beams with Stirrups ,'' *ACI Journal*, Vol. 66, No. 12, December 1969, pp. 986-993.

117. Misic, J., and Warwaruk, J., ``Strength of Prestressed Solid and Hollow Beams Subjected Simultaneously to Torsion, Shear and Bending,'' ACI Publication, No. SP-55, —, pp. 515-546, Detroit.

118. Mitchell, D., and Collins, M.P., ``Detailing for Torsion,'' ACI, No. 9, September 1976, pp. 506-511.

119. Mitchell, D., and Collins, M.P., ``Diagonal Compression Field Theory — A Rational Model for Structural Concrete in Pure Torsion,'' ACI, Vol. 71, No. 8, August 1974, pp. 396-408.

120. Mitchell, D., and Collins, M.P., ``Influence of Prestressing on Torsional Response of Concrete Beams,'' Journal of the Prestressed Concrete Institute, May/June 1978, pp. 54-73.

121. Moretto, O., ``An Investigation of the Strength of Welded Stirrups in Reinforced Concrete Beams,'' Journal of the American Concrete Institute, Vol. 48, No. 2, October 1951, pp. 145-156.

122. Morsch, E, ``Die Schubfestigkeit des Betons,'' Beton und Eisen, Vol. 1 , No. 5, October 1902, pp. 11-12, Berlin.

123. Mukherjee, P.R., and Warwaruk, J., ``Torsion, Bending, and Shear in Prestressed Concrete,'' Journal of the Structural DIvision ASCE, No. ST4, April 1971, pp. 1963-1079.

124. Muller, P., ``Failure Mechanisms for Reinforced Concrete Beams in Torsion and Bending,'' Bericht 65, Insitut fur Baustatik und Konstrucktion ETH, September 1976, Zurich.

125. Murashkin, G.V., ``The Effect of Prestress on Ultimate and Cracking Strengths of Reinforced Concrete Beams Subject to Torsion and Bending,'' Tech. report 10, Beton i Zhelezobeton, October 1965, PCA Foreign Literature Study No. 474, PCA Research and Development Lab., Shokie, Illinois.

126. National Association of Cement Users, NACU Standard No.4, Standard Building Regulations for Reinforced Concrete, 1910, Volume 66, pages 349-361.

127. Nielsen, M.P. and Braestrup, N.W., ``Plastic Shear Strength of Reinforced Concrete Beams,'' Tech. report 3, Bygningsstatiske Meddelelser, 1975, volume 46.

128. Nielsen, M.P., Braestrup, N.W., and Bach, F., Rational Analysis of Shear in Reinforced Concrete Beams, IABSE, 1978.

129. Nielsen, M.P., Braestrup, M.W., Jensen, B.C., and Bach, F.,

141. Rajagopalan, K.S., and Ferguson, P.M., ``Exploratory Shear Tests Emphasizing Percentage of Longitudinal Steel,'' ACI, Vol. 65, August 1968, pp. 634-638.

142. Rangan, B.V., ``Shear Strength of Partially and Fully Prestressed Concrete Beams,'' Uniciv Report R-180, University of New South Wales, February 1979.

143. Rangan, B.V., and Hall, A.S., ``Studies on Prestressed Concrete I-Beams in Combined Torsion, Bending, and Shear,'' Unicev Report R-161, University of New South Wales, October 1976.

144. Rangan, B.V., and Hall, A.S., ``Studies on Prestressed Concrete Hollow Beams in Combined Torsion and Bending,'' Unicev Report R-174, University of New South Wales, February 1978.

145. Rangan, B.V., and Hall, A.S., ``Proposed Modifications to the Torsion Rules in the SAA Concrete Codes,'' Unicev Report R-196, University of New South Wales, July 1980.

146. Rodriguez, J.J., Bianchini, A.C., Viest, I.M., and Kesler, C.E., ``Shear strength of Two-span Continuous Reinforced Concrete Beams,'' ACI Journal, Vol. 30, No. 10, April 1959, pp. 1089-1131.

147. Regan, P.E., ``Shear Tests of Rectangular Reinforced Concrete Beams,'' Tech. report, Polytechnic of Central London, May 1980.

148. Regan, P.E., ``Recommendations on Shear and Torsion: A Comparison of ACI and CEB Approaches,'' ACI, No. SP-59, 1979, pp. 159-175, Bulletin 113, Detroit.

149. Richart, F.E., ``An Investigation of Web Stresses in Reinforced Concrete Beams,'' Bulletin 166, University of Illinois, Urbana, June 1927.

150. Ritter, W., "Die Bauweise Hennebique," Schweizerische Bauzeitung, Vol. 33, No. 5, pp. 41-3; No. 6, pp. 49-52; No. 7, pp. 59, 61; February 1899, Zürich.

151. Robinson, J.R., ``Essals a L'Effort Tranchant des Poutres a Ame Mince en Beton Arme,'' Annales des Ponts et Chaussees, Vol. 132, Mar./Apr. 1961, pp. 225-255, Paris.

152. Sozen, M.A., Zwoyer, E.M. and Siess, C.P., ``Investigation of Prestressed Concrete for Highway bridges, Part 1. Strength in Shear of beams without web reinforcement,'' University of Illinois, Vol. 56, No. 62, April 1959, pp. 62-69.

166. Thürlimann, B., ``Torsional Strength of Reinforced and Prestressed Concrete Beams-CEB Approach,'' Bulletin 113, ACI Publication SP-59, 1979, Detroit.

167. Victor, J.D., and Aravindan, P.K., ``Prestressed and Reinforced Concrete T-Beams Under Combined Bending and Torsion,'' ACI, Vol. 75, No. 10, October 1978, pp. 526-532.

168. Walsh, P.F., Collins, M.P., and Archer,F.E., ``The Flexure-Torsion and Shear-Torsion Interaction Behavior of Rectangular Reinforced Concrete Beams,'' Civil Engineering Transactions, October 1967, pp. 313-319, Australia.

169. Walsh, P.F., Collins, M.P., and Archer, F.E., and Hall, A.S., ``Experiments on the Strength of Concrete beams in Combined Flexure and Torsion,'' UNICIV, No. R-15, February 1966, pp. 59, University of New South Wales,Australia.

170. Werner, M.P., and Dilger, W.H., ``Shear Design of Prestressed Concrete Stepped Beams,'' Journal of the Prestressed Concrete Institute, Vol. 18, No. 4, July/August 1973, pp. 37-49.

171. Withey, M.O., ``Tests of Plain and Reinforced Concrete, Series of 1906,'' Bulletin of the University of Wisconsin, Engineering Series, Vol. 4, No. 1, November 1907, pp. 1-66.

172. Withey, M.O., ``Tests of Plain and Reinforced Concrete, Series of 1907,'' Bulletin of the University of Wisconsin, Engineering Series, Vol. 4, No. 2, February 1908, pp. 71-136.

173. Wyss, A.N., Garland, J.B., and Mattock, A.H., ``A Study of the Behavior of I-Section Prestressed Concrete Girders Subject to Torsion,'' Structures and Mechanics Report SM69-1, March 1969, University of Washington.

174. Zia, P., McGee, W.D., ``Torsion Design of Prestressed Concrete,'' Journal of the Prestressed Concrete Institute, Vol. 19, No. 2, March/April 1974, pp. 46-65.

175. Zia, P., ``What Do We Know About Torsion in Concrete Members?,'' Journal of the Structural Division,ASCE, Vol. 96, No. St 6, June 1970, pp. 1185-1199.

176. Zia,P., ``Torsional Strength of Prestressed Concrete Members,'' ACI, Vol. 57, 1961, pp. 1337-1359.

177. Ramirez, Julio A., "Reevaluation of AASHTO Design Procedures for Shear and Torsion in Reinforced and Prestressed Concrete Beams," Unpublished Ph.D. dissertation, The University of Texas at Austin, December 1983.

183-8 "The Resilient and Fatigue Characteristics of Asphalt Mixtures Processed by the Dryer-Drum Mixer," by Manuel Rodriguez and Thomas W. Kennedy, December 1976.

183-9 "Fatigue and Repeated-Load Elastic Characteristics of Inservice Portland Cement Concrete," by John A. Crumley and Thomas W. Kennedy, June 1977.

183-10 "Development of a Mixture Design Procedure for Recycled Asphalt Mixtures," by Ignacio Perez, Thomas W. Kennedy, and Adedare S. Adedimila, November 1978.

183-11 "An Evaluation of the Texas Blackbase Mix Design Procedure Using the Indirect Tensile Test," by David B. Peters and Thomas W. Kennedy, March 1979.

183-12 "The Effects of Soil Binder and Moisture on Blackbase Mixtures," by Wei-Chou V. Ping and Thomas W. Kennedy, May 1979.

184-1 "The TEXAS Model for Intersection Traffic—Development," by Clyde E. Lee, Thomas W. Rioux, and Charlie R. Copeland, December 1977.

184-2 "The TEXAS Model for Intersection Traffic — Programmer's Guide," by Clyde E. Lee, Thomas W. Rioux, Vivek S. Savur, and Charlie R. Copeland, December 1977.

184-3 "The TEXAS Model for Intersection Traffic—User's Guide," by Clyde E. Lee, Glenn E. Grayson, Charlie R. Copeland, Jeff W. Miller, Thomas W. Rioux, and Vivek S. Savur, July 1977.

184-4F "Application of the TEXAS Model for Analysis of Intersection Capacity and Evaluation of Traffic Control Warrants," by Clyde E. Lee, Vivek S. Savur, and Glenn E. Grayson, July 1978.

188-1 "Behavior of Stage-Cast Inverted T-Beams with the Precast Flange in Tension," by S. A. A. Wahidi and R. W. Furlong, August 1976.

188-2F "Strength and Behavior of Stage-Cast Inverted T-Beams," by Richard W. Furlong, August 1978.

196-1F "Design of Reinforcement for Notched Ends of Prestressed Concrete Girders," by Gangadharan Menon and Richard W. Furlong, August 1977.

198-1F "Control of Cracking on the Side Faces of Large Reinforced Concrete Beams," by G. C. Frantz and J. E. Breen, September 1978.

209-1F "Fatigue Loading of Cantilever Sign Structures from Truck Wind Gusts," by Bruce M. Creamer, Karl H. Frank, and Richard E. Klingner, April 1979.

212-1F "Design Criteria for Median Turn Lanes," by C. Michael Walton, Thomas W. Horne, and William K. Fung, March 1978.

244-1 "Analysis of Single Piles Under Lateral Loading," by Barry J. Meyer and Lymon C. Reese, December 1979.

245-1F "Texas Traffic Data Acquisition Program," by Han-Jei Lin, Clyde E. Lee, and Randy Machemehl, February 1980.

514-1F "Effects of Temperature Change on Plastic Crash Cushions," by Victor N. Toth and Clyde E. Lee, January 1976.

1053-1F "Social Service Agency Transportation Services: Current Operations and the Potential for the Increased Involvement of the Taxi Industry," by Walter L. Cox and Sandra Rosenbloom, August 1977.

RR 16 "The Prediction of Passenger Riding Comfort from Acceleration Data," by Craig C. Smith, David Y. McGehee, and Anthony J. Healey, March 1976.

RR 35 "Perceived Environmental Utility Under Alternative Transportation Systems: A Framework for Analysis," by Pat Burnett, March 1976.

RR 36 "Monitoring the Effects of the Dallas/Fort Worth Regional Airport — Volume I: Ground Transportation Impacts," by William J. Dunlay, Jr., Lyndon Henry, Thomas G. Caffery, Douglas W. Wiersig, and Waldo A. Zambrano, December 1976.

RR 37 "Monitoring the Effects of the Dallas/Fort Worth Regional Airport — Volume II: Land Use and Travel Behavior," by Pat Burnett, David Chang, Carl Gregory, Arthur Friedman, Jose Montemayor, and Donna Prestwood, July 1976.

RR 38 "The Influence on Rural Communities of Interurban Transportation Systems, Volume II: Transportation and Community Development: A Manual for Small Communities," by C. Michael Walton, John Huddleston, Richard Dodge, Charles Heimsath, Ron Linehan, and John Betak, August 1977.

RR 39 "An Evaluation of Promotional Tactics and Utility Measurement Methods for Public Transportation Systems," by Mark Alpert, Linda Golden, John Betak, James Story, and C. Shane Davies, March 1977.

RR 40 "A Survey of Longitudinal Acceleration Comfort Studies in Ground Transportation Vehicles," by L. L. Hoberock, July 1976.

RR 43 "A Pavement Design and Management System for Forest Service Roads — A Working Model," by Freddy L. Roberts, B. Frank McCullough, Hugh J. Williamson, and William R. Wallin, February 1977.

RR 45 "Characteristics of Local Passenger Transportation Providers in Texas," by Ronald Briggs, January 1977.

RR 46 "The Influence on Rural Communities of Interurban Transportation Systems, Volume I: The Influence on Rural Communities of Interurban Transportation Systems," by C. Michael Walton, Richard Dodge, John Huddleston, John Betak, Ron Linehan, and Charles Heimsath, August 1977.

RR 47 "Effects of Visual Distraction on Reaction Time in a Simulated Traffic Environment," by C. Josh Holahan, March 1977.

RR 48 "Personality Factors in Accident Causation," by Deborah Valentine, Martha Williams, and Robert K. Young, March 1977.

RR 49 "Alcohol and Accidents," by Robert K. Young, Deborah Valentine, and Martha S. Williams, March 1977.

RR 50 "Alcohol Countermeasures," by Gary D. Hales, Martha S. Williams, and Robert K. Young, July 1977.

RR 51 "Drugs and Their Effect on Driving Performance," by Deborah Valentine, Martha S. Williams, and Robert K. Young, May 1977.

RR 52 "Seat Belts: Safety Ignored," by Gary D. Hales, Robert K. Young, and Martha S. Williams, June 1978.

RR 53 "Age-Related Factors in Driving Safety," by Deborah Valentine, Martha Williams, and Robert K. Young, February 1978.

RR 54 "Relationships Between Roadside Signs and Traffic Accidents: A Field Investigation," by Charles J. Holahan, November 1977.

RR 55 "Demographic Variables and Accidents," by Deborah Valentine, Martha Williams, and Robert K. Young, January 1978.

RR 56 "Feasibility of Multidisciplinary Accident Investigation in Texas," by Hal L. Fitzpatrick, Craig C. Smith, and Walter S. Reed, September 1977.

RR 60 "A Pavement Design and Management System for Forest Service Roads — Implementation," by B. Frank McCullough and David R. Luhr, January 1979.

RR 61 "Multidisciplinary Accident Investigation," by Deborah Valentine, Gary D. Hales, Martha S. Williams, and Robert K. Young, October 1978.

RR 62 "Psychological Analysis of Degree of Safety in Traffic Environment Design," by Charles J. Holahan, February 1979.

RR 63 "Automobile Collision Reconstruction: A Literature Survey," by Barry D. Olson and Craig C. Smith, December 1979.

RR 64 "An Evaluation of the Utilization of Psychological Knowledge Concerning Potential Roadside Distractors," by Charles J. Holahan, December 1979.